Final Report

ANALYSIS OF SOUTHERN CALIFORNIA WIND PROFILER AND AIRCRAFT DATA

SYSAPP-97-95/091r3

July 1997

Prepared for

Dr. Ash Lashgari
California Air Resources Board
2020 L Street
P.O. Box 2815
Sacramento, California 95814-2815

Prepared by

Sharon G. Douglas
A. Belle Hudischewskyj
Nina K. Lolk
Zitian Guo

Systems Applications International
101 Lucas Valley Road
San Rafael, California 94903
(415) 507-7185

Copyright 1997 by Systems Applications International, Inc.

DISCLAIMER

The statements and conclusions in this report are those of the contractor and not necessarily those of the California Air Resources Board. The mention of commercial products, their source, or their use in connection with material reported herein is not to be construed as actual or implied endorsement of such properties.

ACKNOWLEDGEMENTS

Valley Research Corporation provided and processed a substantial portion of the meteorological and air quality data used in this study.

This report was submitted in fulfillment of ARB Contract Number 94-317 "Analysis of Southern California Wind Profiler and Aircraft Data" by Systems Applications International Incorporated under the sponsorship of the California Air Resources Board. Work was completed as of February 1997.

Contents

Disclaimer and Acknowledgements iii
List of Figures vi
List of Tables xi
Abstract xiii
Executive Summary xv

1 DATA EVALUATION 1-1
Evaluation of the RWP and RASS Data 1-3
Discussion of Aircraft Data 1-42
Summary, Discussion, and Recommendations 1-42

2 ANALYSIS OF WIND AND POLLUTION DISTRIBUTIONS IN THE SOUTH COAST AND THE SOUTHEAST DESERT BASINS 2-1
Determination of Classification Combinations 2-1
Composite Winds and Mixing Heights 2-1
Aircraft Data 2-10
Summary 2-12

3 EVALUATION OF EPISODES IN THE MOJAVE DESERT AND SAN DIEGO AIR BASINS TO DETERMINE SHARED AND LOCAL DAYS 3-1
CART Analysis 3-2
Overview of Meteorology and Air Quality for the Selected Episode Days 3-7
Wind Analysis 3-11
Summary 3-26
Recommendations 3-27

4 SUMMARY AND CONCLUSIONS 4-1

REFERENCES R-1

APPENDIX A1: Scatter plots of u and v wind components and wind speeds and histograms of differences between u and v wind component, wind speed, and wind direction data for Radar Wind Profiler (RWP) and radiosonde site pairs located in the Southeast Desert Air Basin (SEDAB)

APPENDIX A2: Comparison of low and high resolution Radar Wind Profiler (RWP) wind data for the Mojave (MOJ) profiler site with the Edwards radiosonde data

APPENDIX A3: Scatter plots of u and v wind components and wind speeds and histograms of differences between u and v wind component, wind speed, and wind direction data for unedited Radar Wind Profiler (RWP) wind data for the Mojave (MOJ) profiler site with the Edwards radiosonde data

APPENDIX A4: Scatter plots of virtual temperature for RASS and radiosonde site pairs and histograms of the differences for monitoring sites located in the Southeast Desert Air Basin (SEDAB)

APPENDIX B1: Scatter plots of u and v wind components and wind speeds and histograms of differences between u and v wind component, wind speed, and wind direction data for Radar Wind Profiler (RWP) and radiosonde site pairs located in the San Diego Air Basin (SDAB)

APPENDIX B2: Comparison of low and high resolution Radar Wind Profiler (RWP) wind data for the San Diego (SDO) profiler site with the San Diego (MYFR) radiosonde data

APPENDIX B3: Scatter plots of u and v wind components and wind speeds and histograms of differences between u and v wind component, wind speed, and wind direction data for unedited Radar Wind Profiler (RWP) wind data for the San Diego (SDO) profiler site with the San Diego (MYFR) radiosonde data

APPENDIX B4: Scatter plots of virtual temperature for RASS and radiosonde site pairs and histograms of the differences for monitoring sites located in the San Diego Air Basin (SDAB)

APPENDIX C1: Scatter plots of u and v wind components and wind speeds and histograms of differences between u and v wind component, wind speed, and wind direction data for Radar Wind Profiler (RWP) and radiosonde site pairs located in the South Coast Air Basin (SOCAB)

APPENDIX C2: Scatter plots of virtual temperature for RASS and radiosonde site pairs and histograms of the differences for monitoring sites located in the South Coast Air Basin (SOCAB)

APPENDIX D: Comparison of mixing heights estimated using radiosonde data with the C_n^2 (refractive index) derived values

APPENDIX E: Composite Wind Plots

APPENDIX F: Wind Fields and Two- and Three-Dimensional Particle Paths for 20 June 1992

APPENDIX G: Wind Fields and Two- and Three-Dimensional Particle Paths for 25 June 1992

APPENDIX H: Wind Fields and Two- and Three-Dimensional Particle Paths for 29 July 1992

APPENDIX I: Wind Fields and Two- and Three-Dimensional Particle Paths for 27 September 1992

APPENDIX J: Wind Fields and Two- and Three-Dimensional Particle Paths for 30 September 1992

APPENDIX K: Wind Fields and Two- and Three-Dimensional Particle Paths for 11 October 1992

Figures

1-1 Locations of routine and 1992 Southern California field study upper-air monitoring sites 1-6

1-2a. Comparison of the minimum, maximum, and average RWP values with radiosonde data for the north-south component of the wind for the period 1520 to 1640 local time, 6 September, using data collected as part of the 1993 Claremont Study 1-7

1-2b Same as Figure 2-2a, but for the period 1810 to 1920 local time, 7 September 1-8

1-2c Same as Figure 2-2a, but for the period 1030 to 1130 local time, 10 September 1-9

1-3 Comparison of RWP/RASS data for the LAX monitoring site with pibal data for the UCLA monitoring site for September and October 1992 (a) u wind component, (b) v wind component, and (c) virtual temperature 1-10

1-4 Comparison of both edited and unedited RWP data for the Mojave site with radiosonde data for Edwards Air Force Base for 1200 GMT 1-13

1-5a Example plots of the NOAA airflow pattern analysis for 1300 PST for days on which observed ozone concentrations in the SOCAB were low 1-15

1-5b Example plots of the NOAA airflow pattern analysis for 1300 PST for days on which observed ozone concentrations in the SOCAB were high 1-16

1-6a Comparison of RWP/RASS data for the Hesperia monitoring site with radiosonde-derived data for the Edwards Air Force Base monitoring site: Scatter plots comparing RWP and radiosonde derived u and v wind components and wind speed for 0000 and 1200 GMT 1-21

1-6b Frequency distribution plots of the differences between RWP and radiosonde derived u and w wind components for 0000 and 1200 GMT 1-22

1-6c Frequency distribution plots of the differences between RWP and radiosonde derived wind speed and wind direction for 0000 and 1200 GMT 1-23

1-6d Scatter plots comparing RASS and radiosonde derived virtual temperature for 0000 and 1200 GMT 1-24

1-6e Frequency distribution plots of the differences between RASS and radiosonde derived virtual temperature for 0000 and 1200 GMT 1-25

1-7a Comparison of RWP/RASS data for the San Diego monitoring site with radiosonde-derived data for the San Diego monitoring site: Scatter plots comparing RWP and radiosonde derived u and v wind components, and wind speed for 0000 and 1200 GMT 1-29

1-7b. Frequency distribution plots of the differences between RWP and radiosonde derived u and v wind components for 0000 and 1200 GMT 1-30

1-7c Frequency distribution plots of the differences between RWP and radiosonde derived wind speed and wind direction for 0000 and 1200 GMT 1-31

1-7d. Scatter plots comparing RASS and radiosonde derived virtual temperature for 0000 and 1200 GMT 1-32

1-7e. Frequency distribution plots of the differences between RASS and radiosonde derived virtual temperature for 0000 and 1200 GMT 1-33

1-8a Comparison of RWP/RASS data for the Los Angeles International Airport monitoring site with radiosonde-derived data for the UCLA monitoring site: Scatter plots comparing RWP and radiosonde derived u and v wind components and wind speed for1200 GMT 1-37

1-8b Frequency distribution plots of the differences between RWP and radiosonde derived u and v wind components for 1200 GMT 1-38

1-8c. Frequency distribution plots of the differences between RWP and radiosonde derived wind speed and wind direction for 1200 GMT 1-39

1-8d. Scatter plots comparing RASS and radiosonde derived virtual temperature for 1200 GMT 1-40

1-8e. Frequency distribution plots of the differences between RASS and radiosonde derived virtual temperature for 1200 GMT 1-41

1-9 Hourly RASS-derived mixing-height estimates for the Banning Pass monitoring site: 20 June 1992 1-43

1-10a. Comparison of RASS and radiosonde derived virtual temperature for 1 August for HES (0300 PST), and EDWR (0200 PST); comparison of aircraft and radiosonde derived temperature for 1 August for HES (0400 PST) and EDWR (0200 PST) 1-44

1-10b. Comparison of RASS and radiosonde derived virtual temperature for 1 August for HES (1300 PST), and EDWR (1400 PST); comparison of aircraft and radiosonde derived temperature for 1 August for HES (1400 PST) and EDWR (1400 PST) 1-45

1-10c Comparison of RASS and radiosonde derived virtual temperature for 4 August for HES (0300 PST), and EDWR (0200 PST); comparison of aircraft and radiosonde derived temperature for 1 August for HES (0400 PST) and EDWR (0200 PST) 1-46

1-10d Comparison of RASS and radiosonde derived virtual temperature for 4 August for HES (1400 PST), and EDWR (1400 PST); comparison of aircraft and radiosonde derived temperature for 1 August for HES (1400 PST) and EDWR (1400 PST) 1-47

2-1 Air quality monitoring stations used in the data analysis 2-2

2-2a Surface wind sites used in the data analysis 2-4

2-2b Upper-air wind sites used in the data analysis 2-5

2-3 Sample flight path for the SEDAB aircraft flights 2-11

2-4 Vertical profiles of temperature, ozone, NO, and NOx over the Rialto sampling location as measured by the 0413 to 0432 PST aircraft spiral for 27 July 1992 2-12

2-5 Vertical profiles of temperature, ozone, NO, and NOx over the Barstow sampling location as measured by the 0422 to 0439 PST aircraft spiral for 27 July 1992 2-13

2-6 Vertical profiles of temperature, ozone, NO, and NOx over the Rialto sampling location as measured by the 0422 to 0439 PST aircraft spiral for 30 July 1992 2-14

2-7 Vertical profiles of temperature, ozone, NO, and NOx over the Barstow sampling location as measured by the 0510 to 0522 PST aircraft spiral for 30 July 1992 2-15

2-8 Vertical profiles of temperature, ozone, NO, and NOx over the Rialto sampling location as measured by the 0404 to 0418 PST aircraft spiral for 1 August 1992 2-16

2-9 Vertical profiles of temperature, ozone, NO, and NOx over the Barstow sampling location as measured by the 0447 to 0501 PST aircraft spiral for 1 August 1992 2-17

2-10 Vertical profiles of temperature, ozone, NO, and NOx over the Rialto sampling location as measured by the 0408 to 0423 PST aircraft spiral for 9 August 1992 2-18

2-11 Vertical profiles of temperature, ozone, NO, and NOx over the Barstow sampling location as measured by the 0450 to 0502 PST aircraft spiral for 9 August 1992 2-19

2-12 Vertical profiles of temperature, ozone, NO, and NOx over the Rialto sampling location as measured by the 0406 to 0426 PST aircraft spiral for 4 August 1992 2-20

2-13 Vertical profiles of temperature, ozone, NO, and NOx over the Barstow sampling location as measured by the 0502 to 0515 PST aircraft spiral for 4 August 1992 2-23

2-14 Vertical profiles of temperature, ozone, NO, and NOx over the Banning Pass location as measured by the 1711 to 1721 PST aircraft spiral for 4 August 1992 2-24

2-15 Vertical profiles of temperature, ozone, NO, and NOx over the Rialto sampling location as measured by the 0419 to 0438 PST aircraft spiral for 13 August 1992 2-25

2-16 Sampling flight path for the SDAB aircraft flights 2-26

2-17 Vertical profiles of temperature, ozone, NO, and NOx over the Palomar Airport sampling location as measured by the 0940 to 0950 PST aircraft spiral for 2 November 1992 2-27

3-1 Southeast Desert Air Basin classification tree diagram 3-6

3-2 San Diego Air Basin classification tree diagram 3-9

3-3 Surface wind sites used in the data analysis 3-13

3-4 Upper-air wind sites used in the data analysis 3-15

Tables

1-1	Locations of 1992 field study and routine upper-air monitoring sites in Southern California	1-4
1-2	Vertical structure used for validation of the RWP and RASS data	1-6
2-1	Air quality monitoring sites included in the data analysis	2-3
2-2	Frequency of classification combinations	2-4
2-3	Meteorological monitoring sites included in the data analysis	2-6
2-4	Vertical levels used in the preprocessing of wind data	2-7
2-5	Maximum mixing heights for the classification combinations	2-7
3-1	Variables used in the application of CART for the MDAB/SSAB	3-4
3-2	Variables used in the application of CART for the SDAB	3-8
3-3	Surface wind data available for episode days	3-14
3-4	Upper-air wind data availability for episode days	3-16

ABSTRACT

As mandated by the California Clean Air Act of 1988, the California Air Resources Board (ARB) is required to assess the contribution of emissions from upwind air basins to high ozone concentrations in downwind air basins and to develop mitigating emission control strategies that will lead to attainment of the state ozone standard in the affected air basins. In this study, pollutant transport within Southern California, specifically between the South Coast Air Basin (SOCAB) and the Southeast Desert[1] and San Diego Air Basins (SEDAB and SDAB, respectively) is examined using data collected during the 1992 summer field program. These data include Radar Wind Profiler (RWP), Radio Acoustic Sounding System (RASS), and aircraft data. The overall objective of the study was to provide an improved understanding of the three-dimensional meteorological and air quality characteristics of interbasin pollutant transport. The results of this study are summarized in three sections:

Section 1 summarizes the comparison of the RWP and RASS data with routine radiosonde measurements.

Section 2 describes the development of a conceptual model for transport between the SOCAB and the former SEDAB, primarily the Mojave Desert Air Basin (MDAB).

Section 3 contains an analysis of the airflow patterns and calculated trajectories for selected days representing a variety of transport conditions.

The results from each phase of the analysis are summarized in Section 4.

[1] Please note that following the inititation of the study the domain encompassed by the Southeast Desert Air Basin was divided into the South Coast, Mojave Desert, and Salton Sea Air Basins.

EXECUTIVE SUMMARY

The report summarizes methodologies and results of a data analysis study designed to examine pollutant transport within southern California, specifically between the South Coast Air Basin (SoCAB) and (1) the Mojave Desert and Salton Sea Air Basins (MDAB/SSAB) (formerly the Southeast Desert Air Basin, SEDAB) and (2) the San Diego Air Basin (SDAB). Transport conditions were examined using data collected during the 1992 summer field program. These data include Radar Wind Profiler (RWP), Radio Acoustic Sounding System (RASS), and aircraft data. The overall objective of the study was to provide an improved understanding of the three-dimensional meteorological and air quality characteristics of interbasin pollutant transport. The study was comprised of three major components: (1) comparison of the RWP and RASS data with routine radiosonde measurements, (2) development of a conceptual model for transport between the SoCAB and the former SEDAB, and (3) analysis of the airflow patterns and calculated trajectories for selected days representing a variety of transport conditions.

The results of the comparison of the upper-air wind and temperature data indicate that significant differences between measurements obtained using radiosondes and those obtained using RWP and RASS technologies exist. Certainly some differences are expected, given the differences in data collection methodologies and their respective error characteristics. Contamination of the RWP data by migrating birds and the subsequent application of newly developed editing routines may have contributed to the wind component differences. In addition, none of the radiosonde and RWP/RASS sites for which data were compared were collocated. The complex geography of southern California and the corresponding spatial variability in meteorological characteristics introduced by the complex terrain and the land/sea breeze circulation limited the extent to which data from non-collocated sites could be reasonably compared. A more comprehensive, site-specific examination of the agreement between RWP/RASS and radiosonde data that considers instrument calibration, siting, and the use of the moment data in addition to the hourly averages should accompany further monitoring studies of this area.

The results of the data evaluation component of this study further indicate that the use of data from relatively new types of measurement platforms, such as the RWP and RASS instruments, for analysis and modeling purposes, requires a careful review and assessment of data quality and applicability.

In the second phase of the study, each day of the 1992 analysis period was identified as belonging to one of nine categories of combinations of high, moderate, or low ozone concentrations in the SoCAB and MDAB/SSAB (formerly SEDAB) (for example, high ozone concentrations in the SoCAB and moderate ozone in the MDAB/SSAB, or high ozone in the SoCAB and high ozone in the MDAB/SSAB). Analysis of composite surface and upper-level winds and maximum mixing heights for the nine different ozone classification couples indicates numerous similarities in the airflow patterns for all days of the 1992 study period but also some

differences in both the winds and the mixing heights that enable one to distinguish among the categories.

The results of this analysis suggest that there is a strong correlation between high ozone concentrations in the SoCAB and high concentrations in the MDAB and SSAB. During the 1992 study period, moderate to high observed ozone concentrations in the former SEDAB were almost always associated with moderate to high ozone concentrations in the SoCAB. There were no days when high ozone was observed in the former SEDAB and concentrations within the SoCAB were low. The composite winds also indicate that transport of pollutants from the SoCAB to the MDAB/SSAB (previously SEDAB) contributed to the high observed concentrations in the air basin formerly designated the SEDAB; the composite winds (and limited aircraft data) suggest the possibility of pollutant transport both near the surface and aloft.

In the third and final phase of the study, the CART analysis technique was used to categorize the ozone episode days (with respect to meteorological and air quality conditions) and representative episodes from the major classification categories were selected for further analysis. The ozone episode days were then classified as "local" or "shared" events; the "shared" events were further categorized as "overwhelming", "significant", or "inconsequential" transport days. Based on the results of the CART analyses, six episodes were selected for further analysis. Of these, two episode days indicated the possibility of transport into the MDAB or SSAB (formerly SEDAB) from the SoCAB, one indicated the possibility of local causes within the former SEDAB and remaining three episodes indicated the possibility of transport into the SDAB from the SoCAB.

Analyses of the transport characteristics of these episode days were carried out through trajectory analysis. Two- and three-dimensional particle paths were calculated using gridded wind fields, and the potential for interbasin transport for the selected days, as well as for meteorologically similar days, was examined.

The results of two- and three-dimensional particle path analyses for the MDAB/SSAB (formerly SEDAB) indicate that although local causes for one of the days was indicated by CART, all three episode days appear to be shared events. These and meteorologically similar days (according to the CART analysis) comprise more than 80 percent of the exceedance days included in this analysis. Thus most ozone episodes that occurred within the SEDAB during the summer of 1992 can be characterized as shared. The influence of transport was further classified as "significant."

The results of two- and three-dimensional particle path analyses for the SDAB indicate that all three episode days appear to be shared events. Trajectories from both the SCCAB and SoCAB, as well as from points to the south of the SDAB, indicate the possibility of transport of ozone and precursor into the SDAB; meandering trajectories remaining over the SDAB indicate local influences. These and meteorologically similar days (according to the CART analysis) comprise 90 percent of the exceedance days included in this analysis. Thus most ozone episodes that occurred within the SDAB during the summer of 1992 can be characterized as shared. The influence of transport was further classified as "significant" with a note that with slightly different criteria a designation of "inconsequential" would have been obtained.

1 DATA EVALUATION

As mandated by the California Clean Air Act of 1988, the California Air Resources Board (ARB) is required to assess the contribution of emissions from upwind air basins to high ozone concentrations in downwind air basins and to develop mitigating emission control strategies that will lead to attainment of the state ozone standard in the affected air basins. In a previous study (ARB, 1990), the ARB concluded that transport of ozone and precursor emissions from the South Coast Air Basin (SoCAB) contributes to ozone concentrations in excess of the state standard (9 pphm) in both the Southeast Desert and San Diego air basins (SEDAB and SDAB)[1]. This conclusion was based on analyses of routine surface meteorological and air quality data for selected episode days. In this study, the transport issue is further examined using supplementary data (including Radar Wind Profiler (RWP), Radio Acoustic Sounding System (RASS), and aircraft data) collected during the 1992 summer field program to improve understanding of the three-dimensional meteorological and air quality characteristics associated with interbasin transport of pollutants.

The advent of the RWP and RASS measurement techniques has provided meteorological and air quality analysis and modeling researchers the opportunity to evaluate and potentially to improve existing conceptual and simulation models pertaining to the characteristics and properties of the lower atmosphere, as well as the recirculation and transport of pollutants, both within and above the boundary layer. Data obtained using these measurements techniques are essentially continuous in time and well distributed aloft (such that the mesoscale vertical structure of the atmosphere is accurately resolved). As with all measurement platforms, however, the monitoring network configuration (the spatial distribution of monitoring sites) relative to complex terrain and other geographical features will determine the utility of the data for analysis and for modeling purposes.

The RWP/RASS network for the 1992 summer field program was designed to enable, using existing analysis and modeling techniques, the assessment of interbasin pollutant transport. The instruments were sited such that the airflow and thermal features that are thought to contribute to or be associated with transport between the SoCAB and the MDAB/SSAB (previously SEDAB), such as airflow through the mountain passes, could be observed and quantified.

The data were also collected to provide a more comprehensive database (compared to those incorporating only routine measurements) for the application and evaluation of meteorological and air quality modeling tools. Current state-of-the-science meteorological

[1] Please note that following initiation of this study, the domain encompassed by the SEDAB was divided into the SOCAB and the Mojave Desert and Salton Sea Air Basins, MDAB and SSAB, respectively. To the extent possible, the new designations have been incorporated into this report.

models, such as the Pennsylvania State University/National Center for Atmospheric Research (PSU/NCAR) Mesoscale Model, Version 5 (MM5) support the four-dimensional assimilation of observational data. By incorporating the data into the model simulation, this technique ensures that the observed, day-specific meteorological features are represented. This is an especially important consideration if the output from the meteorological model is used as input to an air quality simulation model.

Aircraft data collected during the field study provided information regarding pollutant concentrations aloft that can be used in the development/refinement of a conceptual model for pollutant recirculation and transport and in the evaluation of air quality modeling results.

The specific objectives of this data analysis study are (1) to validate the 1992 RWP and RASS data against conventional radiosonde data, (2) to use these data in conjunction with the surface and upper-air (aircraft) air quality data to develop a conceptual model of the three-dimensional recirculation and/or pollutant transport between the SoCAB and the MDAB/SSAB (previously SEDAB), and (3) to classify all days for which the state standard was exceeded during the summer of 1992 in the downwind air basins, the MDAB/SSAB (previously SEDAB) and the SDAB, according to transport potential.

The validation of the RWP and RASS data through comparison with conventional radiosonde data may be limited by differences in the location and design of the measurement platforms. Specifically, differences in locations of the monitoring sites for which data are being compared and differences in data acquisition and averaging procedures may contribute to apparent differences between RWP/RASS and radiosonde data.

The data acquired for this study have already been subjected to certain quality assurance procedures by the National Oceanic and Atmospheric Administration (NOAA, 1994). This review has indicated that the data may have been contaminated by interference caused by migrating birds during the nighttime hours, especially during the spring/early summer and late summer/early autumn periods. Editing routines developed by NOAA were used to removed the contaminated data from the data set, and this has resulted in some missing data for the nighttime hours. The field study data were validated using (1) scatter plots illustrating the correlation between the RWP/RASS data and the radiosonde data and (2) histograms illustrating the frequency of differences between the two measurement systems. Differences between the high- and low-resolution data and the edited and unedited data were also examined.

Preliminary analysis of the data collected during the 1992 field study (NOAA, 1994) has also indicated that the amount of transport, and thus potential for transported pollutants to influence ozone concentrations in the MDAB/SSAB (previously SEDAB), appears to be related to the depth of the mixed layer. The NOAA researchers used radar reflectivity measurements from the RWP instruments to estimate mixing heights at the profiler sites during the study period. The mixing-height estimates derived from the RWP reflectivity data were also compared with the radiosonde inversion heights for 1600 PST.

This section of the report describes results of the data validation and the conceptual model development tasks. Results of the transport assessment for the downwind air basins are presented in Sections 2 and 3.

EVALUATION OF THE RWP AND RASS DATA

Upper-air data were collected during the 1992 summer field study using Radar Wind Profiler (RWP) and Radio Acoustic Sounding System (RASS) instrumentation. Before using these data in the analysis of ozone and precursor pollutant transport in southern California, they were validated against more conventional and routinely available data from radiosonde monitoring sites for the area of interest. The RWP and RASS data were provided by the ARB and included data for 13 monitoring sites located in the SoCAB, MDAB/SSAB (previously SEDAB), and SDAB. Radiosonde data were obtained from the Western Regional Climate Center (WRCC) and included data from the National Weather Service (NWS), the South Coast Air Quality Management District (SCAQMD), and two military installations. Locations of all the monitoring sites are listed in Table 1-1 and plotted in Figure 1-1.

To facilitate the comparison of the RWP and RASS data with the radiosonde data, the wind and virtual temperature data were vertically interpolated to 18 vertical levels (Table 1-2). Scatter plots illustrating the correlation between the RWP/RASS and the radiosonde data were prepared for u and v wind components, wind speed, and virtual temperature for two times (0000 and 1200 GMT) and four levels (100, 300, 1000, 2000 meters above ground level, or m agl). The comparison was limited to two times per day, 0400 and 1600 PST, which correspond to the times for which the NWS routinely collects upper-air data. However, because measurement times for the two military locations were highly variable, data for these monitoring sites were included in the comparison if the measurement time occurred within 2 hours of the selected comparison time (no temporal interpolation was performed). Each RWP and RASS monitoring site was paired with a collocated or nearby radiosonde monitoring site, and scatter plots were prepared illustrating the correlation between the data collected from the two different measurement systems. For those RWP/RASS and radiosonde pairs that are not geographically collocated, some differences between the data from the two types of monitoring sites are expected. This is especially true at low levels, where the influence of terrain is most pronounced.

Radiosondes are sounding balloons that are equipped with meteorological sensors and transmitters that radio measured values of temperature, pressure, and humidity to a ground-based receiver. The receiver can also determine the balloon elevation angle and azimuth. Elevation is inferred from pressure. The movement of the balloon is used to determine the upper-level winds. With the exception of the wind data, the data represent point measurements of the various parameters. Winds are typically averaged over layers that are 45 to 75 meters deep, thus gradients tend to be smoothed. Data are reported for preassigned (mandatory) pressure levels which include the 1000, 900, 850, 700, and 500 millibar pressure levels as well as for significant pressure levels which are determined according to the observed temperature and moisture gradients.

Radiosondes represent the most commonly used instrument for the routine collection of upper-air meteorological data. Standardized data collection and quality assurance procedures enhance the consistency and the utility of the measurements.

TABLE 1-1. Locations of 1992 field study and routine upper-air monitoring sites in Southern California.

Site Name	Site ID	Source	UTM-Easting (km)	UTM-Northing (km)
1992 Field Study Monitoring Sites				
San Clemente Island	SCI[b]	NOAA/ERL	351.5	3654.4
Point Loma	PTL[b]	NOAA/ERL	476.6	3617.9
El Cajon	ELC[a,b]	NOAA/ERL	501.9	3630.0
San Diego	SDO[a]	NOAA/ERL	485.1	3647.8
Los Angeles International Airport	LAX[b]	NOAA/ERL	366.9	3756.2
Point Mugu	PTM[b]	NOAA/ERL	304.4	3775.1
Palmdale	PAL[a]	NOAA/ERL	404.6	3827.9
Mojave	MOJ[a]	NOAA/ERL	395.1	3880.1
Barstow	BAR[a]	NOAA/ERL	489.0	3855.1
Hesperia	HES[a,b]	NOAA/ERL	462.3	3804.2
San Bernardino	SBO[b]	NOAA/ERL	464.1	3781.0
Banning	BAN[a]	NOAA/ERL	509.2	3752.0
Whitewater	WWR[a]	NOAA/ERL	529.6	3750.9
Routine Monitoring Sites				
San Diego	MYFR	WRCC	486.9	3628.9
Univ. California, Los Angeles	UCLR	SCAQMD	369.0	3760.0
Pt. Mugu Naval Air	NTDR	WRCC	304.8	3776.9
Edwards Air Force Base	EDWR	WRCC	419.6	3862.1

[a] C_n^2-derived mixing heights.
[b] Site equipped with RASS instrumentation.

A Radar Wind Profiler (RWP) is a vertically pointing Doppler radar capable of measuring horizontal and vertical wind components. Pulsed energy from a transmitter is reflected backward by discontinuities in the atmosphere. This reflected signal is then used to infer the three-dimensional structure of the velocity fields. The temporal resolution of the data can be as frequent as every six minutes; hourly averaged values are then computed. The vertical resolution is related to the operating parameters (for example, pulse length and peak power) and higher-resolution "low" and lower-resolution "high" modes are available. For the 1992 Southern California summer field program, these corresponded to approximately 100 and 400 m intervals between data values. The vertical extent of the RWP measurements reached approximately 2000 meters for the low mode and 4000 meters for the high mode.

A Radio-Acoustic Sounding System (RASS) is a method of remotely measuring atmospheric temperature profiles by combining acoustic and radar techniques. Specifically, RASS measures the vertical profile of the speed of sound using Doppler radar to observe the propagation of an acoustic wave. This can be related (to a very good approximation) to

virtual temperature. The achievable temporal and vertical resolution of the RASS measurements is similar to that for a wind profiler. The vertical extent of RASS, however, is limited to the lower troposphere.

Additional discussion of the RWP and RASS technologies is provided by STI (1996).

In order to validate the RASS virtual temperature data collected during the 1992 field study, the radiosonde temperature and moisture data were converted to virtual temperature. Virtual temperature T_v is defined as the temperature of dry air having the same values of pressure and specific volume as the moist air considered. It is defined as $T_v = (1 + 0.61q)T$, where q is specific humidity and T is air temperature in kelvins. As for the wind data, the temperature data were vertically interpolated to the levels listed in Table 1-2. Scatter plots comparing the RASS and radiosonde-derived virtual temperature data for 0400 and 1600 PST were prepared for seven site pairs.

The plots presented in this section include (1) scatter plots, illustrating the correlation between the RWP or RASS and radiosonde derived values of the wind, temperature, and mixing height, and (2) frequency distribution plots indicating the frequency of occurrence of calculated differences between the RWP or RASS and radiosonde derived values (in the frequency distribution plots for wind direction the non-shaded area corresponds to those data points with wind speeds less than 2 ms^{-1}). Note that the RWP data used for this comparison represent hourly averaged data; each average comprises some variable number of measurements. Thus, some disagreement between the RWP and radiosonde data may be acceptable, especially if the radiosonde data are within the range of the minimum and maximum RWP values. To illustrate this point, example comparisons of the minimum, maximum, and average RWP values with radiosonde data, using data collected as part of the 1993 Claremont Study, are provided in Figure 1-2.

Previous studies have compared RWP/RASS and radiosonde measurements. NOAA (1994) performed some comparisons using data from the 1991 Northern California Transport Study and found qualitatively good agreement between RWP and radiosonde-derived wind components for most of the eight monitoring sites. In this case, the RWP and radiosonde monitoring sites were collocated and the radiosonde data were obtained at three hourly intervals.

Durkee and Cassmassi (1991) also compared RWP/RASS data with airsonde data for the South Coast Air Basin, specifically the LAX-UCLA site pair. Their findings suggest that the RASS and airsonde data depicted the vertical structure of virtual temperature similarly but that the RWP winds were unreliable (especially during the nighttime and early morning hours) due to possible interference. The authors concluded that this, coupled with the physical distance between the two sites, differences in monitoring methods, and the limited number of airsonde-derived observations, resulted in some large differences between the RWP and airsonde wind data. Examples of their results are provided in Figure 1-3. These

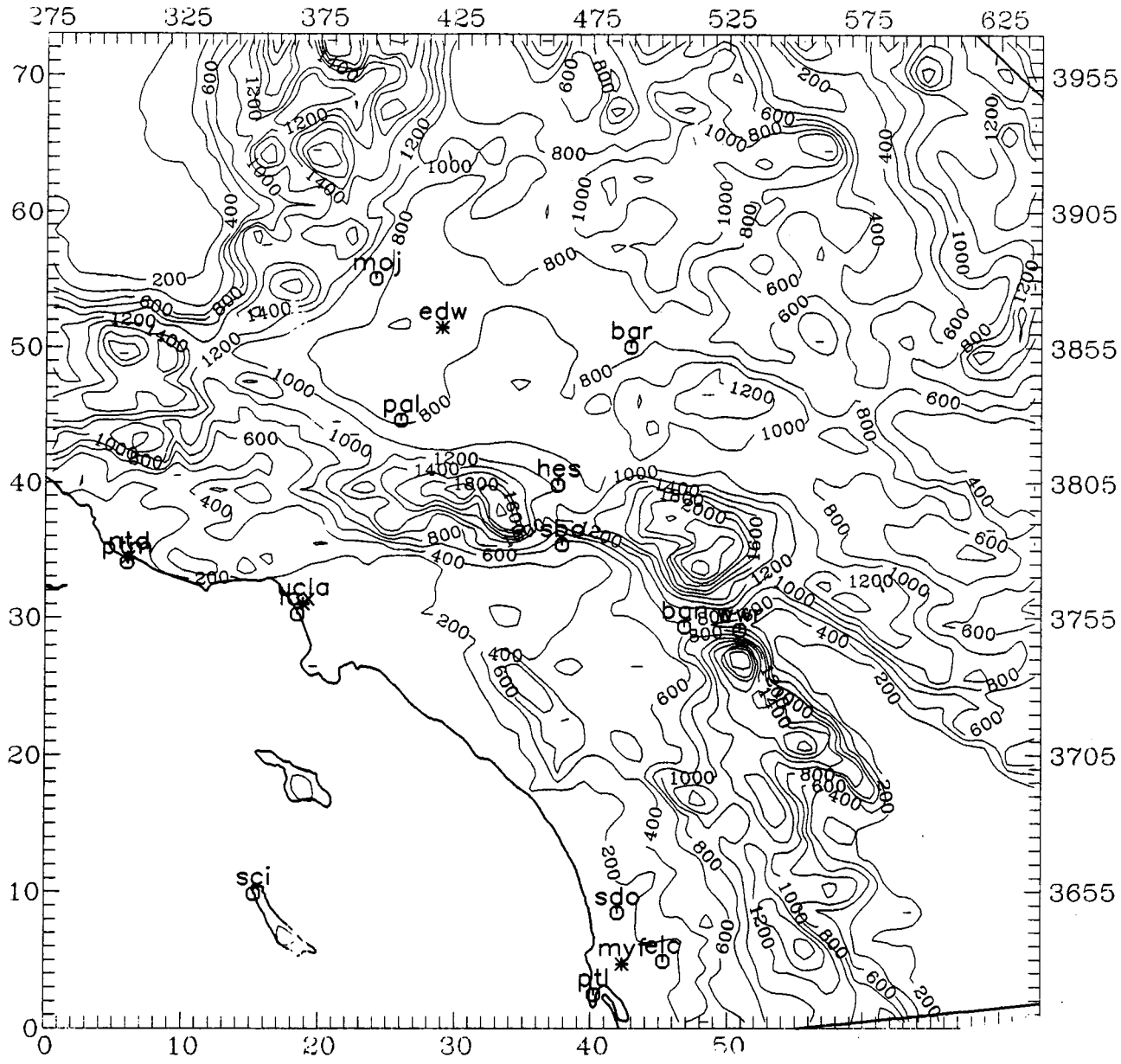

FIGURE 1-1. Locations of routine and 1992 Southern California field study upper-air monitoring sites. The symbol "*" denotes a routine site.

TABLE 1-2. Vertical structure used for validation of the RWP and RASS data.

Level	Height (m agl)	Level	Height (m agl)
1	10	10	800
2	50	11	1000
3	100	12	1200
4	200	13	1500
5	300	14	2000
6	400	15	2600
7	500	16	3200
8	600	17	4000
9	700	18	5000

1993 Claremont Study
September 6 - 15:20 to 16:40 PM Local Time-North-South Portion of Wind Vector (N+)
Quality Assurance Comparison of 10 min Avg RWP (h-highest;l-lowest;avg-average) & RawinSonde Data

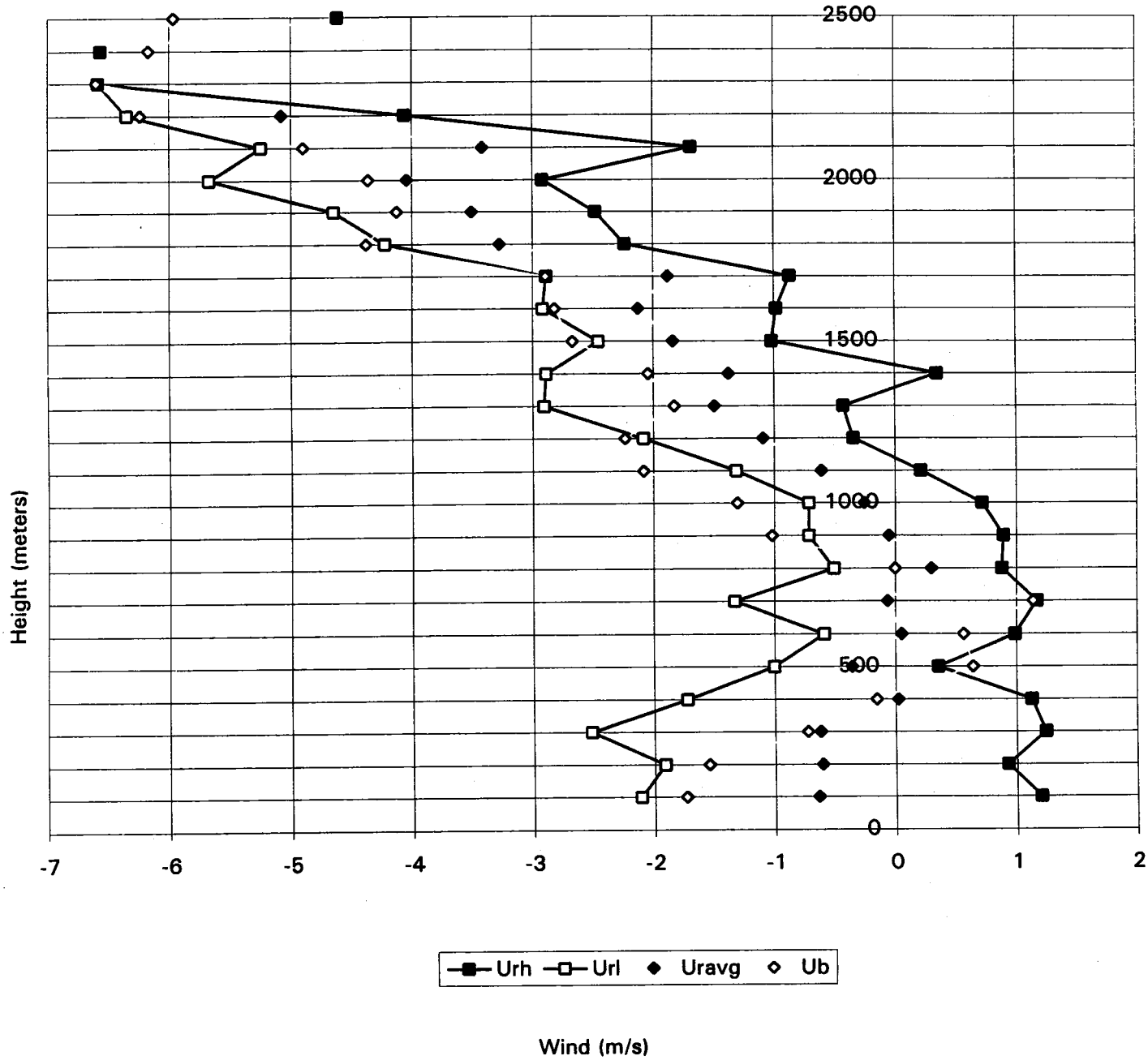

FIGURE 1-2a. Comparison of the minimum, maximum, and average RWP values with radiosonde data for the north-south component of the wind for the period 1520 to 1640 local time, 6 September, using data collected as part of the 1993 Claremont Study. In the figure Urh is the highest value of the north-south wind component used in the average for each level, Url is the lowest value, Uavg is the average value, and Ub is the radiosonde-derived value.

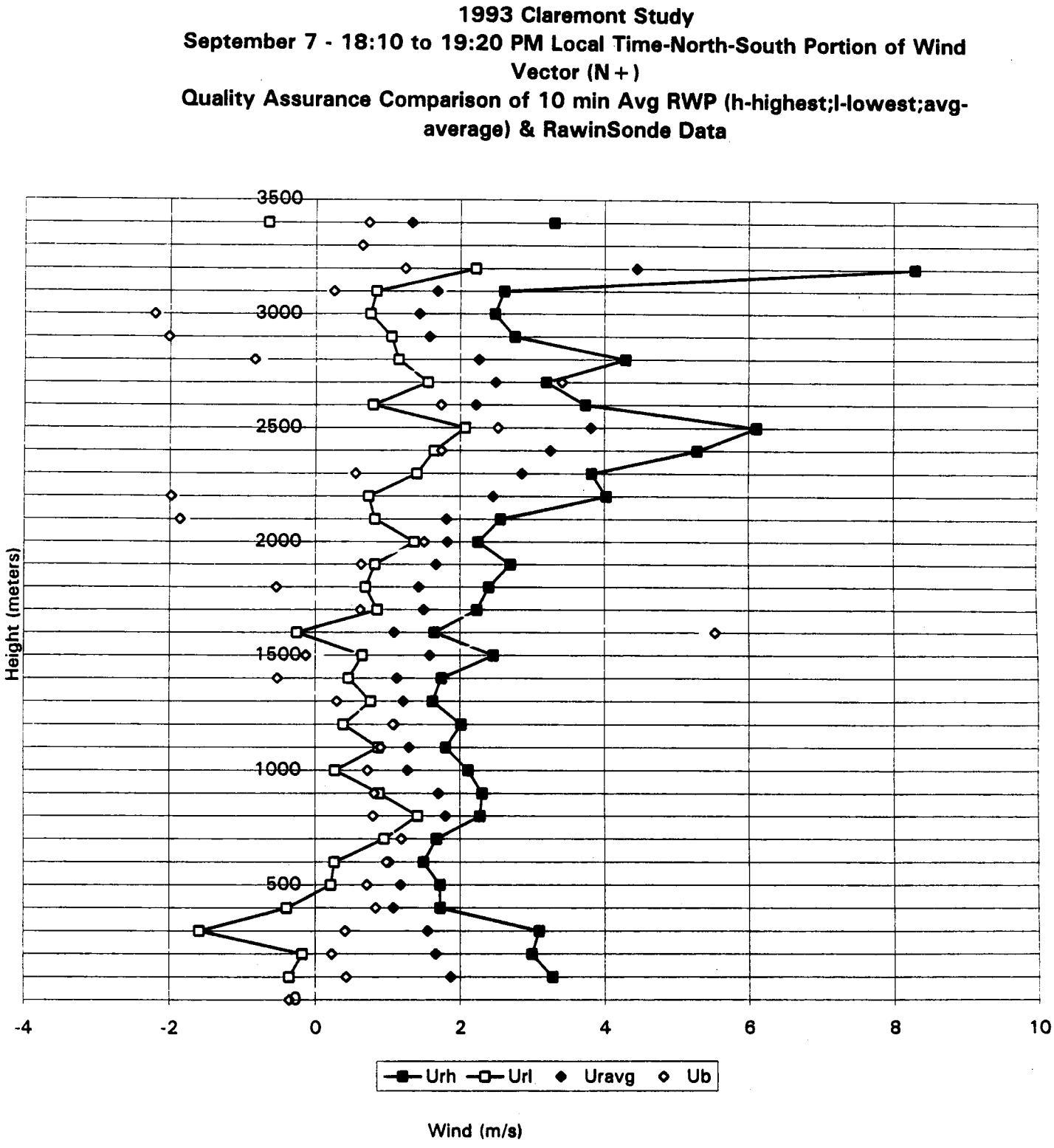

FIGURE 1-2b. Same as Figure 2-2a, but for the period 1810 to 1920 local time, 7 September.

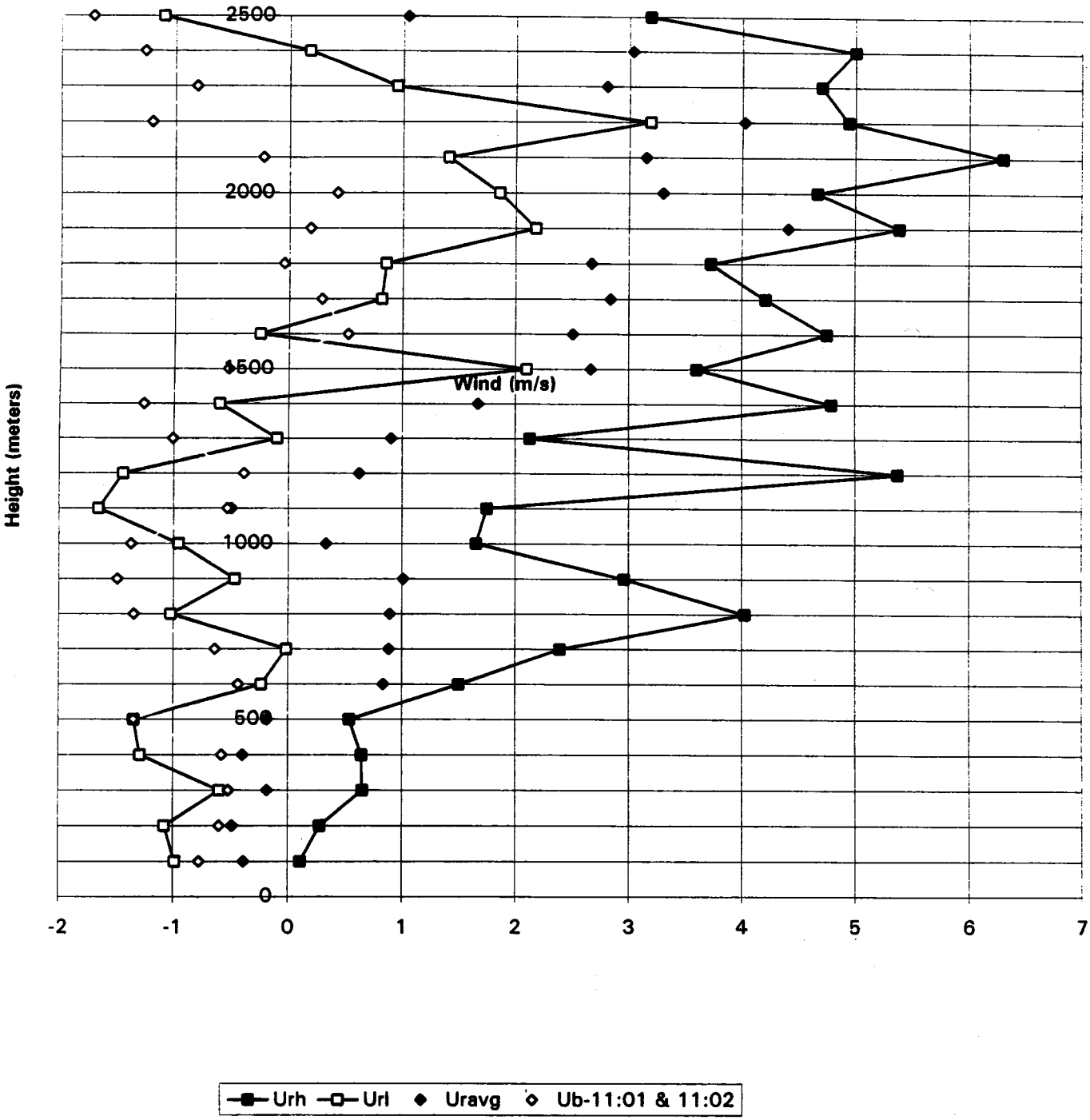

FIGURE 1-2c. Same as Figure 1-2a, but for the period 1030 to 1130 local time, 10 September.

(a)

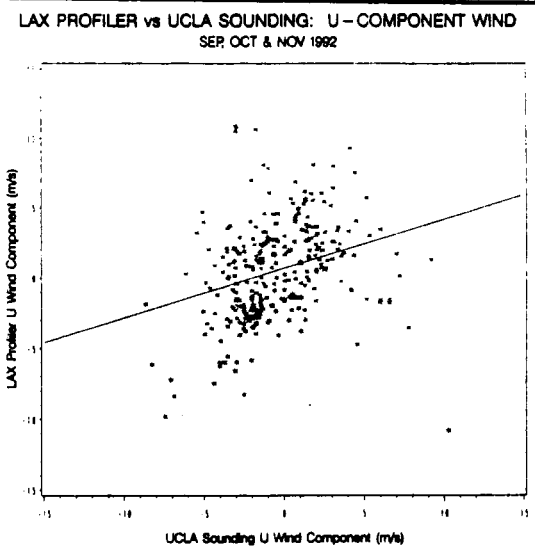

(b)

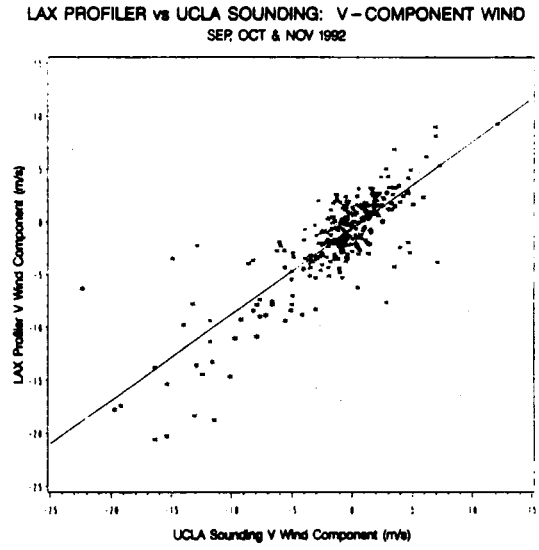

(c)

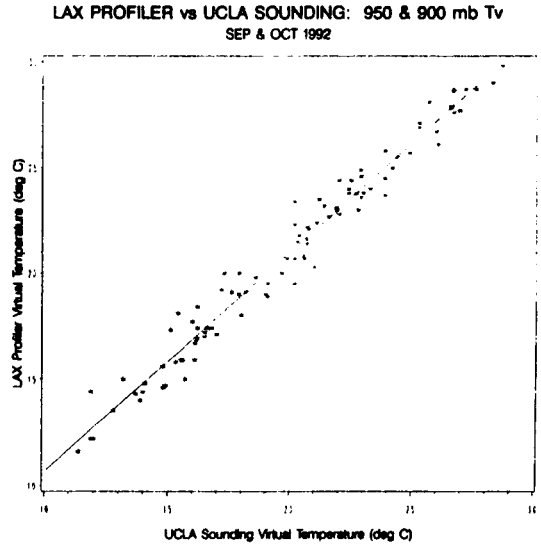

FIGURE 1-3. Comparison of RWP/RASS data for the LAX monitoring site with pibal data for the UCLA monitoring site for September and October 1992 (a) u wind component, (b) v wind component, and (c) virtual temperature. The diagonal line represents the least squares fit to the data. (Source: Durkee and Cassmassi, 1991)

illustrate good agreement between the RASS and airsonde data and larger differences between the RWP and airsonde derived measurements.

Even when collocated, RASS/RWP and radiosonde measurements can differ by as much as 1°C and 20 degrees, respectively. This is attributable to differences in the sampling techniques with respect to both the measured quantities and instrument accuracy (Golden et al., 1986). For temperature, radiosondes typically utilize thermistors which measure temperature to within 0.5°C. RASS-derived virtual temperatures are calculated from measurements of the speed of sound; their accuracy is less well known but is also expected to be within approximately 0.5°C. Note that for direct comparison of these measurements, conversion of temperature to virtual temperature or the reverse is required. This conversion may enhance the differences. Radiosonde-derived wind measurements are based on the movement of the balloon and typically represent a depth of 45 to 75 meters, thus vertical gradients in the wind fields tend to be smoothed. Errors are also introduced into the measurements through the calculation of balloon height (conversion of pressure to altitude). RWP measurements are derived from backscattered energy from a Doppler radar. Each pulse samples all levels of the atmosphere (Golden et al., 1986) and, thus, these data are essentially point measurements. The accuracy of the RWP instrument is limited by electrical and convective interference, false targets, and weak returns under conditions of laminar flow. Given these differences and limitations, wind directions differences of 20 degrees or more between collocated RWP and radiosonde instruments ~~is~~ are not unexpected.

This report presents the results of a comparison study using RWP and RASS data collected during the 1992 summer field study. The RWP/RASS monitoring sites are paired with existing radiosonde sites; in only a few of the cases are the site pairs collocated or nearby. Thus, both data quality as well as representativeness are combined in this assessment. A more comprehensive, site-specific examination of the agreement between RWP/RASS and radiosonde data that considers instrument calibration, siting, and the use of the moment data in addition to the hourly averages should accompany further monitoring studies of this area.

Overview of the 1992 NOAA RWP/RASS Monitoring Network for Southern California

The monitoring network for the 1992 summer field study consisted of thirteen monitoring sites that were equipped with RWP instrumentation, seven of these sites were also equipped with RASS. The sites are listed and delineated with respect to type of equipment in Table 1-1. As noted earlier in this section, the site locations are plotted in Figure 1-1. Most of the monitoring sites were operational for less than the entire field study period, as indicated in the operational summaries provided by NOAA (1994). This was due to occasional radar downtime (resulting from equipment failures) as well as the redistribution of equipment during the course of the summer. In particular, the focus shifted from the MDAB/SSAB (previously SEDAB) air basins during May through August to the SDAB during August through October.

The study was designed as a test of a RWP/RASS network for Southern California. The equipment used for the study, although state-of-the art in 1992, has since been significantly improved. More importantly, the procedures and algorithms associated with data collection, processing, quality control, and calculation of parameters such as mixing heights have also been more thoroughly tested and subsequently improved.

All RWP/RASS networks have inherent limitations pertaining to electrical and electronic interference, false targets, weak returns under conditions of laminar flow, and the presence of clouds. Numerous problems were manifested during the 1992 Southern California study. Of greatest concern, was the contamination of the RWP data by migratory birds. Editing routines were developed and applied to remove the contaminated data (the data were postprocessed using the Weber-Würtz algorithm). Figure 1-4 illustrates the comparison of both edited and unedited RWP data for the Mojave site (MOJ and MOJR, respectively) with radiosonde data for Edwards Air Force Base (EDWR) for 1200 GMT. The agreement is clearly much better for the edited data. Nevertheless, data completeness (and potentially data accuracy) may have been affected by the editing procedures.

As noted earlier, the following comparison of RWP/RASS and radiosonde data is limited by the fact that the monitoring sites were not collocated. Lack of higher resolution moment data (detailing the distribution of values that comprise the hourly averages) also limited the comparison to the extent that this information would represent a more appropriate comparison with the radiosonde data (which are not hourly averages but essentially point measurements).

Summary of Findings from the 1992 Southern California Transport Study

Additional analysis of these data was performed by NOAA (1994). The findings of this analysis included: (1) wind directions indicating transport from the SoCAB to the MDAB/SSAB (previously SEDAB) occur frequently during the summer and early autumn months, (2) synoptic weather patterns do not significantly influence the observed airflow patterns but do influence the mixing heights, and (3) the depth of the mixed layer can influence the amount of pollutant transport between the SoCAB and the MDAB/SSAB (previously SEDAB). Example plots from the airflow pattern analysis are provided in Figure 1-5 for 1300 PST (2100 GMT) for days on which observed ozone concentrations in the SoCAB (at the San Bernardino monitoring site) were low (Figure 1-5a) and high (Figure 1-5b). These plots illustrate the average surface and upper-air airflow patterns that were associated with the different concentration regimes during the 1992 study period as well as the potential for both ozone precursor (under low ozone conditions in San Bernardino) and ozone (under high ozone conditions in San Bernardino) transport. A similar analysis was not performed for the SoCAB/SDAB transport couple.

Mojave Desert/Salton Sea (Previously Southeast Desert) Air Basin Monitoring Sites

Data for six RWP sites located within the MDAB/SSAB (previously SEDAB) were compared with the Edwards Air Force Base (EDWR) radiosonde data. Scatter plots illustrating the correlation between the data from the EDWR radiosonde and the data from each of the six RWP monitoring sites, including Mojave (MOJ), Palmdale (PAL), Barstow (BAR), Hesperia (HES), Banning (BAN), and Whitewater (WWR), and frequency distribution plots of the differences are presented in Appendix A1. In general, the correlation between the radiosonde and the

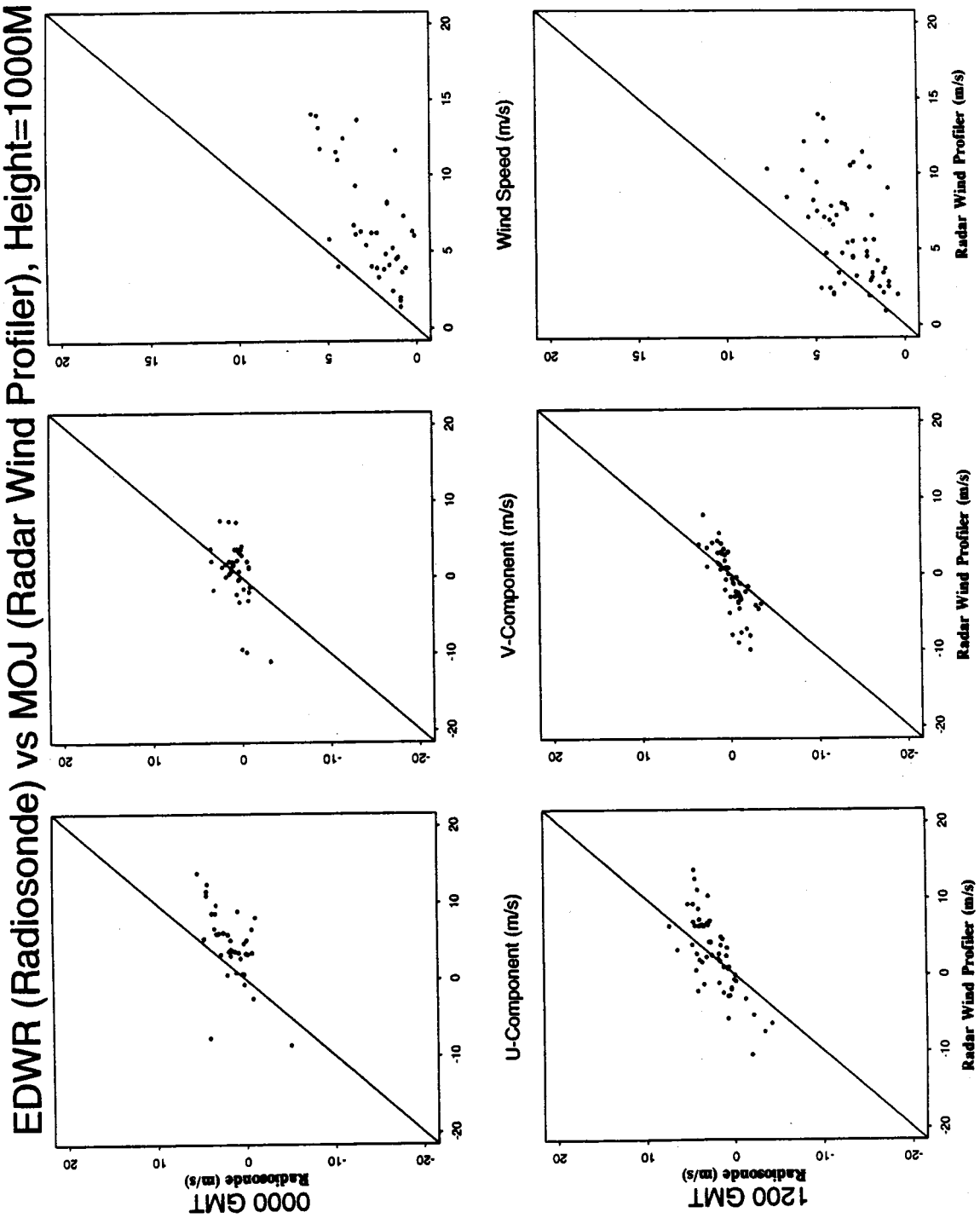

FIGURE 1-4. Comparison of both edited and unedited RWP data for the Mojave site (MOJ and MOJR, respectively) with radiosonde data for Edwards Air Force Base (EDWR) for 1200 GMT.

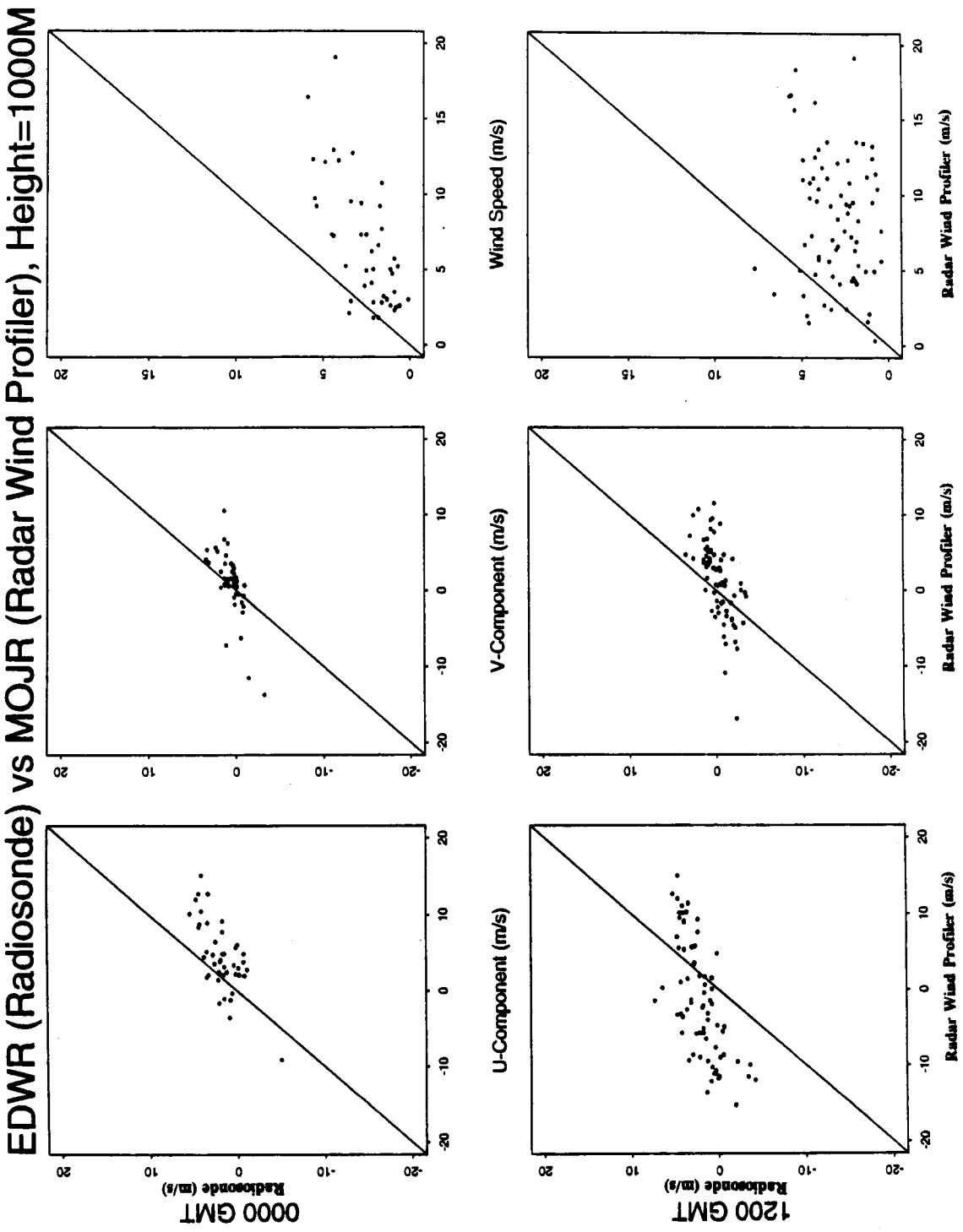

FIGURE 1-4. Concluded.

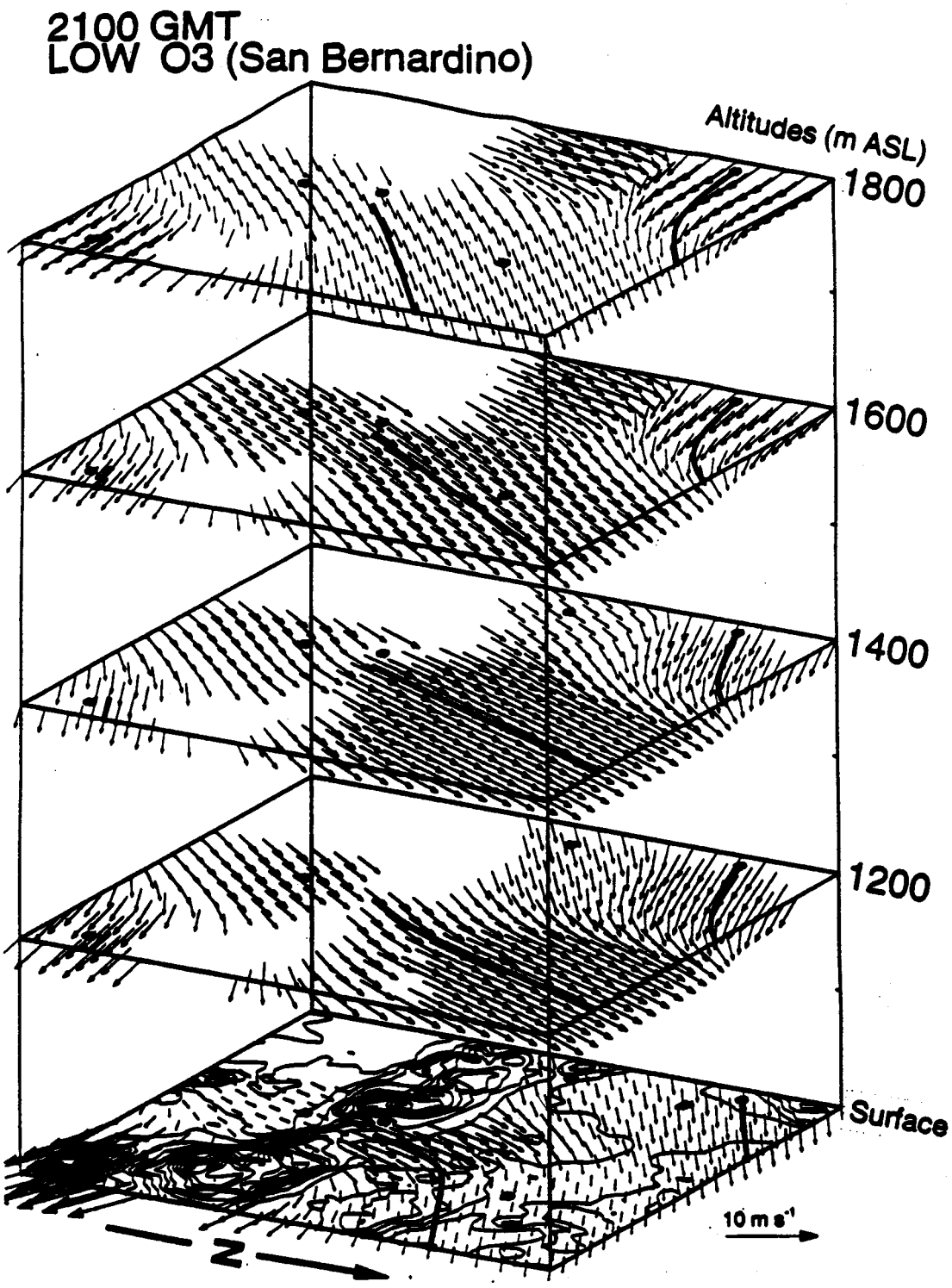

FIGURE 1-5a. Example plots of the NOAA airflow pattern analysis for 1300 PST (2100 GMT) for days on which observed ozone concentrations in the SOCAB (at the San Bernardino monitoring site) were low. (Source: NOAA, 1994)

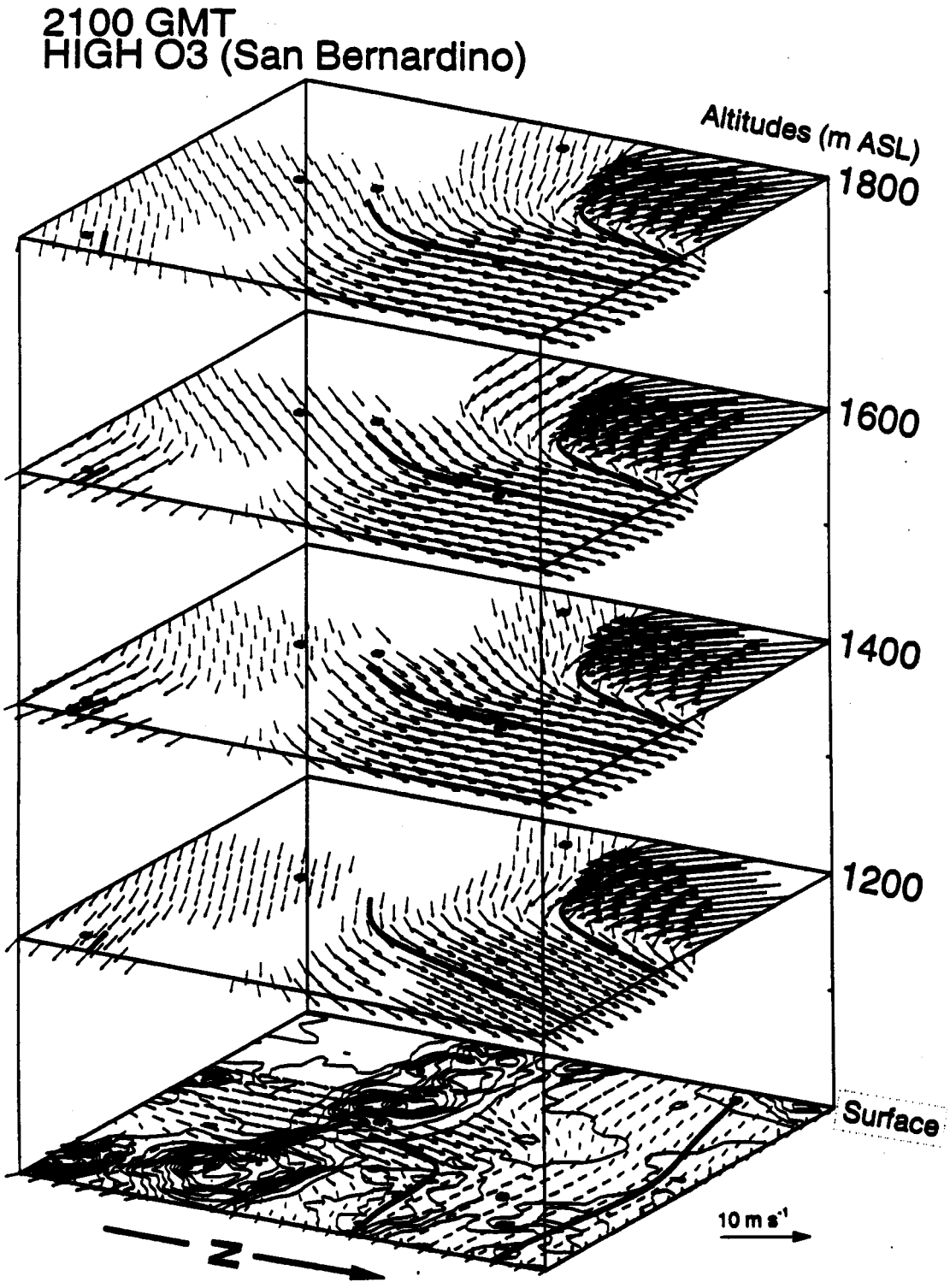

FIGURE 1-5b. Example plots of the NOAA airflow pattern analysis for 1300 PST (2100 GMT) for days on which observed ozone concentrations in the SOCAB were high. (Source: NOAA, 1994)

profiler data depends to some extent on the locations of these sites with respect to each other. Locations of the six profiler sites and the radiosonde site at Edwards are shown in Figure 1-1. This plot illustrates that the EDWR radiosonde site and the MOJ and PAL profiler sites are located north of the San Gabriel Mountains in the western part of the Antelope Valley, while the BAR and the HES profiler sites are located in the eastern part of the valley. The BAN and WWR profiler sites are located in the Banning Pass to the south of the San Bernardino Mountains. Thus, while comparison of the EDWR site with the other profiler sites located in the Antelope Valley is in principle appropriate, comparison of the BAN and WWR data with the EDWR data (due to the distances between the sites and the potential complicating effects of terrain) is perhaps not.

Wind Data

EDWR–MOJ

The EDWR–MOJ scatter plots suggest better correlation between the RWP and the radiosonde data for 1000 and 2000 m agl than for 300 m agl (no data were available for 100 m agl for this site). At 300 m agl, the RWP u and v component data as well as the wind speed data have a broader range of values than the radiosonde data. At this level, for example, the RWP u-components range from approximately -8 to 14 ms^{-1}, whereas the radiosonde data range from -2 to 4 ms^{-1}. Frequency distribution plots of difference in u and v components between these two sites also show that for 300 m agl, a majority of the differences are often more than 5 ms^{-1} while for 1000 and 2000 m agl differences are mostly less than 5 ms^{-1}. Overestimation of wind speed by the RWP data is suggested for all three levels, though it is most pronounced at 300 m agl; for this level differences in wind direction are also frequently more than 30 degrees. Note also that the overestimation of wind speeds for this level appears to be due to overestimation of the u-components. Better correlation in the morning (1200 GMT) than in the afternoon (0000 GMT) is also suggested by the scatter plots. Note that these two sites are 30 km apart. In addition, this type of pairwise comparison of RWP and radiosonde data ignores the differences in the statistical nature of the two data sources and may, therefore, account for some of the differences. Hourly RWP data represent population averages and comparison with radiosonde data should attempt to accommodate this fact. For example, through the use of the individual measurements, the 1993 Claremont study, as illustrated in Figure 1-2, provides a more complete comparison.

EDWR–BAR

These scatter plots comparing data for the EDWR and BAR monitoring sites indicate some correlation between the u- and v-component data but systematically higher wind speeds from the radar profilers. The frequency distribution plots for this pair indicate smaller differences for 1200 GMT than for 0000 GMT. Note that these two sites are located approximately 70 km apart.

EDWR–PAL

Again, the RWP wind speeds are generally higher than the radiosonde wind speeds. While the scatter plots suggest little variation with height in the correlation between wind speeds and wind components, the frequency distribution plots show that a large proportion of the wind direction differences occur in the 60–90 degree range for the 300 m agl level. These two sites are located approximately 38 km apart. Note that insufficient data were available for the PAL site at 1200 GMT to perform this comparison.

EDWR–HES

For the HES monitoring site, the correlation with the radiosonde wind speeds is better than for any of the previous sites, though the tendency for the radar wind profiler to exhibit higher wind speeds than the radiosonde is also evident here, particularly for the 2000 m agl level. The scatter plots suggests that the RWP v-components are consistently more variable (exhibit a wider range of values) than the radiosonde v-components. Significant differences are also noted in the wind direction data, possibly because these sites are located approximately 72 km apart.

EDWR–BAN

The correlation between the RWP and radiosonde wind data improves with height. Large wind direction differences are evident for the 300 m agl level. This is not unreasonable given the considerable distance between the sites (approximately 142 km) and the differences in the surrounding terrain; both the BAN and the WWR monitoring sites are located more than 100 miles to the southeast of the EDWR radiosonde monitoring site, on the other side of the San Bernardino Mountains. Note that insufficient data were available for 1200 GMT for the BAN site to perform this comparison.

EDWR–WWR

The WWR site is located approximately 156 km from the EDWR radiosonde site. As for the BAN profiler site, good correlation is not expected for the lower levels. The frequency distribution plots show several occurrences of large differences in the wind speed (up to 16 ms^{-1}) for the 300 and 1000 m agl levels. However, the wind direction data are fairly well correlated; for all three levels a majority of the differences are less than 60 degrees.

Comparison of High- and Low-Resolution RWP data

Typically, a radar wind profiler is configured to collect and archive wind data in two modes. In the low mode, only the lower portion of the atmosphere (generally below 2000 m agl) is sampled, allowing high resolution (100 m interval) measurements; in the high mode, the range of the instrument is increased and the resolution of the wind measurements is lower (on the order of 400 m). To examine whether differences between the RWP and radiosonde data are

affected by the resolution of the RWP data, a set of scatter plots was prepared for two RWP-radiosonde pairs (EDWR–MOJ, within the MDAB/SSAB (previously SEDAB), and MYFR–SDO, within the SDAB), contrasting the radiosonde data with the high- and low-resolution data separately. The comparisons for the Mojave site are presented in Appendix A2. For these plots, the RWP three-character site name was modified to reflect whether the high (i.e., MOJH) or the low resolution (i.e., MOJL and SDOL) data were used.

For the MOJ radar wind profiler, the scatter plots suggest that the differences between the high- and low-resolution data are small. Some variation is apparent in the wind speed and wind direction difference frequency distribution plots. For the 300 m agl level, wind direction differences of more than 30 degrees and wind speed differences of more than 10 ms^{-1} are more frequent for the high-resolution data than for the low-resolution data. There are no significant differences between the low- and high-resolution wind data bins for the 1000 and 2000 m agl levels. However, more observations are available at 2000 m agl from the low resolution data. Thus, it seems that use of either the high- or low-resolution data alone would not improve the quality of the RWP data and that combination of the two modes provides enhanced resolution near the surface (if needed) and increased data availability for the upper levels. The larger difference with the high-resolution data at the 300 m level may be attributable to the distance between the sites and the effects of terrain.

Comparison of Edited and Unedited RWP Data

The data acquired for this study were subjected to certain quality assurance procedures (NOAA, 1994). Editing routines were applied to remove data points that were found to be contaminated due to interference caused by migrating birds. To examine the effects of the editing routine on data quality and data availability, additional scatter plots were prepared for the EDWR–MOJ and MYFR–SDO pairs using the unedited RWP data. Those for the Mojave site are presented in Appendix A3. For these plots, the MOJR site name denotes the use of the unedited or raw data.

Comparison of the EDWR–MOJ (edited) and EDWR–MOJR (unedited) scatter plots indicates that the edited data compare more favorably with the radiosonde data then the unedited data. Note the availability of unedited data for the 100 m level. Several outliers were removed in the editing process. While the number of wind observations in the edited data set is notably less than for the raw data set, the reduction in sample size does not appear to excessively limit the informational content.

Virtual Temperature Data

Virtual temperature data were collected at the Hesperia (HES) monitoring site for a short period of time during the 1992 field study. Scatter plots comparing the HES and EDWR virtual temperature data for 300 and 1000 m agl are presented in Appendix A4. In general, the RASS instrument measures cooler temperatures than the radiosonde. Because this bias is apparent for both levels and measurement times, the discrepancy might in part be explained by the distance between the locations of the two monitors. To the extent that temperatures at

the Hesperia monitoring site were influenced by the sea breeze intrusion from the SoCAB, the cooler temperatures are expected.

Summary

The comparison of RWP/RASS and radiosonde data for the MDAB/SSAB (previously SEDAB) does not indicate that the data are well correlated. An example set of scatter and frequency distribution plots for the Hesperia (HES) monitoring site (at the 1000 m level) is provided in Figure 1-6. The RWP/RASS data for Hesperia are compared with the Edwards Air Force Base (EDWR) radiosonde data. As illustrated in this figure, the u and v wind components from the RWP dataset exhibit a broader range of values than those calculated using the radiosonde data. The RWP data range from approximately -10 to 10 ms^{-1} while the radiosonde data range from approximately -5 to 5 ms^{-1}. This is consistent with the distribution of wind speeds; the RWP derived wind speeds are typically greater than the radiosonde derived values (these differences are typically within 5 ms^{-1}). Most of the wind direction differences are within 30 degrees for the 0000 GMT (afternoon) comparison and within 60 degrees for the 1200 GMT (morning) comparison. However, given the location of the two sites with respect to the terrain features (in particular the San Gabriel Mountains), these differences are not unexpected nor indicative of problems with either instrument. Also included in Figure 1-6, is a comparison of the RASS-derived temperatures for the Hesperia monitoring site with the radiosonde-derived temperatures for EDWR. The RASS-derived temperatures are on the order of 2-4 degrees cooler than those for Edwards. As noted earlier, the temperatures at HES could be influenced by the sea breeze (lower temperatures in the SoCAB and airflow through Cajon Pass) and, thus, the temperature differences are physically realistic.

The comparison of RWP/RASS and radiosonde data for the MDAB/SSAB (previously SEDAB) is limited by the distance between the monitoring sites. The complexity of the terrain surrounding the MDAB and SSAB and the location of the monitoring sites with respect to the terrain (refer to Figure 1-1) further limit this comparison. However, two inferences can be drawn from the comparison. First, since it is expected that meteorological data are representative of the meteorological conditions within a given radius of influence, it can be inferred that within the lowest 1,000 meters of the atmosphere (e.g., the boundary layer), the radius of influence for meteorological monitoring sites in the air basin previously identified as the SEDAB may be less than 30 km, which is the smallest distance between any RWP/radiosonde site pair. Second, the comparison also suggests that wind speeds associated with the hourly averaged RWP data are systematically higher than those obtained from the radiosonde data (for all sites and all layers).

San Diego Air Basin Monitoring Sites

Data for four RWP monitoring sites located in the SDAB were compared with the San Diego NWS radiosonde data. These include San Clemente Island (SCI), San Diego (SDO), Point Loma (PTL), and El Cajon (ELC). As indicated by Figure 1-1, three of the profiler sites (SDO, ELC, and PTL) are fairly close to the radiosonde site. Although these sites are close together, the coastal location of the San Diego area may result in differences between the

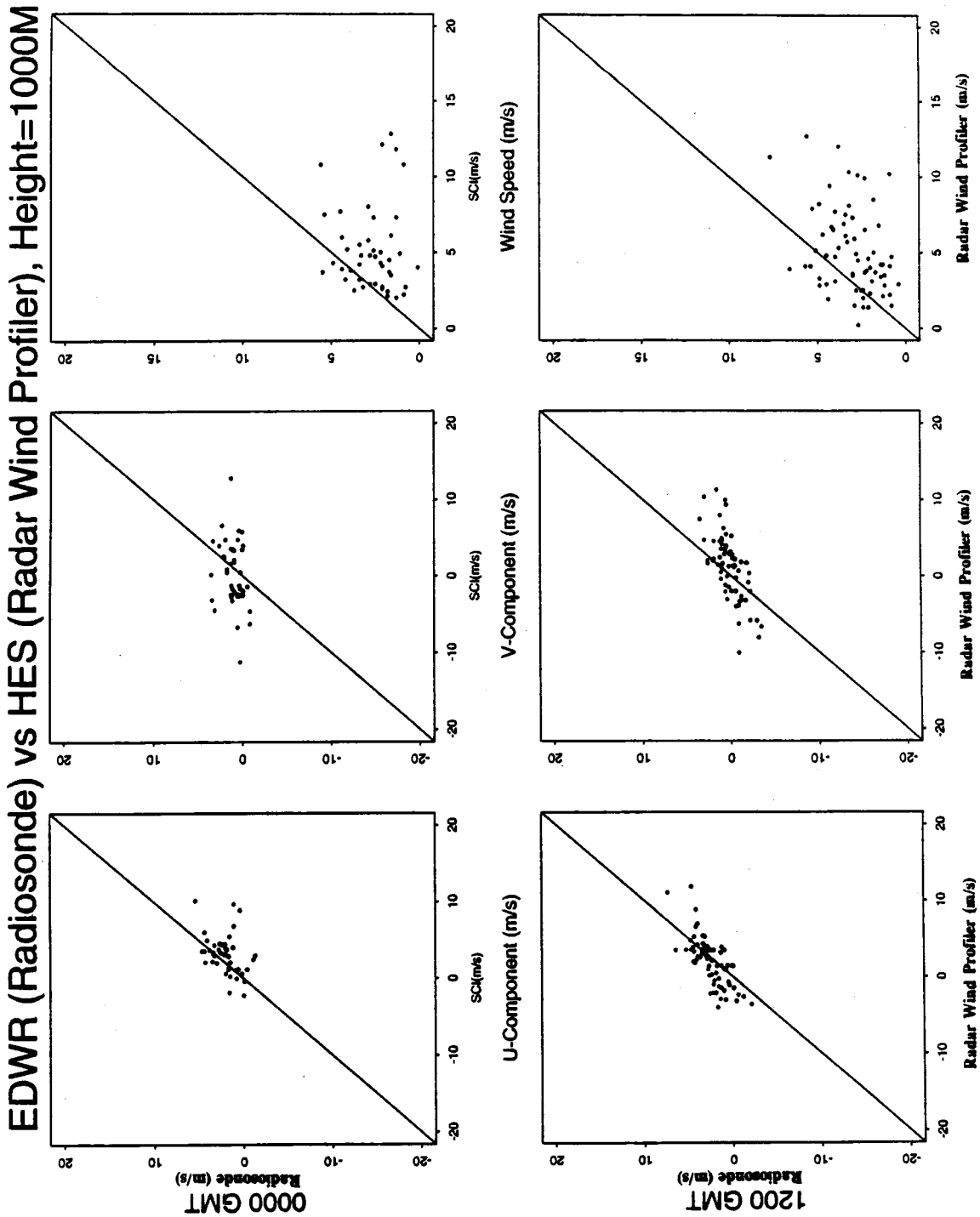

FIGURE 1-6a Comparison of RWP/RASS data for the Hesperia (HES) monitoring site with radiosonde-derived data for the Edwards Air Force Base (EDWR) monitoring site: Scatter plots comparing RWP and radiosonde derived u and v wind components and wind speed for 0000 and 1200 GMT.

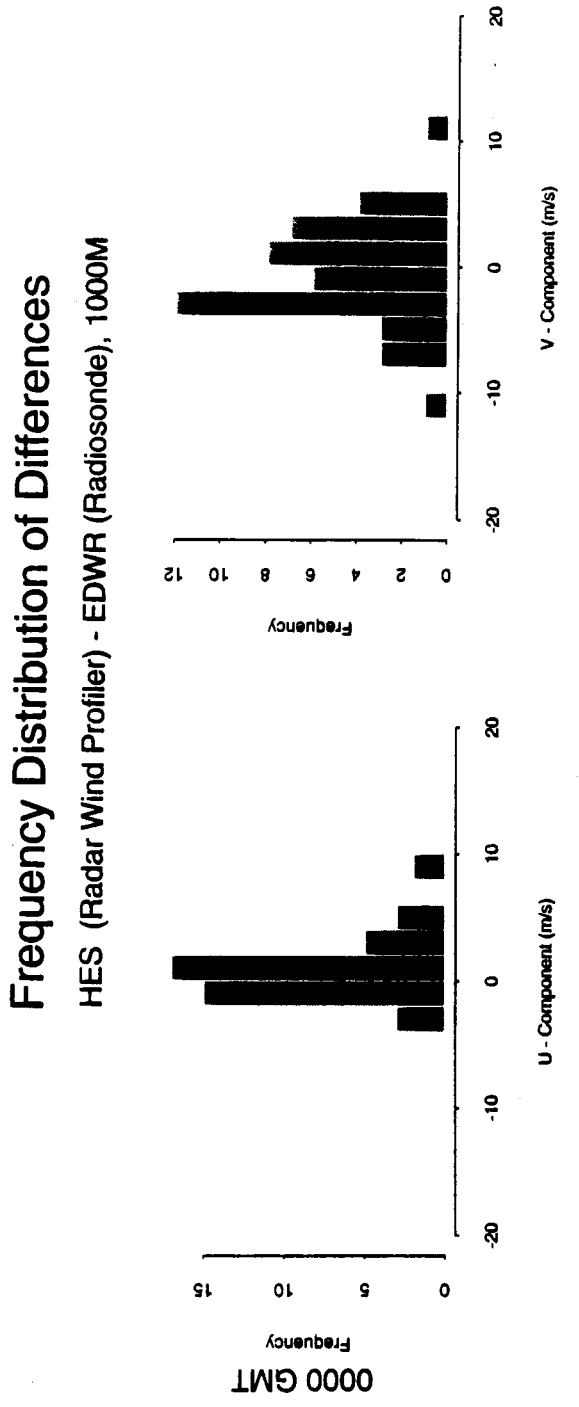

FIGURE 1-6b. Frequency distribution plots of the differences between RWP and radiosonde derived u and v wind components for 0000 and 1200 GMT.

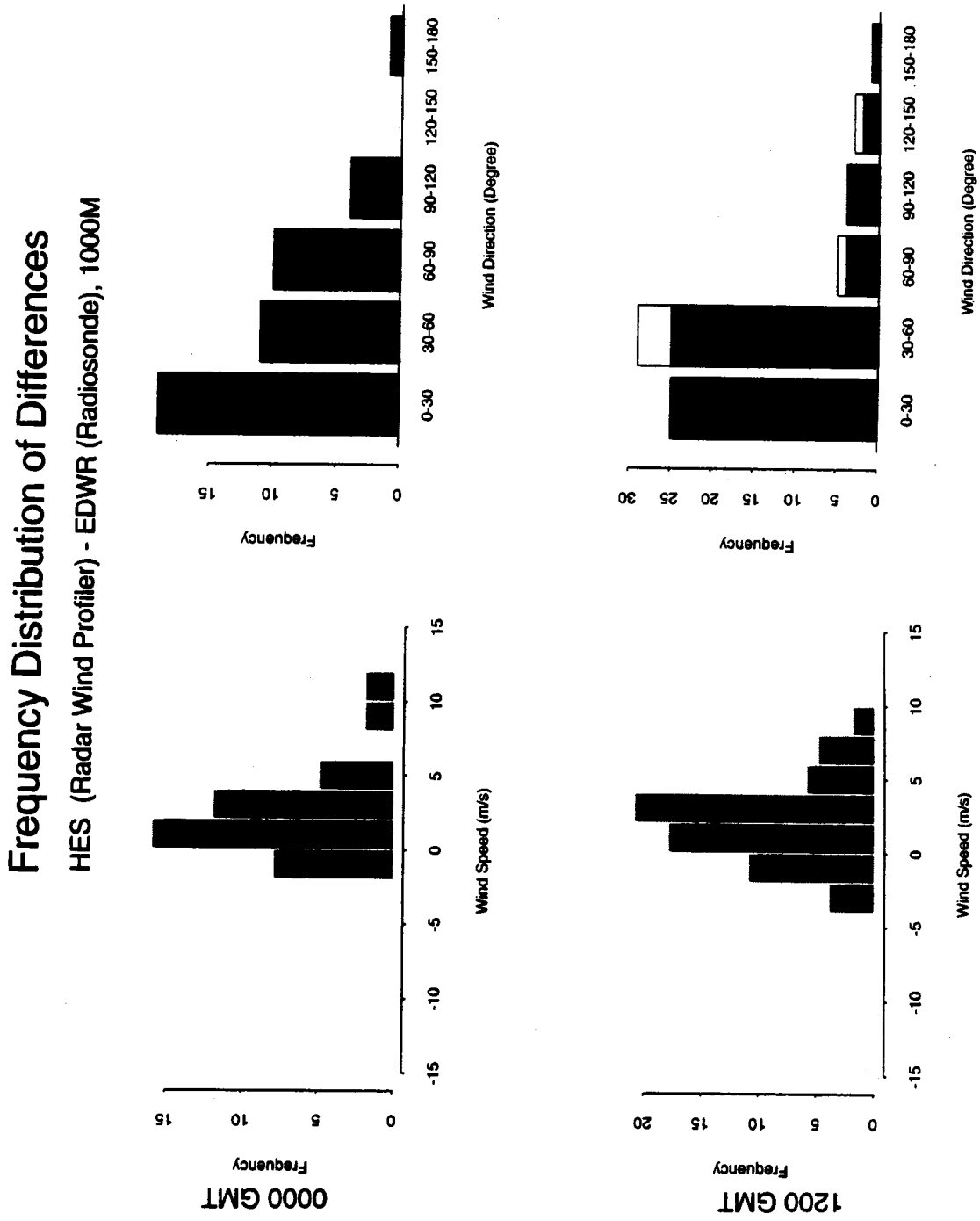

FIGURE 1-6c. Frequency distribution plots of the differences between RWP and radiosonde derived wind speed and wind direction for 0000 and 1200 GMT.

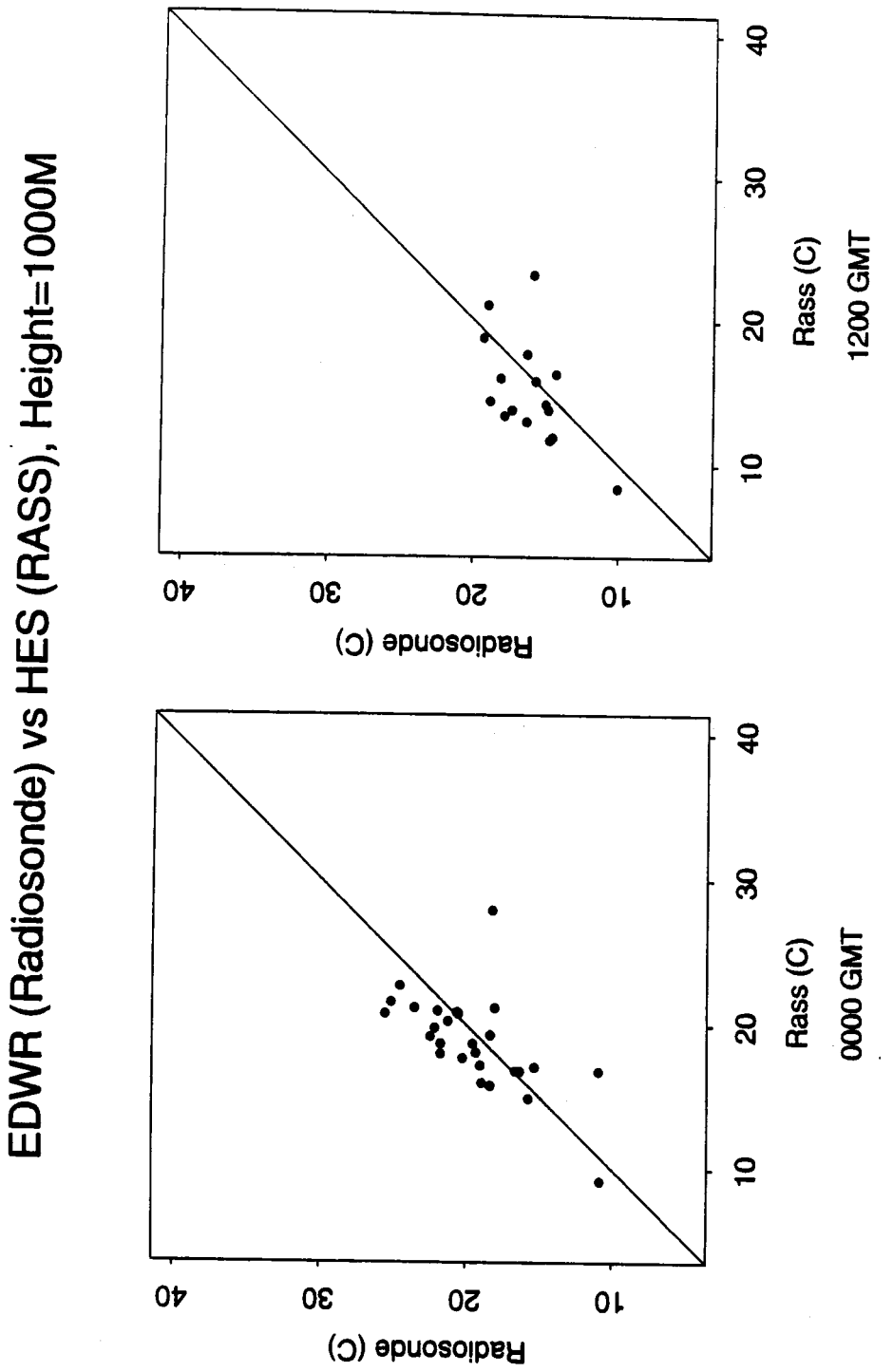

FIGURE 1-6d. Scatter plots comparing RASS and radiosonde derived virtual temperature for 0000 and 1200 GMT.

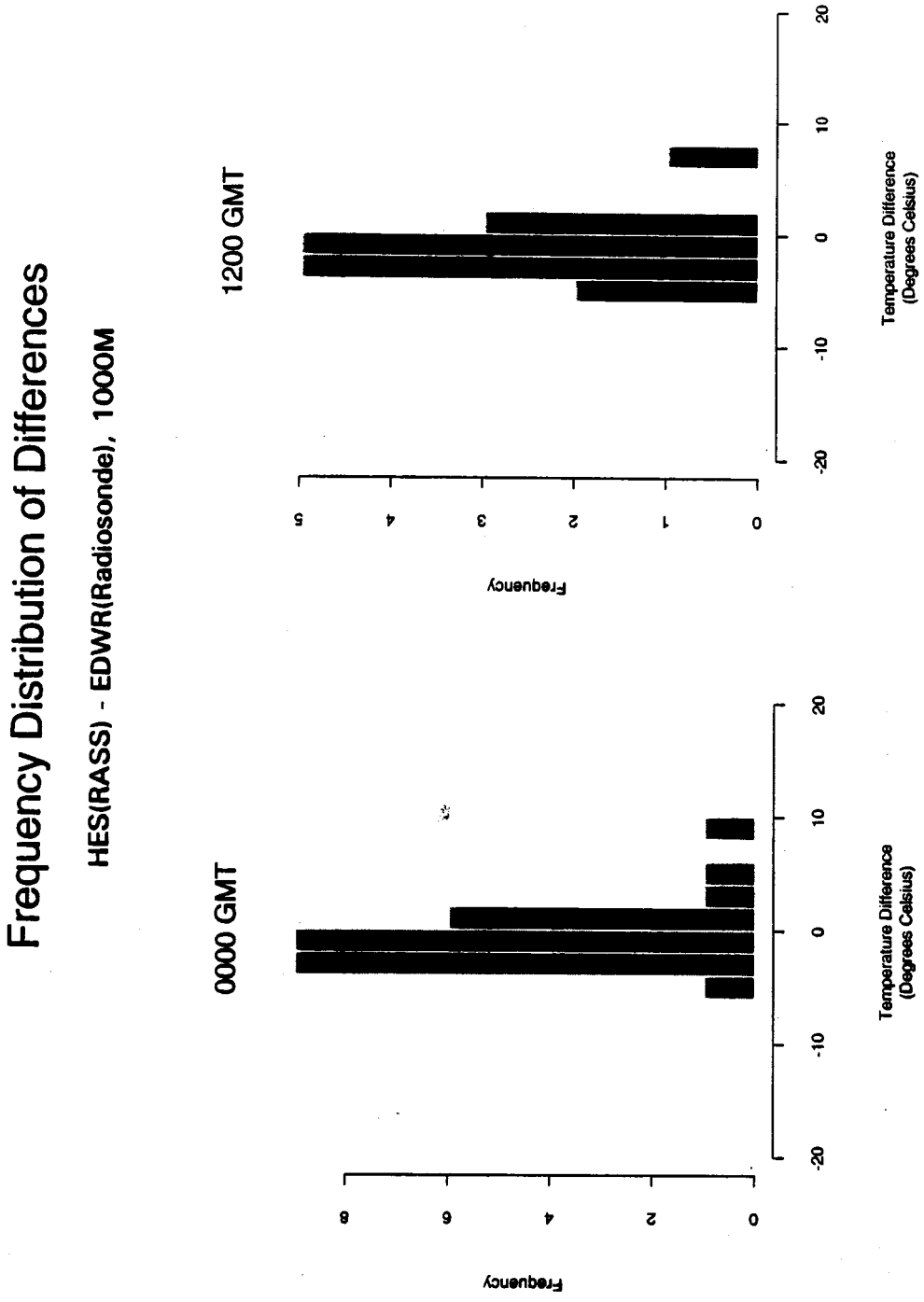

FIGURE 1-6e. Frequency distribution plots of the differences between RASS and radiosonde derived virtual temperature for 0000 and 1200 GMT.

sites due to daily variations in the inland extent of marine air influence. The SCI site is located on San Clemente Island, approximately 150 km west of San Diego; discrepancies between these data and the MYFR data are likely to be due to the distance between the two monitors. Scatter plots and plots of the frequency distribution of differences for each of these monitoring site pairs are shown in Appendix B1.

Wind Data

MYFR–SDO

The MYFR–SDO scatter plots indicate that the RWP and the radiosonde u and v wind components for all three levels are well correlated (no data were available for 100 m agl). Wind speed differences for 300 and 1000 m agl are typically within 2 ms^{-1}; some outliers associated with high radiosonde wind speeds are evident in the plot for the 300 m agl level. At 2000 m agl, the RWP wind speeds are higher than the radiosonde wind speeds (for 1200 GMT differences of 5 ms^{-1} or greater characterize approximately 25 percent of the dataset). The frequency distribution plots also suggest that the agreement between the radiosonde and RWP u- and v-components diminishes with height. This is different from the comparison for the MDAB and SSAB (previous SEDAB) where the agreement improved somewhat with height. Note that the distance between these two sites is approximately 10 km.

MYFR–SCI

Scatter plots for the SCI monitoring site indicate that there is more variation in the profiler wind data than in the radiosonde wind data. Better correspondence aloft is expected for the SCI data considering the significant distance between the radiosonde and the SCI profiler site. The data for 1200 GMT (the morning sounding) at 1000 m agl are particularly well correlated. However, at 2000 m agl, differences in the u- and v-components are frequently more than 4 ms^{-1}, and wind direction differences of more than 60 degrees occur approximately 50 percent of the time. This could be attributable to the distance between the sites or possibly to differences between the marine (SCI) and coastal (MYFR) environments. Note that the distance between these two sites is approximately 138 km.

MYFR–PTL

The 100 and 300 m agl level wind speeds for the PTL RWP monitoring site are consistently higher than the radiosonde wind speeds, particularly for the 0000 GMT data. The scatter plots for these levels and the 0000 GMT time period indicates that the radiosonde wind speeds are generally less than 3 ms^{-1}, whereas the RWP wind speeds range from 2 to 14 ms^{-1}. For the 1000 and 2000 m agl levels, the u and v components as well as the wind speeds are better correlated; however, the tendency for higher RWP wind speeds is again evident. Differences in the wind direction data are frequently between 30 and 60 degrees at and below 1000 m agl; above this level differences are mostly less than 30 degrees. These sites are located approximately 15 km apart.

MYFR–ELC

The ELC data show better correspondence with the MYFR radiosonde data than the SDO, SCI, and PTL RWP wind data. This is evident in the scatter plots as well as in the frequency plots of the differences. The frequency plots show that differences in the magnitude of the wind components and the wind speeds are mostly within 2 ms^{-1}. The wind direction data are well correlated for the 2000 m agl level but differences for the 300 and the 1000 m agl levels are distributed among the bins with some differences of 90 degrees or more; this may be due to the relatively low wind speeds recorded for the lower levels (note the preponderance of wind speeds less than 5 ms^{-1}). The distance between these sites is approximately 15 km.

Comparison of High- and Low-Resolution RWP Data

As for the MOJ RWP site discussed previously, the differences between the high (SDEH) and low (SDEL) resolution data for the San Diego (SDO) RWP monitoring site are small. The scatter plots (see Appendix B2) suggest that the correlation of the radiosonde data with the high-resolution data is slightly better for the 300 m agl level but worse for the 1000 and 2000 m agl levels. The frequency distributions of the differences are similar for the two data sets for the 300, 1000, and 2000 m agl levels. Comparison of the frequency plots for the high- and low-resolution data with those for the combined data suggests that combination of the data tends to improve the quality of the RWP data overall. In all cases, where the majority of differences in the u and v component are greater than 2 ms^{-1} with a subset of the data (for examples, see the SDEL 1000 m agl plot for 1200 GMT and the SDEH 2000 m agl plot for 0000 GMT), the highest frequency of differences shifts to the 0–2 ms^{-1} class when the data are combined.

Comparison of Edited and Unedited RWP Data

The editing routines applied to the SDO profiler data resulted in removal of all wind data for the 100 m agl level and a notable number of measurements for the 300, 1000, and 2000 m levels. This reduction in sample size is the most notable difference between the edited and unedited data sets. The scatter plots (see Appendix B3) indicate that these routines removed some outliers in the unedited data, but also suggest that they removed a number of points that appeared to show good agreement with the radiosonde data. As the frequency distribution plots show, however, differences between the radiosonde and profiler wind direction data do appear to be somewhat smaller for the edited data.

Virtual Temperature Data

RASS virtual temperature data are available for three field study monitoring sites in the SDAB: SDO, PTL, and SCI. Scatter plots for these sites are presented in Appendix B4. For the MYFR–SDO pair, the plots show that the differences between the radiosonde and the RASS data range from approximately 0 to 10°C. Surface temperature differences of 10°C between the coastal and inland areas are observed in the San Diego area, thus, the inland

location of the SDO RASS monitor compared to the location of the radiosonde monitoring site could explain some of the deviations from the radiosonde measurements. However, the PTL and MYFR data also exhibit some differences of up to 10°C, even though they are both located near the coast. The differences between the MYFR and the SCI data are more evenly distributed about the x=y line and indicate higher temperatures over MYFR during the afternoon (0000 GMT), as expected. Please keep in mind that some of these differences could be attributed to errors introduced by the conversion of the radiosonde temperature and moisture data into virtual temperature.

Summary

The comparison of RWP/RASS and radiosonde data for the SDAB is more favorable than that for the MDAB and SSAB (previously SEDAB), likely as a result of the closer proximity of the monitoring sites (with the exception of San Clemente Island) and fewer effects from complex terrain. However, for this area, spatial variations in the timing, as well as the horizontal and vertical extent of the land/sea breeze circulation limit our ability to compare the data from sites that are not collocated. Thus, while better than that for the MDAB/SSAB (previously SEDAB) monitoring sites, the comparison of RWP/RASS and radiosonde data for the SDAB does not indicate that the data are well correlated. An example set of scatter and frequency distribution plots for the San Diego (SDO) monitoring site (at the 1000 m level) is provided in Figure 1-7. The RWP/RASS data for SDO are compared with the San Diego NWS (MYFR) radiosonde data. As illustrated in this figure, the u and v wind components from the RWP dataset typically differ from those calculated using the radiosonde data by as much as 4 ms^{-1}. RWP derived wind speeds for this level are higher than the radiosonde derived values for 0000 GMT (by as much as 10 ms^{-1}) but do not show a consistent bias with respect to the radiosonde data for 1200 GMT. Wind direction differences are distributed among the bins (and somewhat irregularly for 1200 GMT). As noted earlier, this could be attributable, in part, to variations in the land/sea breeze characteristics affecting the two sites. Also included in Figure 1-7, is a comparison of the RASS-derived temperatures for the SDO monitoring site with the radiosonde-derived temperatures for MYFR. While large differences are noted (as much as 10°C), the temperature differences are somewhat evenly distributed along the x=y line.

In summary, the comparison of RWP/RASS and radiosonde data for the SDAB is also limited by the effective distance between the monitoring sites. The spatially varying influence of the land/sea-breeze circulation renders this comparison difficult. It is not clear to what extent the differences between the RASS-derived and radiosonde-derived temperatures are due to the distances between the sites. Some of these differences could also be due to inaccuracies introduced by the calculation of virtual temperature for the radiosondes using point measurements of temperature and dew point temperature. Accurate characterization of the vertical distribution of moisture is required and this may be difficult to obtain within coastal areas. An important consideration arising from the comparison for the SDAB is that the utility of the high-resolution RASS-derived virtual temperature measurements (e.g. for modeling purposes) may, under certain circumstances, depend upon the availability of equally highly resolved observations of the vertical distribution of moisture.

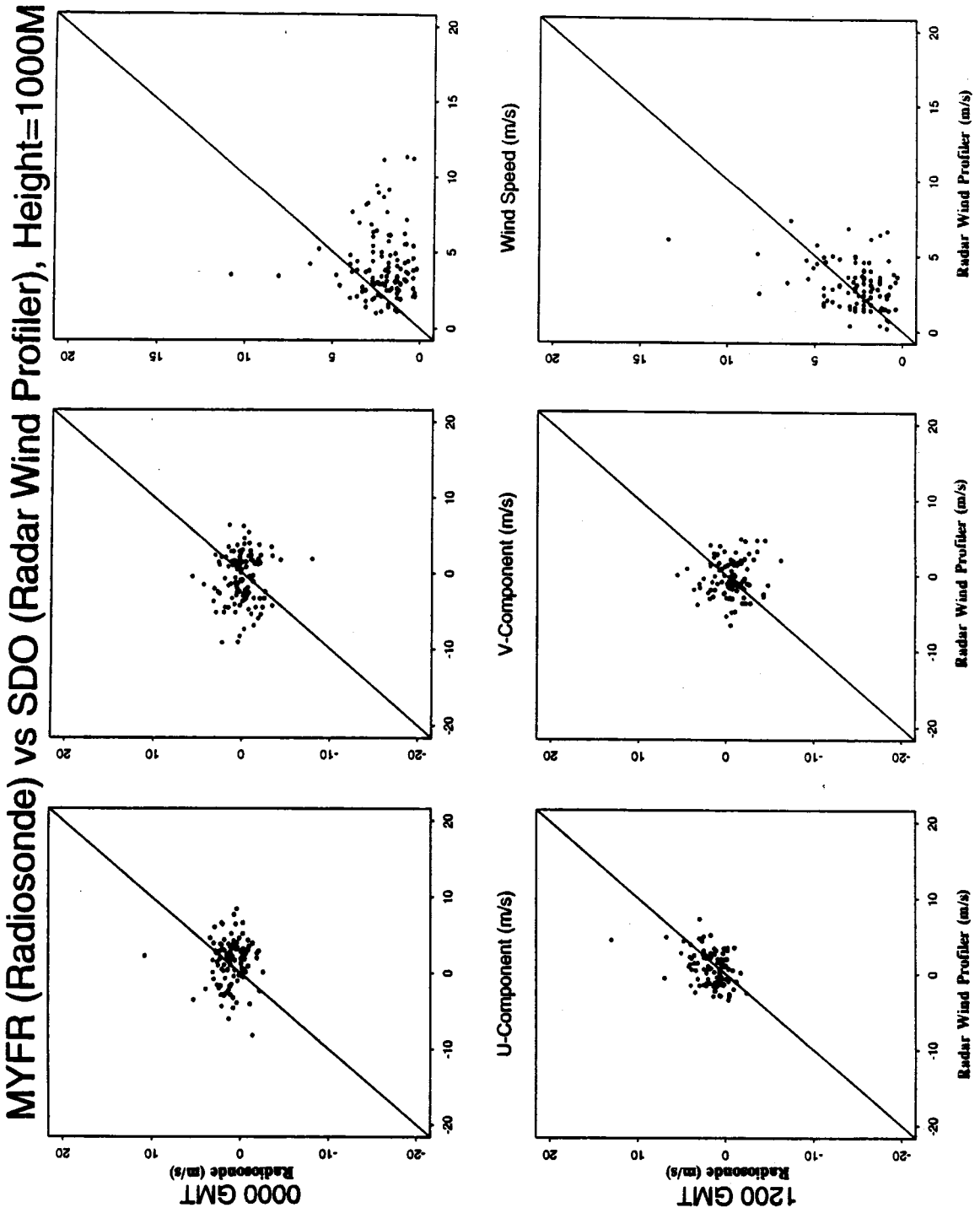

FIGURE 1-7a. Comparison of RWP/RASS data for the San Diego (SDO) monitoring site with radiosonde-derived data for the San Diego (MYFR) monitoring site: Scatter plots comparing RWP and radiosonde derived u and v wind components and wind speed for 0000 and 1200 GMT.

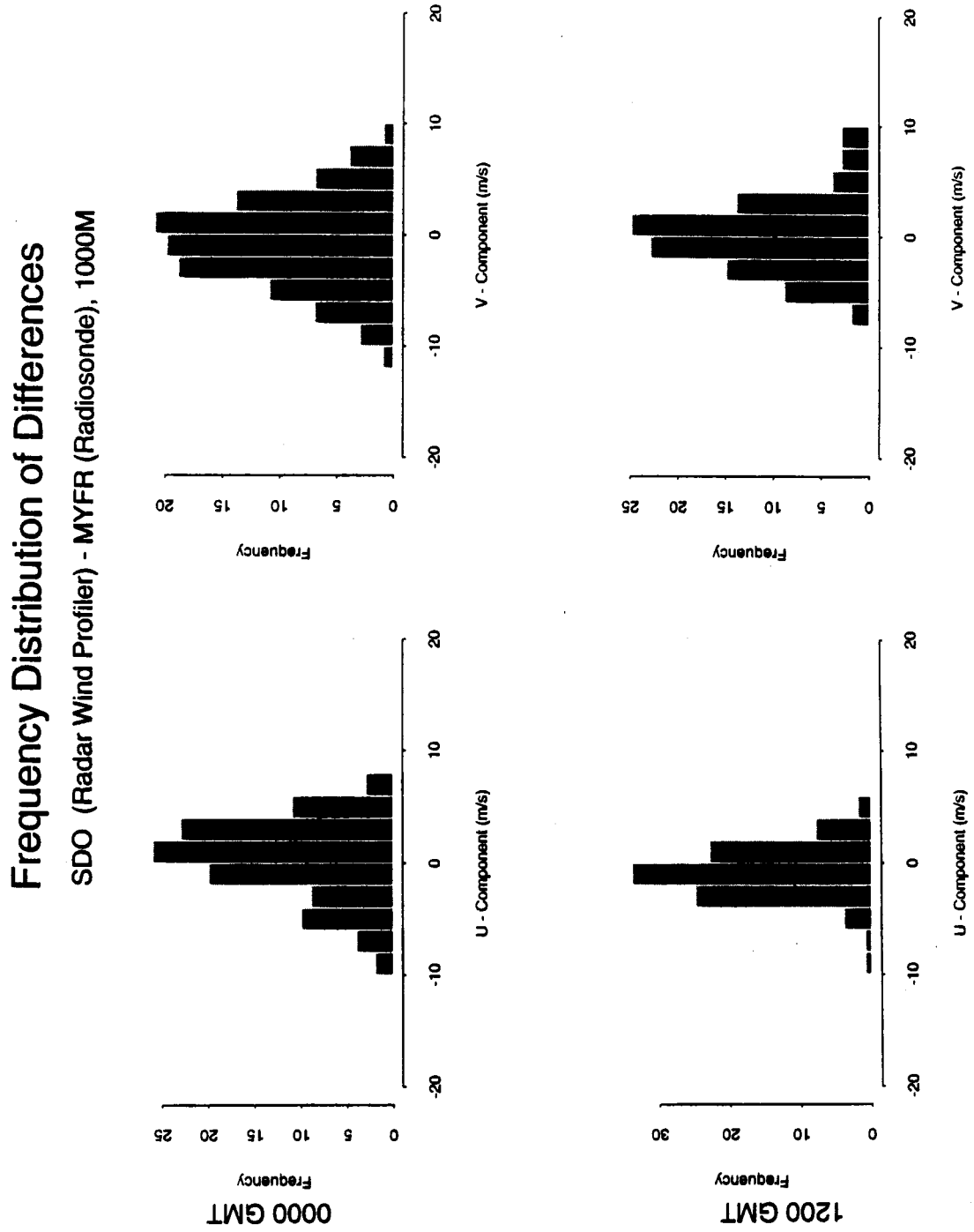

FIGURE 1-7b. Frequency distribution plots of the differences between RWP and radiosonde derived u and v wind components for 0000 and 1200 GMT.

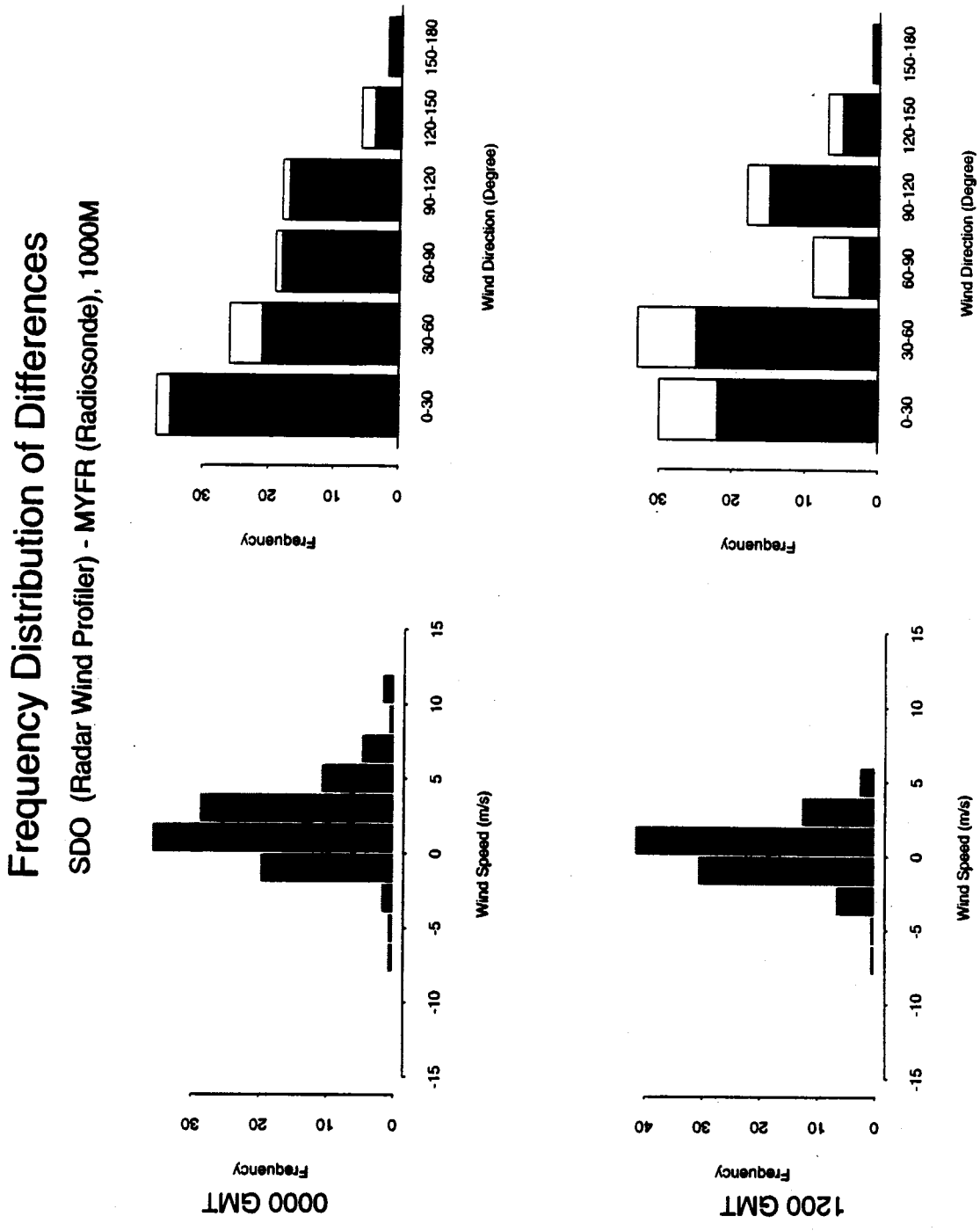

FIGURE 1-7c. Frequency distribution plots of the differences between RWP and radiosonde derived wind speed and wind direction for 0000 and 1200 GMT.

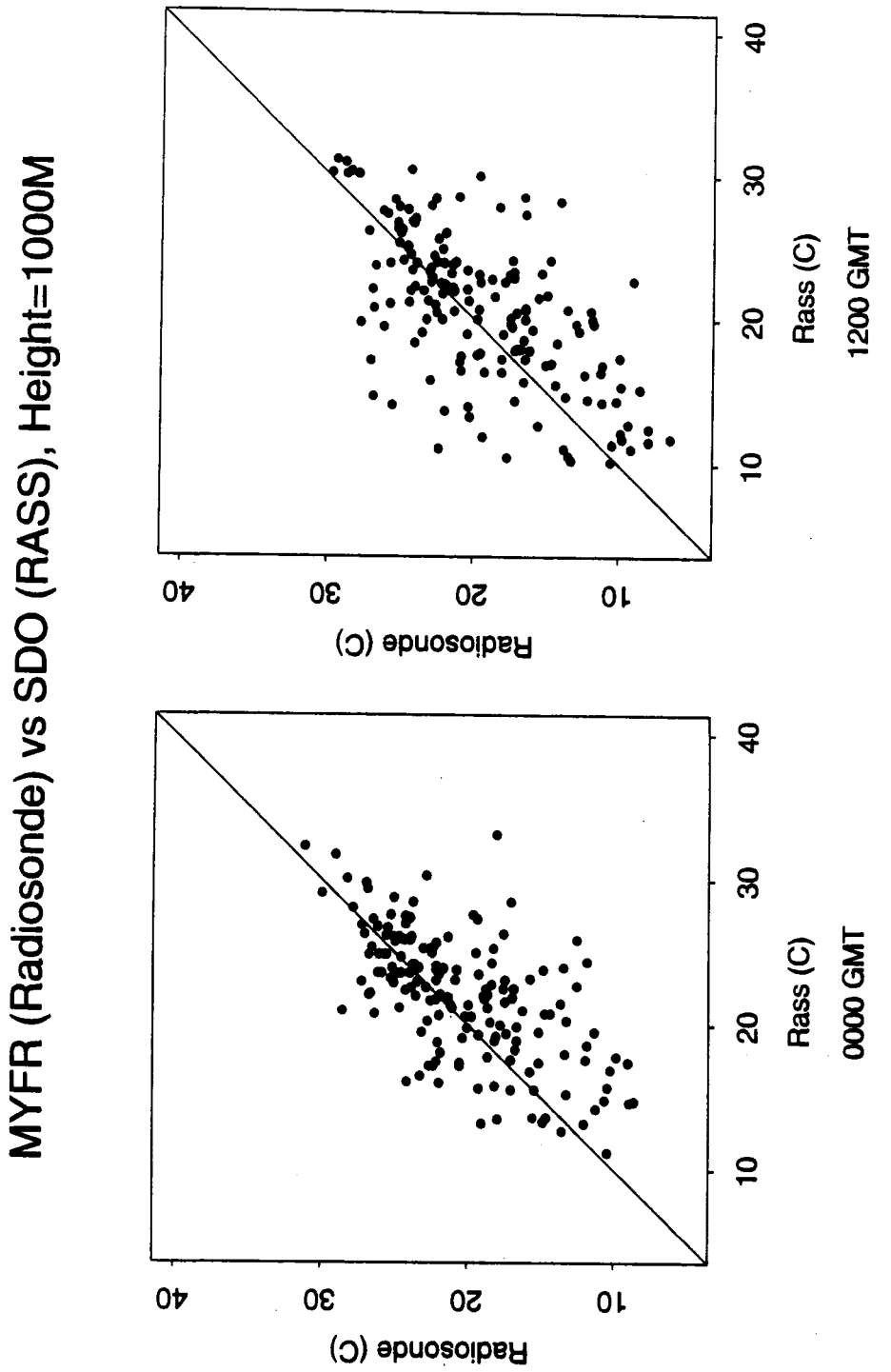

FIGURE 1-7d. Scatter plots comparing RASS and radiosonde derived virtual temperature for 0000 and 1200 GMT.

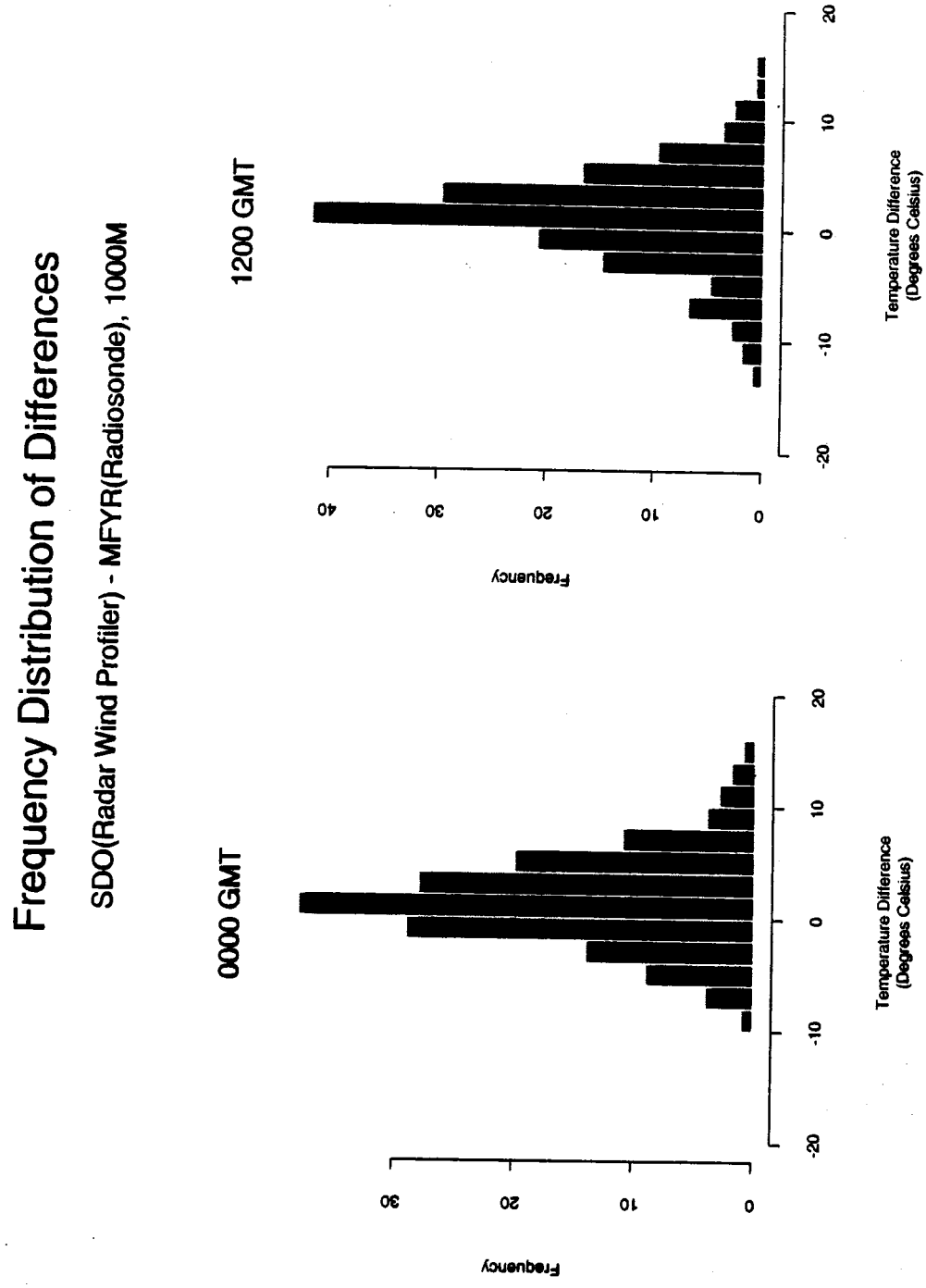

FIGURE 1-7e. Frequency distribution plots of the differences between RASS and radiosonde derived virtual temperature for 0000 and 1200 GMT.

South Coast Air Basin Monitoring Sites

Radar wind profiler and RASS sites were operated at two locations in the SoCAB during the 1992 field study; these include the Los Angeles International Airport (LAX) and San Bernardino (SBO). Although it is not located within the SoCAB, data for Point Mugu (PTM) are also discussed in the section. The LAX and SBO data were compared with radiosonde data from the UCLA monitoring site (UCLR); the PTM data were compared with radiosonde data from the Pt. Mugu Naval Air Station (NTDR). The LAX and UCLA sites as well as the PTM and NTDR sites are nearly collocated and are expected to be representative of the same atmospheric conditions at any given time. In contrast, the SBO profiler site is located approximately 100 km inland from the UCLA site; comparison of these data with the UCLA data is thus not as appropriate in this case, especially for the lower levels. Additional comparison of the LAX data with radiosonde and sodar data is presented by Durkee and Cassmassi (1993) and Cassmassi et al. (1994). Scatter plots and histograms of differences for the SoCAB RWP-radiosonde pairs are shown in Appendix C1.

Wind Data

NTDR–PTM

Data availability from the Point Mugu (PTM) wind profiler site is somewhat limited for the 1992 time period. Scatter plots of the u and v components suggest reasonable agreement with the radiosonde data; the profiler wind speeds are consistently higher than those for the radiosonde. The frequency distribution plots suggest that differences in the RWP and radiosonde u and v components are less than 6 ms^{-1} for the 300 and 1000 m agl levels and less than 8 ms^{-1} for the 2000 m agl level. For a majority of the observations, wind direction differences are less than 60 degrees. Note that these sites are nearly collocated (2 km apart).

UCLR–LAX

Data for the UCLA radiosonde monitoring site are available for 1200 GMT only. Scatter plots of the wind data for this site pair suggest that the RWP u and v wind components are generally within 5 ms^{-1} of those corresponding to the radiosonde data for the 100 and 300 m agl levels but within 10 ms^{-1} for the 1000 and 2000 m agl levels, where outliers occur more frequently. This pattern is also evident in the histograms. A propensity for the RWP to measure higher wind speeds is evident for all levels. These two sites are approximately 5 km apart.

UCLR–SBO

No data were available for the 100 and 300 m agl levels for this site pair. The RWP and radiosonde wind components agree to within approximately 5 ms^{-1} at the 1000 m agl level

and within 10 ms^{-1} at the 2000 m agl level. The histograms show large differences in both wind speed and direction for the 2000 m agl. These differences are likely due to the distance between the monitors (97 km). The UCLA radiosonde site is located near the coast, and the SBO monitoring site is located in the eastern part of the Los Angeles basin (the airflows in this region are influenced by the higher terrain to the east and north of Los Angeles.)

Virtual Temperature Data

All three wind profiler sites in the SoCAB were equipped with RASS monitors. Scatter plots comparing virtual temperature data for each RASS monitor with those derived from the radiosonde data are included in Appendix C2. As for the wind data, plots were prepared for 1200 GMT only and, for two of the pairs, data are available for the 300 and 1000 m agl levels only. With a few exceptions, the radiosonde and RASS data are within a few degrees C. For all three pairs, the plots suggest a tendency for RASS virtual temperatures to be slightly higher than the radiosonde data.

NTDR–PTM

The sample size for this comparison is very limited. For a large proportion of the sample, temperature differences are within 2°C.

UCLR–LAX

The scatter plots of the radiosonde versus the RASS data suggest that the RASS data are unreliable for the 2000 m agl level, most likely because this level is near the upper range of the instrument. The RASS-derived virtual temperatures for the 100, 300, and 1000 m agl levels are generally within 2°C of the radiosonde-derived values. This level of agreement is also noted by Durkee and Cassmassi (1991).

UCLR–SBO

Data are only available for the 1000 m agl level for the SBO RASS site. The scatter plot for this level suggests good agreement with the radiosonde data, particularly for virtual temperatures above approximately 20°C. For the lower temperature data, the scatter plots show somewhat greater discrepancies between the two instruments. The frequency distribution plots of the differences indicate that the RASS virtual temperatures tend to be higher than those for the radiosonde.

Summary

The comparison of RWP/RASS and radiosonde data for the SoCAB (including Point Mugu) includes two nearly collocated sites. An example set of scatter and frequency distribution plots for one of these site pairs (Los Angeles at the 1000 m level) is provided in Figure 1-8. The RWP/RASS data for UCLA are compared with the Los Angeles International Airport (LAX) radiosonde data. Although these monitoring sites are located only 5 km apart, differences in the wind components are frequently larger than 2 ms-1. Wind speeds differ by as much as 10 ms-1 and wind direction differences of greater than 90 degrees are found for this level. Also included in Figure 1-8, is a comparison of the RASS-derived virtual temperatures for the UCLA monitoring site with the radiosonde-derived virtual temperatures for LAX. Temperature differences are typically within 2°C. These results are consistent with those obtained by Durkee and Cassmassi (1993).

The comparison of RWP/RASS and radiosonde data for the SoCAB suggests that even small differences in location can contribute to differences in the observed wind data. However, the comparison also strongly suggests that the type of RWP instrument used in the 1992 Southern California summer field study consistently provided wind speeds that were higher than those obtained using standard radiosonde technology. The consistency of the RASS and radiosonde derived temperature estimates is, however, encouraging.

Mixing Height Data Validation

Using radar reflectivity measurements (or refractive index, C_n^2) from the wind profiler instruments, NOAA researchers estimated mixing heights for some of the profiler sites during the study period. Specifically, the vertical profile of radar C_n^2 was examined and the peak or maximum value was identified. The level at which the peak value occurred was used as an estimate of the top of the mixed layer or capping inversion height (NOAA, 1994). This technique is based on descriptions of the behavior of C_n^2 in the unstable boundary layer that characterize this parameter as decreasing in the surface layer, remaining relatively constant throughout the mixed layer, increasing to a peak value at the top of the mixed layer, and decreasing to a free tropospheric value above this layer (NOAA, 1994). The C_n^2-derived mixing height estimates were compared with the mixing heights estimated using radiosonde data for 1600 PST for the selected RWP and radiosonde site pairs.

The radiosonde-derived mixing-height estimates were calculated as follows. The radiosonde potential temperature data were used to calculate the height of the temperature inversion. Specifically, the potential temperature sounding data were examined and the mixing height was estimated to be the height at which a positive change in potential temperature with height was reported. This approach follows White (1993).

Scatter plots for eight pairs for which C_n^2-derived mixing height estimates were available are presented in Appendix D. Both methods generate relatively low mixing heights for the SDAB site pairs (SDO/MYFR and ELC/MYFR). For most sites located in the Antelope Valley, the scatter plots suggest some disagreement between the radiosonde and RWP derived mixing heights especially for the higher radiosonde mixing heights. Given the geographical differences and simple method for estimating the radiosonde mixing heights, this

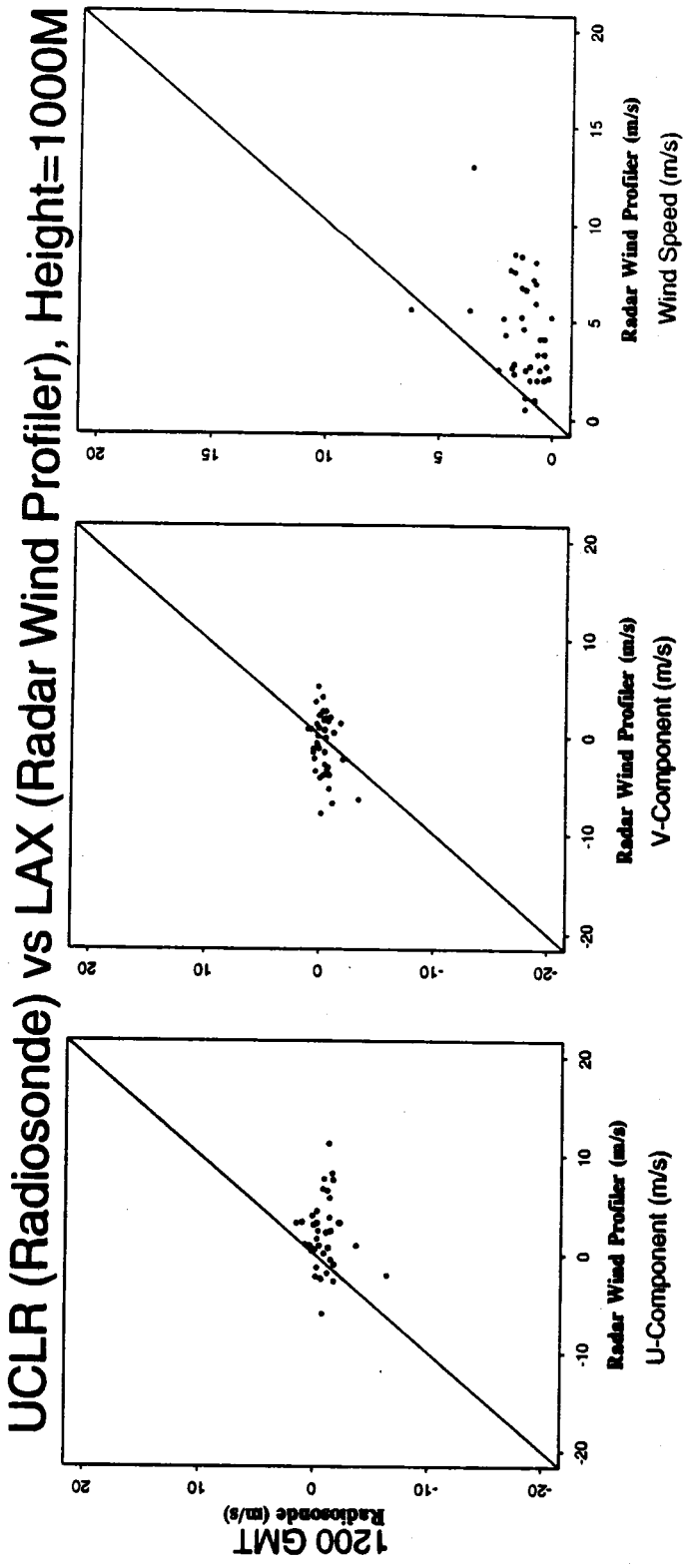

FIGURE 1-8a. Comparison of RWP/RASS data for the Los Angeles International Airport (LAX) monitoring site with radiosonde-derived data for the UCLA (UCLR) monitoring site: Scatter plots comparing RWP and radiosonde derived u and v wind components and wind speed for 1200 GMT.

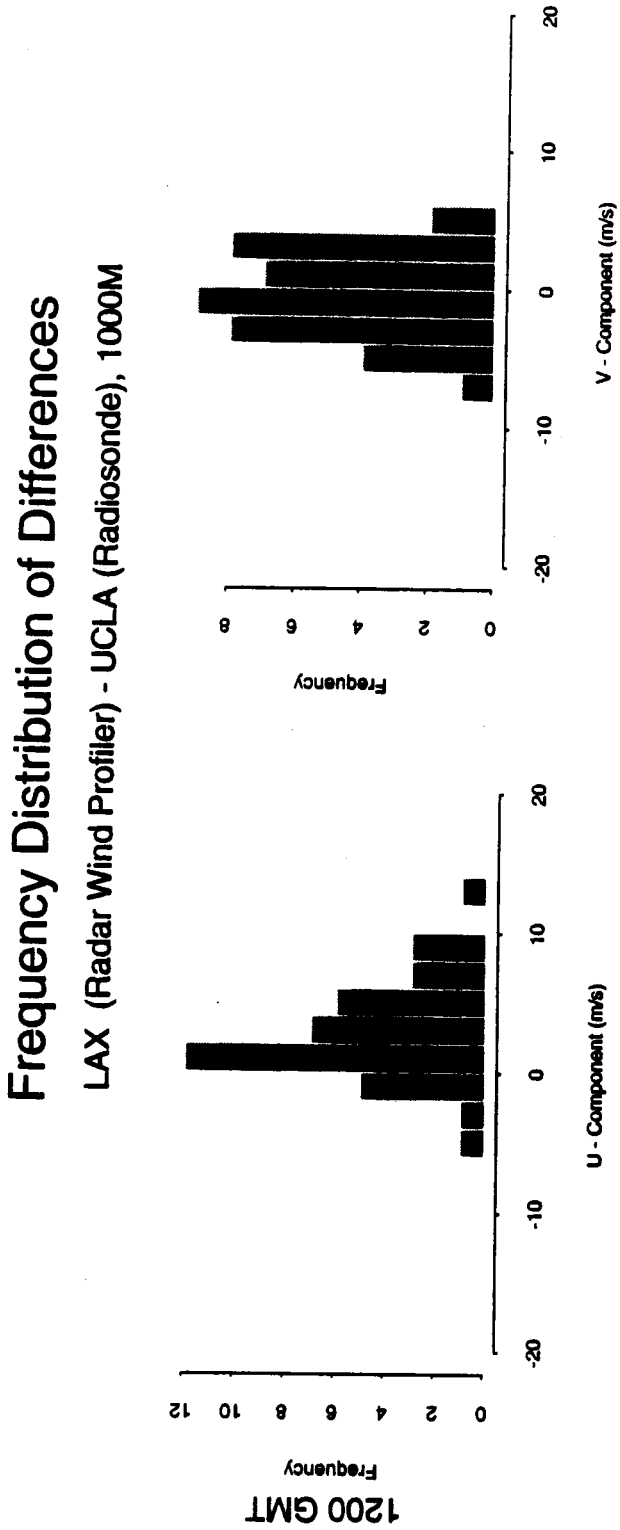

FIGURE 1-8b. Frequency distribution plots of the differences between RWP and radiosonde derived u and v wind components for 1200 GMT.

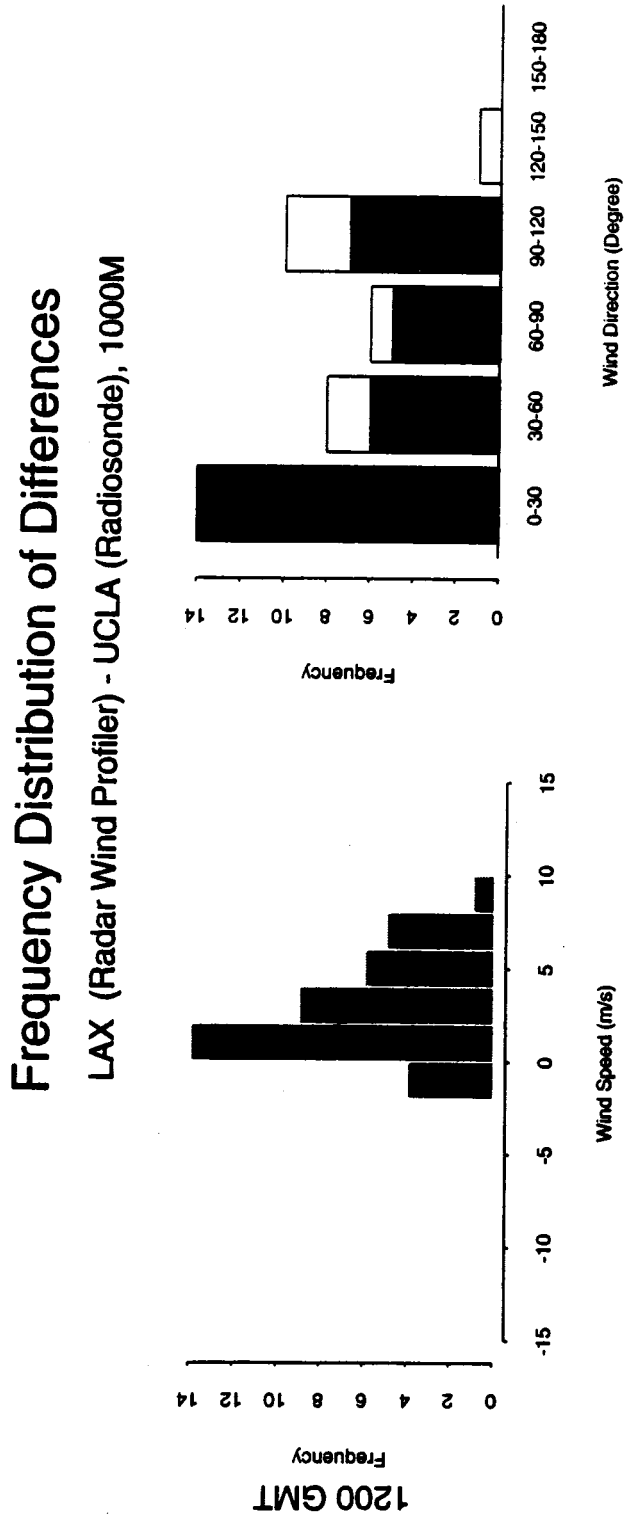

FIGURE 1-8c. Frequency distribution plots of the differences between RWP and radiosonde derived wind speed and wind direction for 1200 GMT.

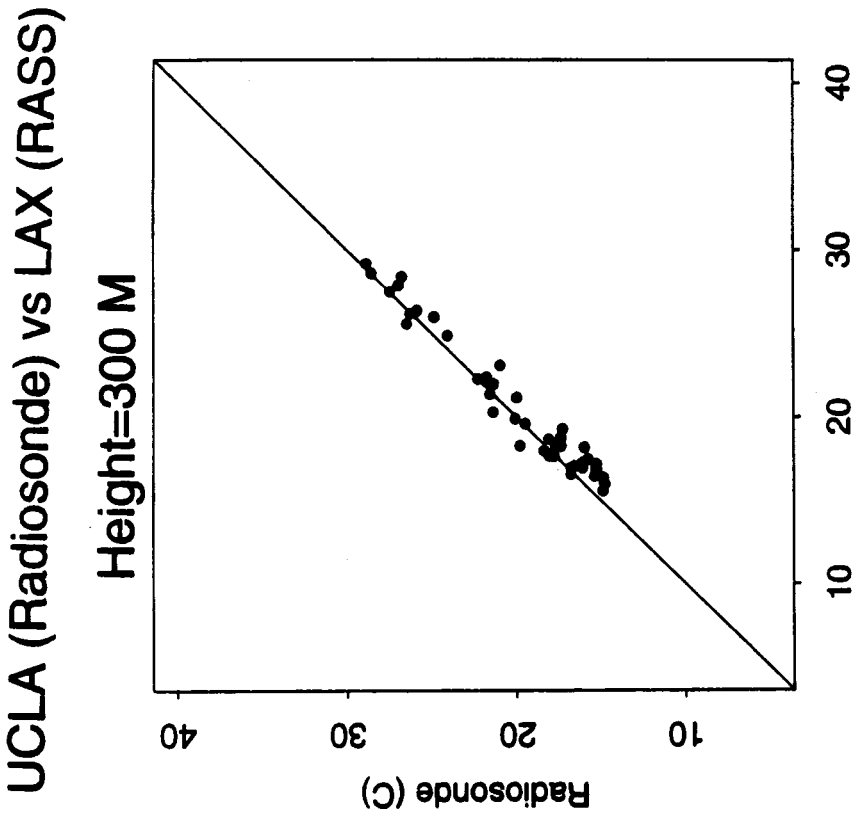

FIGURE 1-8d. Scatter plots comparing RASS and radiosonde derived virtual temperature for 1200 GMT.

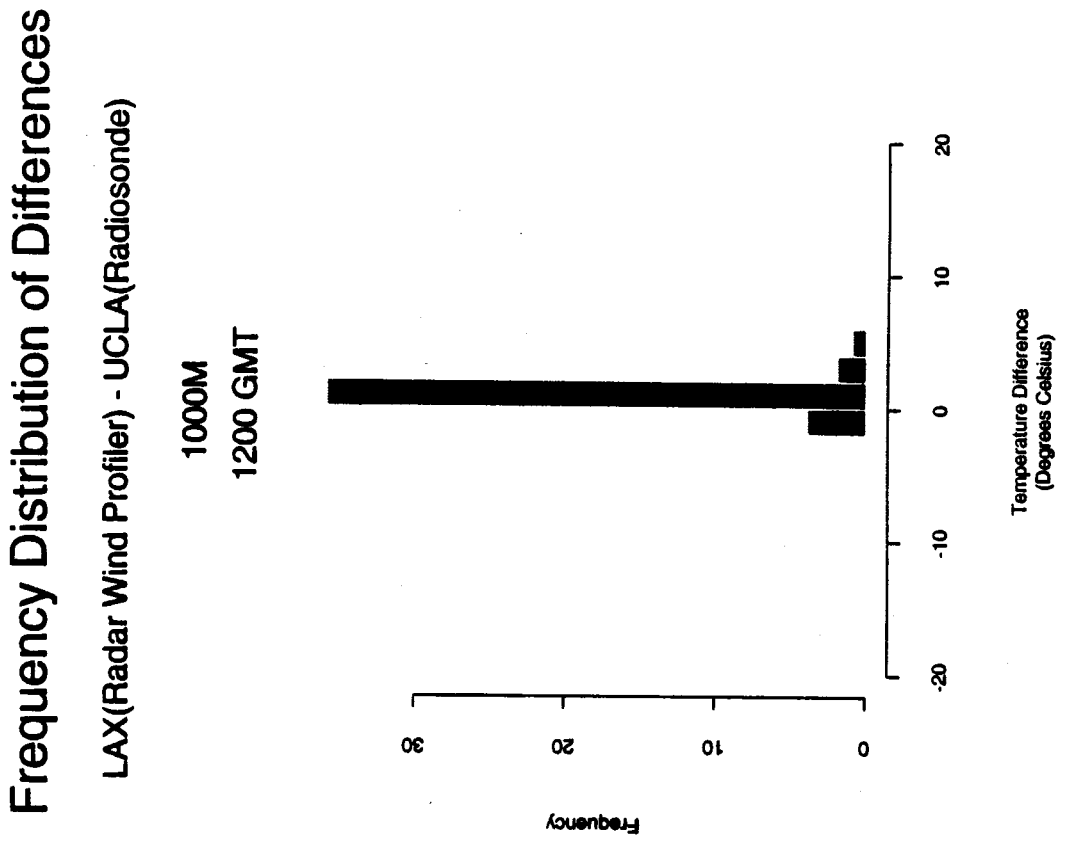

FIGURE 1-8e. Frequency distribution plots of the differences between RASS and radiosonde derived virtual temperature for 1200 GMT.

is perhaps expected. Additionally, note that the times at which the sounding data for Edwards Air Force Base were available varied from day to day and that some data were typically available during the mid to late morning hours. This corresponds to the period when the RASS-derived mixing heights change most rapidly (see, for example, Figure 1-9) and could account for some of the differences between the RASS-derived and radiosonde-derived mixing-height estimates.

DISCUSSION OF AIRCRAFT DATA

Additional meteorological and air quality data were collected during the 1992 Southern California Transport Study using an instrumented aircraft (Anderson et al., 1993). The aircraft was flown on selected days (typically twice per day) and along selected flight paths; the flights are described in detail in the referenced report. Measurements/reported parameters include: time, position, altitude, temperature, dew-point temperature, turbulence, backscatter, ultraviolet and total solar radiation, ozone, and NO-NO_x.

The aircraft sampling flight paths consisted of horizontal traverses and vertical spirals. One spiral location (Hesperia) was coincident with a RASS monitoring site (HES). To examine whether the aircraft temperature data provide any insights into the differences between the RASS and radiosonde data, the aircraft temperature data were compared with the radiosonde data (for the EDWR site). This comparison is presented side-by-side with a comparison of the RASS and radiosonde derived virtual temperature data in Figure 1-10. Due to the availability of the aircraft data at times corresponding to the radiosonde data, this comparison was obtained for only two days: 1 August and 4 August 1992. Note that the times differ slightly.

The comparison indicates that the difference between the RASS and radiosonde data are no larger than those between the aircraft and radiosonde data, however, the differences are more variable with height (a consistent bias is indicated for the aircraft data). This suggest that both differences in location as well as differences in measurement technique contribute to the temperature differences.

SUMMARY, DISCUSSION, AND RECOMMENDATIONS

Summary of Data Evaluation

Field study data were collected for 13 locations throughout southern California during 1992 using radar wind profiler and RASS instrumentation. These data were evaluated against radiosonde data using scatter plots and frequency distribution plots of differences for selected RWP-radiosonde site pairs and for two times, 0000 and 1200 GMT. Plots were generated for four levels, 100, 300, 1000, and 2000 m agl. The most notable feature of these plots is the tendency of the RWP to measure higher wind speeds than the radiosonde. This is evident for all four levels and both time periods. Because the site pairs were very rarely collocated, differences between the two instruments are very likely due, in part, to differences in the local terrain and/or surface cover. As a result of the differences in location as well as differences in

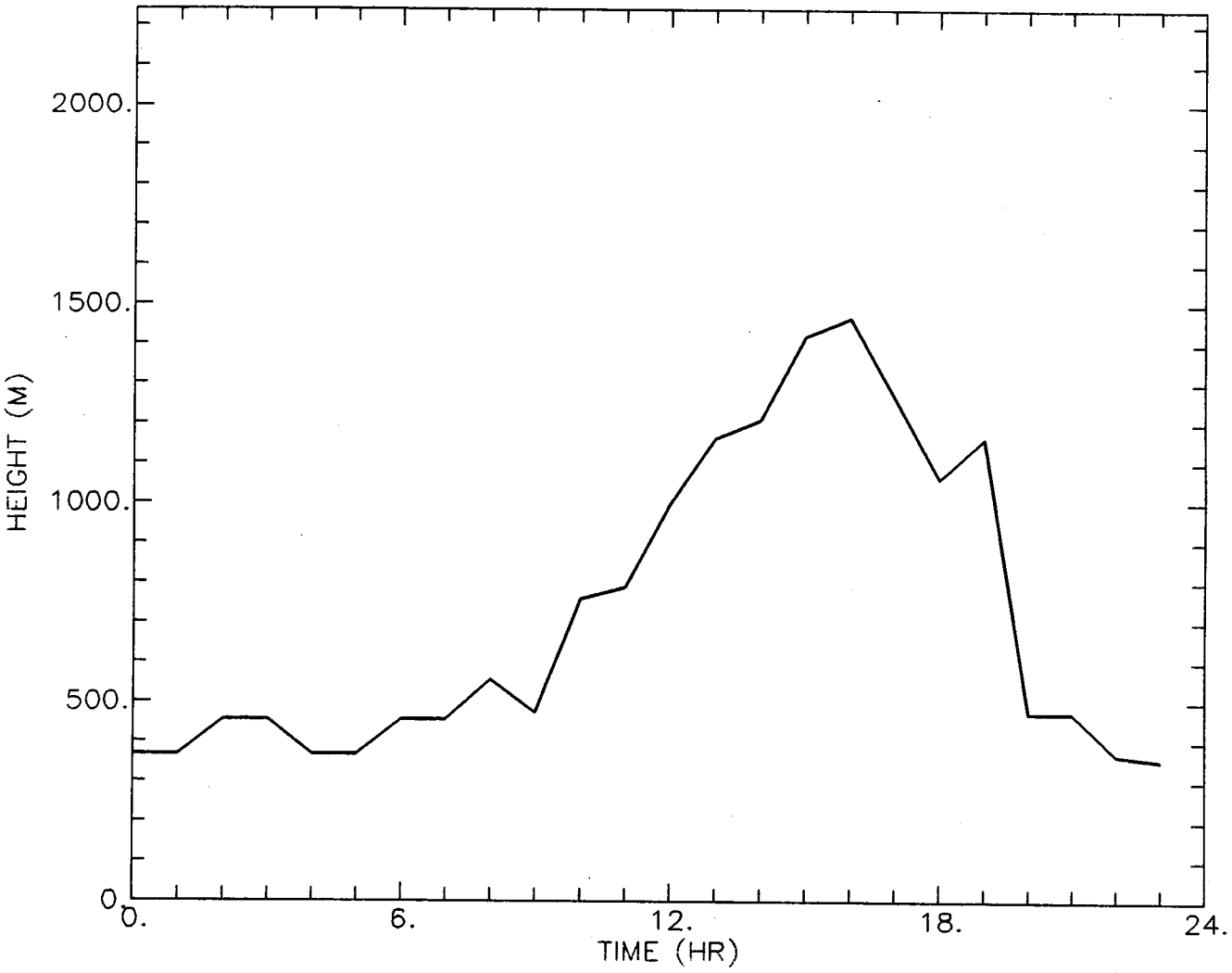

FIGURE 1-9. Hourly RASS-derived mixing-height estimates for the Banning Pass (BAN) monitoring site: 20 June 1992.

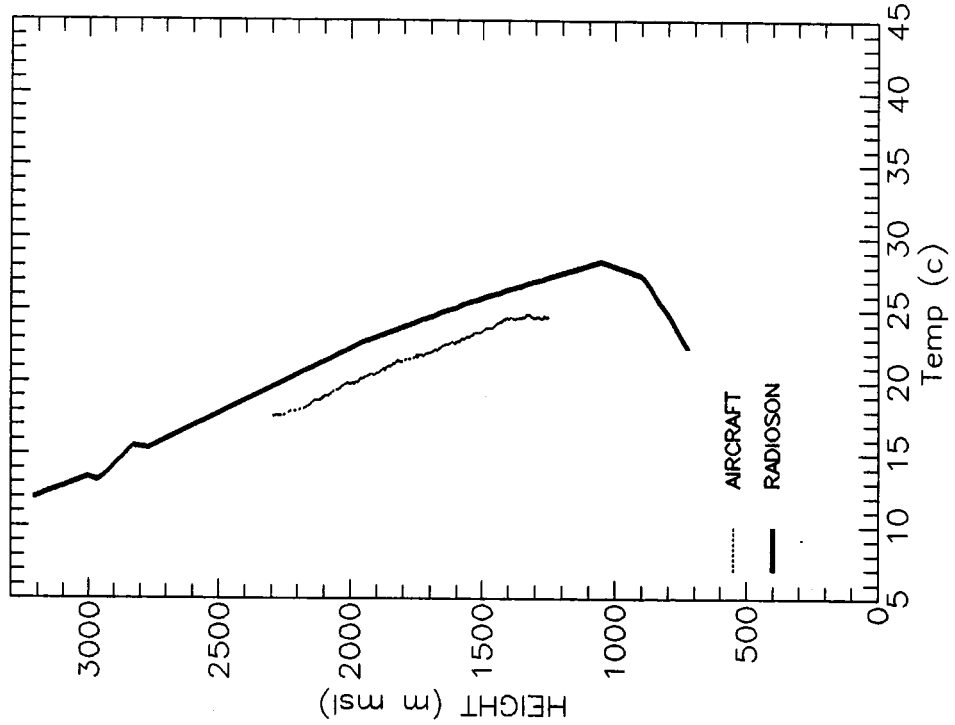

AIRCRAFT: HES, 400 PST 1AUG92
RADIOSONDE: EDW, 200 PST 1AUG92

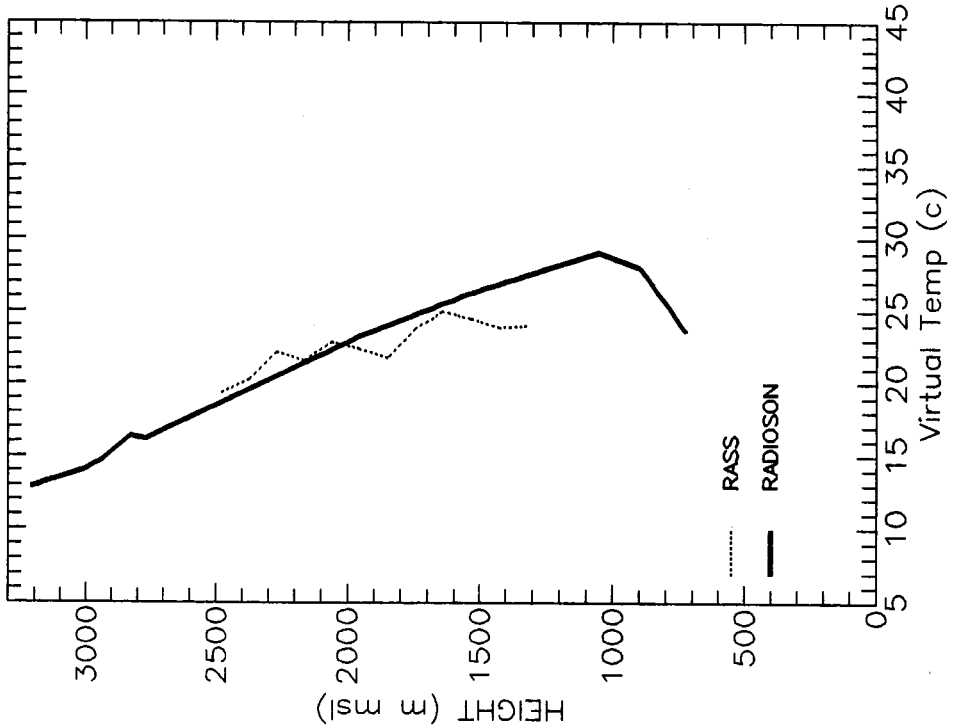

RASS: HES, 300 PST 1AUG92
RADIOSONDE: EDW, 200 PST 1AUG92

FIGURE 1-10a. Comparison of RASS and radiosonde derived virtual temperature for 1 August for HES (0300 PST) and EDWR (0200 PST) (left); comparison of aircraft and radiosonde derived temperature for 1 August for HES (0400 PST) and EDWR (0200 PST).

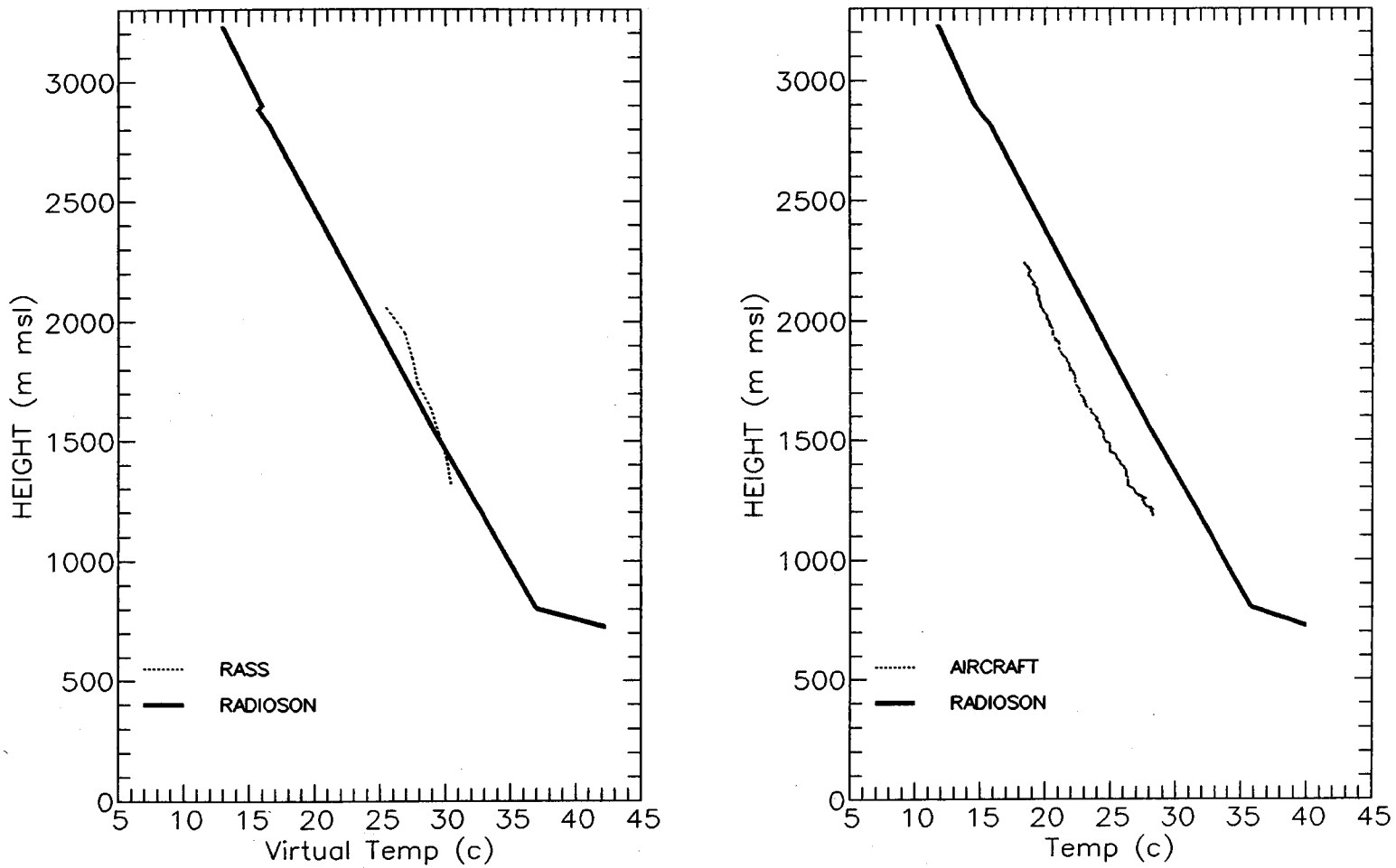

FIGURE 1-10b. Comparison of RASS and radiosonde derived virtual temperature for 1 August for HES (1300 PST) and EDWR (1400 PST) (left); comparison of aircraft and radiosonde derived temperature for 1 August for HES (1400 PST) and EDWR (1400 PST).

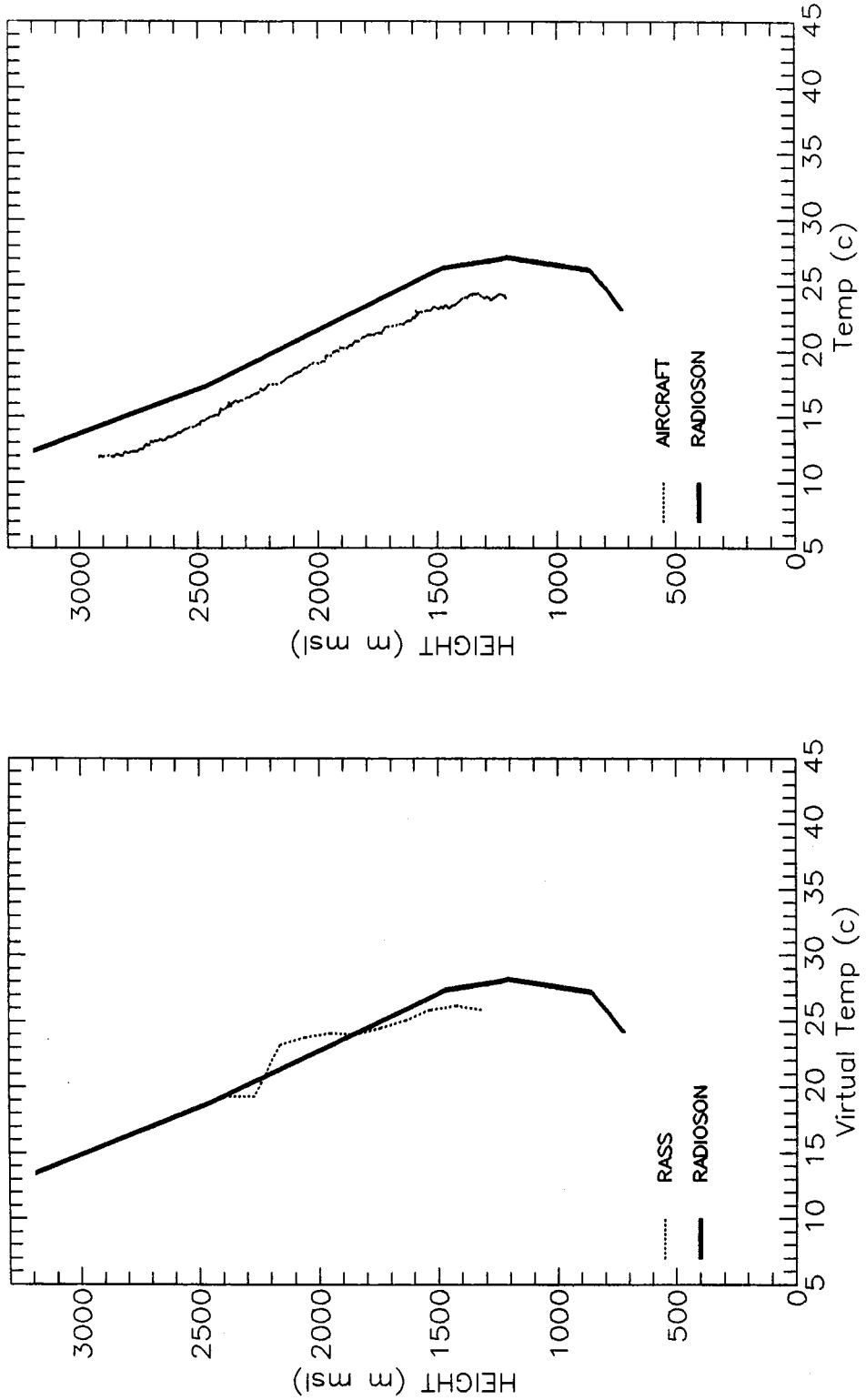

RASS: HES, 300 PST 4AUG92
RADIOSONDE: EDW, 200 PST 4AUG92

AIRCRAFT: HES, 400 PST 4AUG92
RADIOSONDE: EDW, 200 PST 4AUG92

FIGURE 1-10c. Comparison of RASS and radiosonde derived virtual temperature for 4 August for HES (0300 PST) and EDWR (0200 PST) (left); comparison of aircraft and radiosonde derived temperature for 1 August for HES (0400 PST) and EDWR (0200 PST).

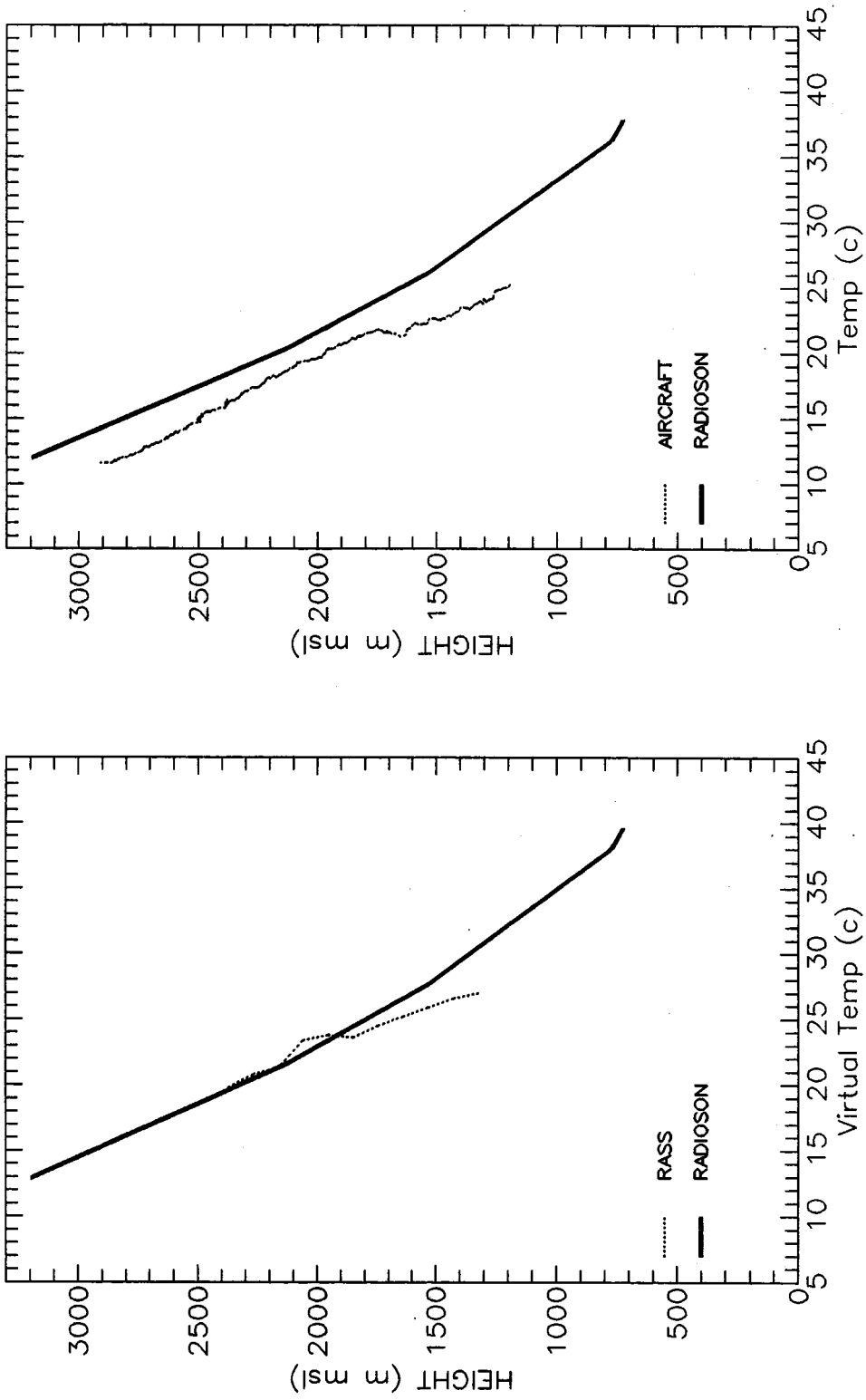

FIGURE 1-10d. Comparison of RASS and radiosonde derived virtual temperature for 4 August for HES (1400 PST) and EDWR (1400 PST) (left); comparison of aircraft and radiosonde derived temperature for 1 August for HES (1400 PST) and EDWR (1400 PST).

the timing and temporal resolution of the measurements, the field study data cannot be completely evaluated.

Differences between the low- and high-resolution RWP data were also examined, by preparing scatter plots for each resolution. A data set consisting of the high- and low-resolution data combined was found to agree with the radiosonde data better than either the high- or the low-resolution data separately. Similarly, scatter plots were prepared for the edited and unedited RWP data for two collocated RWP-radiosonde site pairs in San Diego (MYFR+SDO) and in the Antelope Valley (EDWR+MOJ). These scatter plots suggest that a notable number of data points were removed by the editing routines and that they removed several outliers, but also many points that appeared to be well correlated with the radiosonde data.

Scatter plots of the RASS and radiosonde virtual temperature data indicated mixed agreement. Generally, the discrepancies did not appear to be related to differences in the locations of the RASS and radiosonde sites. Agreement between the two instruments for the SoCAB and MDAB/SSAB (previously SEDAB) site pairs was better than that for the SDAB site pairs. The reasons for the relatively poor agreement of the San Diego RASS and radiosonde data are not clear.

Mixing height estimates derived from the C_n^2 (refractive index) data were also plotted against mixing heights calculated using the radiosonde data for seven site pairs. Scatter plots contrasting the two data sets did not indicate any problems with the C_n^2-derived estimates. The radiosonde data appeared to be characterized by more scatter for some of the MDAB/SSAB (previously SEDAB) monitoring sites. Good correlation was indicated for the San Diego sites.

The aircraft data collected as part of the field study provide a limited basis for comparison with RASS and radiosonde data. A comparison of the RASS, radiosonde, and aircraft data for the one site for which both RASS and aircraft spiral temperature data were obtained and the results support the hypothesis that the differences between the RASS and radiosonde temperature measurements are largely due to differences in the measurement techniques. The distance between the RASS and radiosonde sites potentially adds to these inherent differences.

Quality Control/Quality Assurance Issues

Discussion

It is well recognized that quality control of meteorological data is an important, if not critical, aspect of any data collection or field study program. The results of this study further indicate that the use of data from relatively new types of measurement platforms, such as the RWP and RASS instruments, for analysis and modeling purposes, requires a careful review and assessment of data quality and applicability. This review should include an assessment of the effectiveness of any editing routines and the compatibility of data for the low and high modes (for the RWP instrument).

The results of this study indicate that significant differences between measurements obtained using radiosonde and those obtained using RWP and RASS technologies exist. Certainly some differences are expected, given the differences in data collection methodologies and their respective error characteristics. Contamination of the RWP data by migrating birds and the subsequent application of newly developed editing routines may have contributed to the wind component differences. In addition, none of the radiosonde and RWP/RASS sites for which data were compared were collocated. The complex geography of southern California and the corresponding spatial variability in meteorological characteristics introduced by the complex terrain and the land/sea breeze circulation limited the extent to which data from non-collocated sites could be reasonably compared.

Recommendations

Further assessment/use of the RWP/RASS instruments for meteorological data collection within southern California should consider:

- careful siting of the instruments such that the data are representative of the spatial scales that are to be studied/modeled

- establishing collocated radiosonde (or other routine monitoring equipment) and RWP/RASS monitoring sites at several locations representing the different geographical characteristics of the area under study (e.g., coastal, inland valley, etc.) for a more accurate validation of the data

- obtaining sufficiently temporally resolved data from these other routine data acquisition sources for validation of the RWP and RASS data (e.g., every three hours)

- obtaining high resolution moisture data for conversion of the RASS virtual temperature data to a more useful format (this may be important for certain types of analyses or required by certain modeling systems)

- obtaining meteorological data within the lowest 500 to 700 m of the atmosphere, where RWP and RASS data are not available

Additional discussion of these and other issues related to the use of RWP and RASS upper-air monitoring systems is provided by STI (1996).

Use of RWP/RASS Data for Analysis and Modeling Purposes

The RWP and RASS instruments provide nearly continuous, high-vertical-resolution measurements of wind and virtual temperature that offer enormous possibilities with respect to improving our ability to understand, to describe, and to simulate the atmosphere.

In this study, for example, development of a conceptual model for ozone transport between the SoCAB and the SEDAB and SDAB was enhanced by the availability of these data. As described in Section 3 of this report, RWP wind data for the Barstow (BAR), Hesperia

(HES), and Whitewater (WWR) monitoring sites were key parameters in classifying high and low ozone days according to transport/airflow characteristics (using the Classification and Regression Technique, CART, analysis technique). The construction of composite winds (Section 2 of this report) and detailed, hourly wind fields (using a diagnostic wind modeling technique) and the subsequent calculation of particle paths (Section 3 of this report) for the purposes of examining the potential for interbasin pollutant transport was also significantly enhanced by the RWP data (data from the routine monitoring upper-air network for southern California does not provide sufficient spatial or temporal resolution to support such an analysis).

A major deficiency in the database for this additional analysis was the lack of data for the lowest levels of the atmosphere. To some extent this may have been due to the editing procedures. However, both the RASS and RWP instruments are limited in this respect; the lowest measurement level is typically on the order of 100 m agl. This represents a serious limitation in using these data for the analysis or modeling of the boundary layer. Use of other instruments (such as sodar at key locations) may have mitigated this problem.

The RWP/RASS data also represent a source of information for the application of data-assimilating prognostic meteorological models. The lack of data for the lowest layers of the atmosphere and the lack of high-resolution moisture data may affect the utility of the RWP/RASS measurements for four-dimensional data assimilation. The RWP/RASS data should be representative of the spatial scales that are to be simulated by the meteorological model. Thorough quality control/quality assurance of the data is also essential, since the assimilation of erroneous data can adversely affect the simulation of the structure and evolution of the meteorological fields.

Finally, through improved characterization of the meteorological characteristics within the area of interest, the RWP and RASS data may (1) enhance the episode selection process accompanying the application of an air quality model, through the more detailed identification of representative episode days and (2) provide an improved basis for the review and evaluation of the meteorological input fields and the corresponding air quality modeling results.

2 ANALYSIS OF WIND AND POLLUTANT DISTRIBUTIONS IN THE SOUTH COAST AND THE SOUTHEAST DESERT AIR BASINS

Observed air quality, wind, and mixing-height data collected during the 1992 Southern California summer field study were examined and classified according to combinations of daily maximum ozone concentrations in the SoCAB and the MDAB and SSAB (previously SEDAB). Each day of the period was identified as belonging to one of nine categories of combinations of high, moderate, or low ozone concentrations in the SoCAB and MDAB/SSAB (for example, high ozone concentrations in the SoCAB and moderate ozone in the MDAB/SSAB, or high ozone in the SoCAB and high ozone in the MDAB/SSAB). The objective of this exercise was to characterize the airflow patterns for each of these classification combinations using composite hourly wind and mixing-height data corresponding to averages for each site of all the days within each category. Three-dimensional conceptual models of the airflow patterns associated with each of these combinations were developed based on examination of 3-hourly plots of the composite wind data for the surface, 1000, and 2000 meters above ground level (m agl).

DETERMINATION OF CLASSIFICATION COMBINATIONS

Surface air quality data for the 31 March – 22 October 1992 period for monitoring sites located within the SoCAB and the MDAB/SSAB (previously SEDAB) were obtained and the daily maximum ozone concentration for each air basin was determined. The air quality monitoring locations are plotted in Figure 2-1 and listed in Table 2-1. A total of 201 days were classified into nine classification combinations; these are summarized in Table 2-2. A day is classified as "high" if the observed daily maximum ozone concentration at any site within the air basin was greater than 12 parts per hundred million by volume (pphmV), "moderate" if this concentration was between 9 and 12 pphmV, and "low" if this concentration was lower than 9 pphmV.

As indicated by Table 2-2, the most frequent combination is high ozone in the SoCAB and high ozone in the former SEDAB. No cases with low ozone in the SoCAB and high ozone in the former SEDAB were observed.

COMPOSITE WINDS AND MIXING HEIGHTS

Composite winds and mixing heights were calculated by averaging the hourly wind data for each site for which data were available for the days within each of the categories listed in Table 2-2. The surface and upper-air meteorological monitoring site locations are plotted in Figure 2-2 and listed in Table 2-3. The wind observations were first preprocessed to provide hourly data for 18 vertical levels as listed in Table 2-4. Three-hourly plots of the averaged wind data for each category are presented in Appendix E. Mixing-height estimates derived from radar wind profiler (RWP) data were averaged in a fashion similar to that used for the winds. Maximum mixing height estimates for Banning and San Bernardino monitoring

sites represent the daytime mixing height conditions in the SoCAB, while the average of maximum mixing height estimates for the Barstow, Hesperia, Mojave, Palmdale, and White Water monitoring sites represent the mixing conditions in the MDAB/SSAB (previously SEDAB). These values are summarized in Table 2-5.

Several notable surface and upper-level airflow features are characteristic of many of the ozone-concentration categories; some categories (such as the "High-High" and the "High-Moderate" classes) exhibit similar surface characteristics, but different airflow characteristics aloft. Those features that enable one to distinguish among the categories include (1) wind direction aloft at Banning and Cajon Passes, (2) surface wind speeds over the Los Angeles Basin, (3) extent and timing of sea-breeze development, and (4) maximum mixing height. Composite winds and mixing heights for each of the categories are described, compared, and contrasted in the remainder of this section.

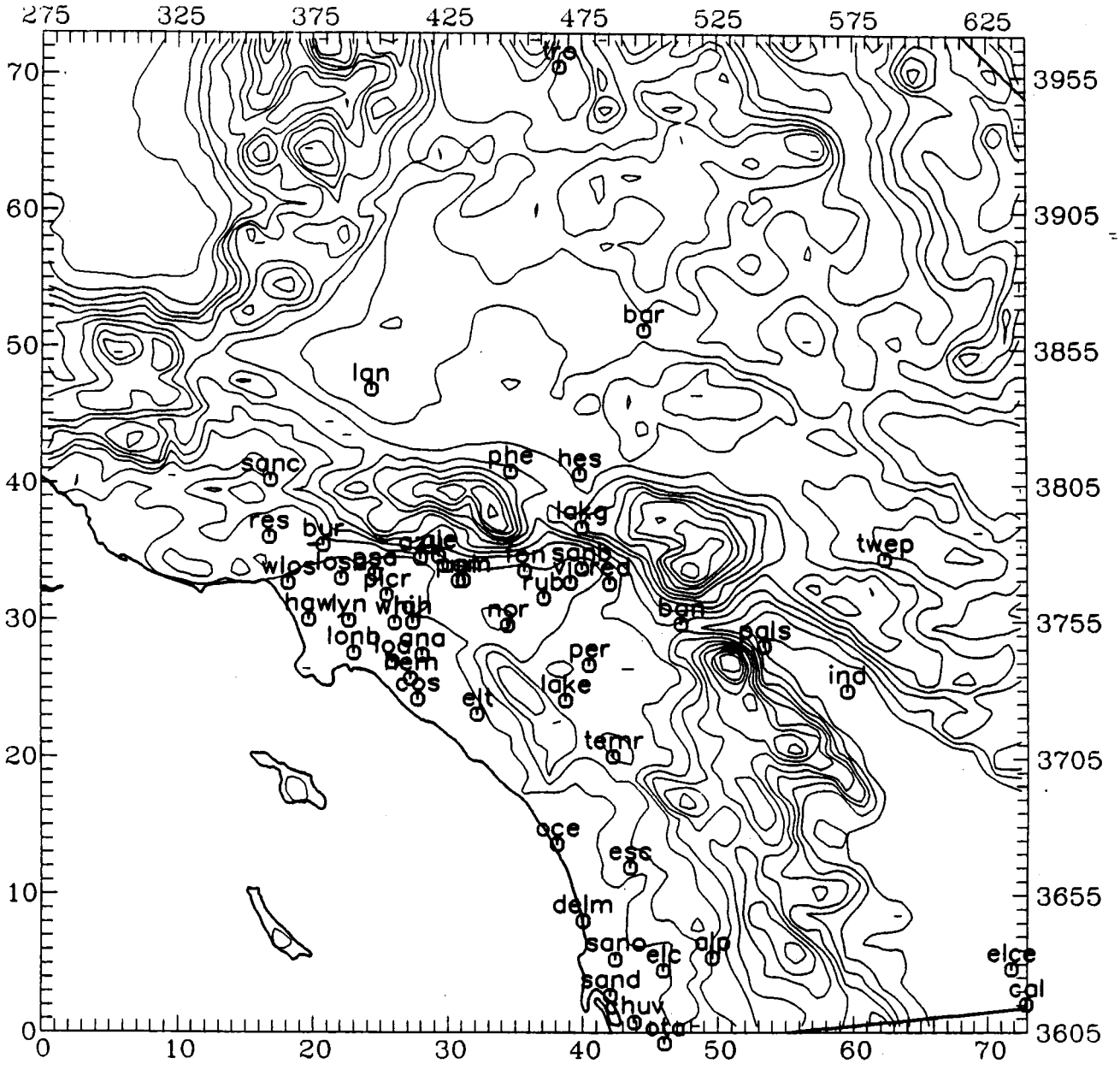

FIGURE 2-1. Air quality monitoring stations used in the data analysis.

TABLE 2-1. Air quality monitoring sites included in the data

ID	Site Name	UTM Easting	UTM Northing
alp	Alpine	523.40	3632.65
ana	Anaheim	415.48	3742.44
azu	Azusa	414.91	3777.41
ban	Banning	511.68	3753.96
bar	Barstow	497.84	3861.20
bur	Burbank	378.70	3782.27
cal	Calexico	640.36	3615.94
chuv	Chula Vista	494.74	3609.28
cos	Costa Mesa	413.81	3726.29
delm	Del Mar	475.39	3645.86
elc	El Cajon	505.46	3627.97
elce	El Centro	634.68	3628.92
elt	El Toro	435.97	3720.88
esc	Escondido	493.08	3665.26
fon	Fontana	453.42	3773.10
gle	Glendale	421.53	3778.24
haw	Hawthorne	373.47	3755.11
hem	Hemet	411.23	3733.73
hes	Hesperia	473.84	3808.35
ind	Indio	572.82	3729.93
lah	La Habra	412.12	3754.18
lake	Lake Elsinore	468.84	3725.98
lakg	Lake Gregory	474.75	3789.04
lan	Lancaster	396.32	3839.08
loa	Los Alamitos	404.47	3739.80
lonb	Long Beach	390.00	3743.04
losa	Los Angeles	385.40	3770.11
lyn	Lynwood	388.19	3754.77
nor	Norwood	447.18	3753.30
oce	Oceanside	465.80	3673.67
ota	Otay Mesa	505.87	3601.43
pals	Palm Springs	542.40	3745.98
per	Perris	477.58	3738.89
phe	Phelan	448.26	3809.35
picr	Pico Rivera	402.28	3764.13
pom	Pomona	430.72	3769.64
psa	Pasadena	397.76	3771.76
red	Redlands	485.26	3768.63
res	Reseda	358.72	3785.14
rub	Rubidoux	460.65	3763.18
sanb	San Bernardino	474.79	3773.88
sanc	Santa Clarita	359.01	3805.99
sand	San Diego - 12th Ave.	485.68	3618.84
sano	San Diego - Overland	487.52	3632.10
temr	Temecula	486.50	3705.61
tro	Trona	466.20	3957.19
twep	Twentynine Palms	586.82	3778.10
upl	Upland	428.84	3769.47
vic	Victorville	470.52	3768.94
whi	Whittier	405.28	3753.97
wlos	West Los Angeles	365.68	3768.55

TABLE 2-2. Frequency of classification combinations.

	SoCAB	MDAB/ SSAB	Frequency of Occurrence	Percent of Total Days
1	High	High	101	50
2	High	Moderate	48	24
3	High	Low	5	2.5
4	Moderate	High	6	3
5	Moderate	Moderate	25	12.5
6	Moderate	Low	3	1.5
7	Low	High	0	0
8	Low	Moderate	9	4.5
9	Low	Low	4	2

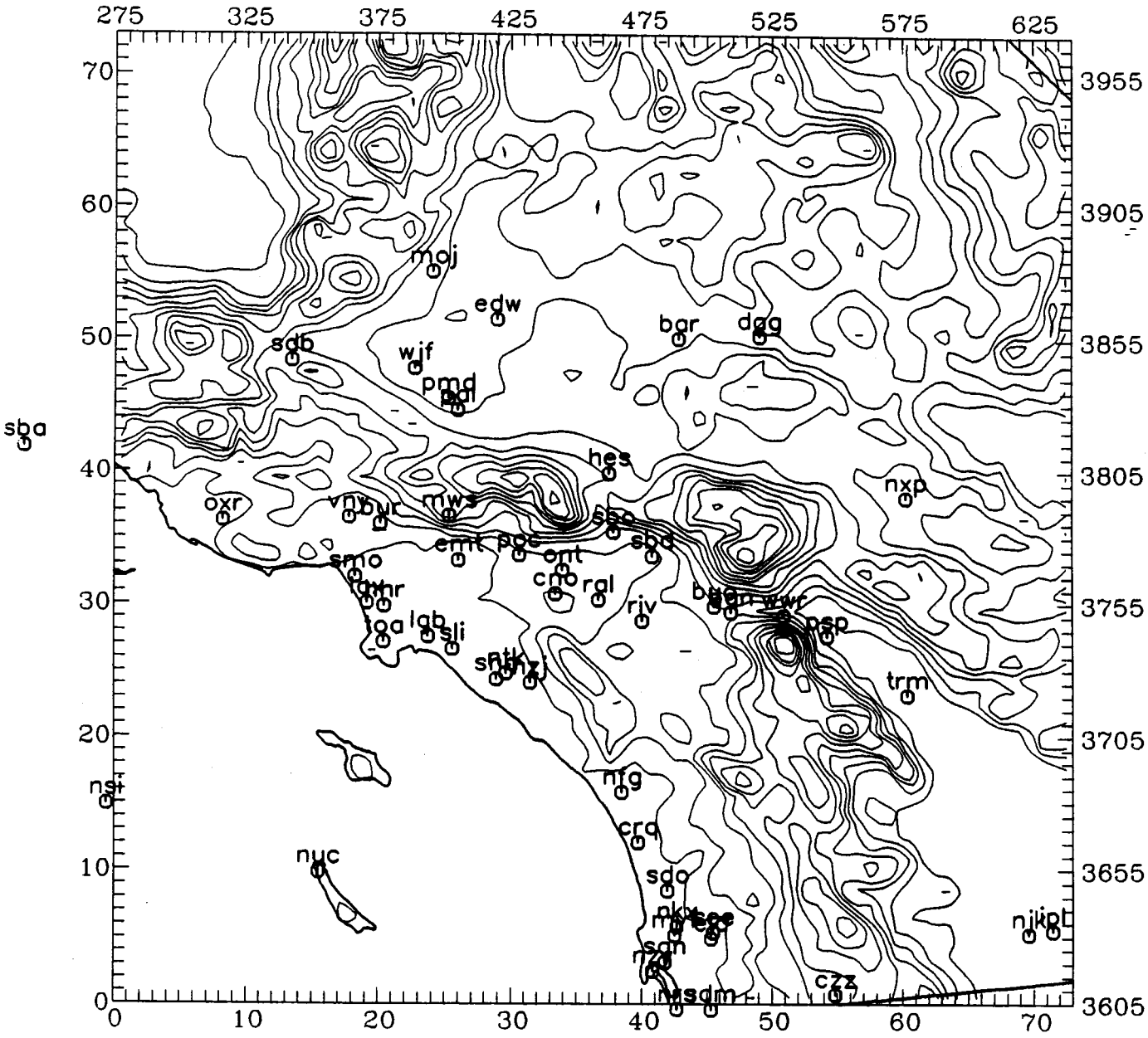

FIGURE 2-2a. Surface wind sites used in the data analysis.

High-High

Days within this category are characterized by predominant southwesterly surface winds. Air flow through the passes from the SoCAB to the MDAB/SSAB (previously SEDAB) is apparent throughout much of the day. The sea breeze dominates the airflow over the SoCAB from approximately 1000 to 2200 PST; at other times winds are light and variable. Winds aloft at 1000 and 2000 m agl maintain a westerly component through Banning Pass and a southerly component through Cajon Pass throughout most of the day. Winds along the coast (e.g., at Pt. Mugu, LAX, and San Diego) are generally northwesterly but are southerly at 2000 m agl between the hours of 1000 and 1900 PST. Maximum mixing heights (as defined earlier in this section) for this category are relatively low over the SoCAB (approximately 1000 m) and somewhat higher over the MDAB/SSAB (approximately 1300 m).

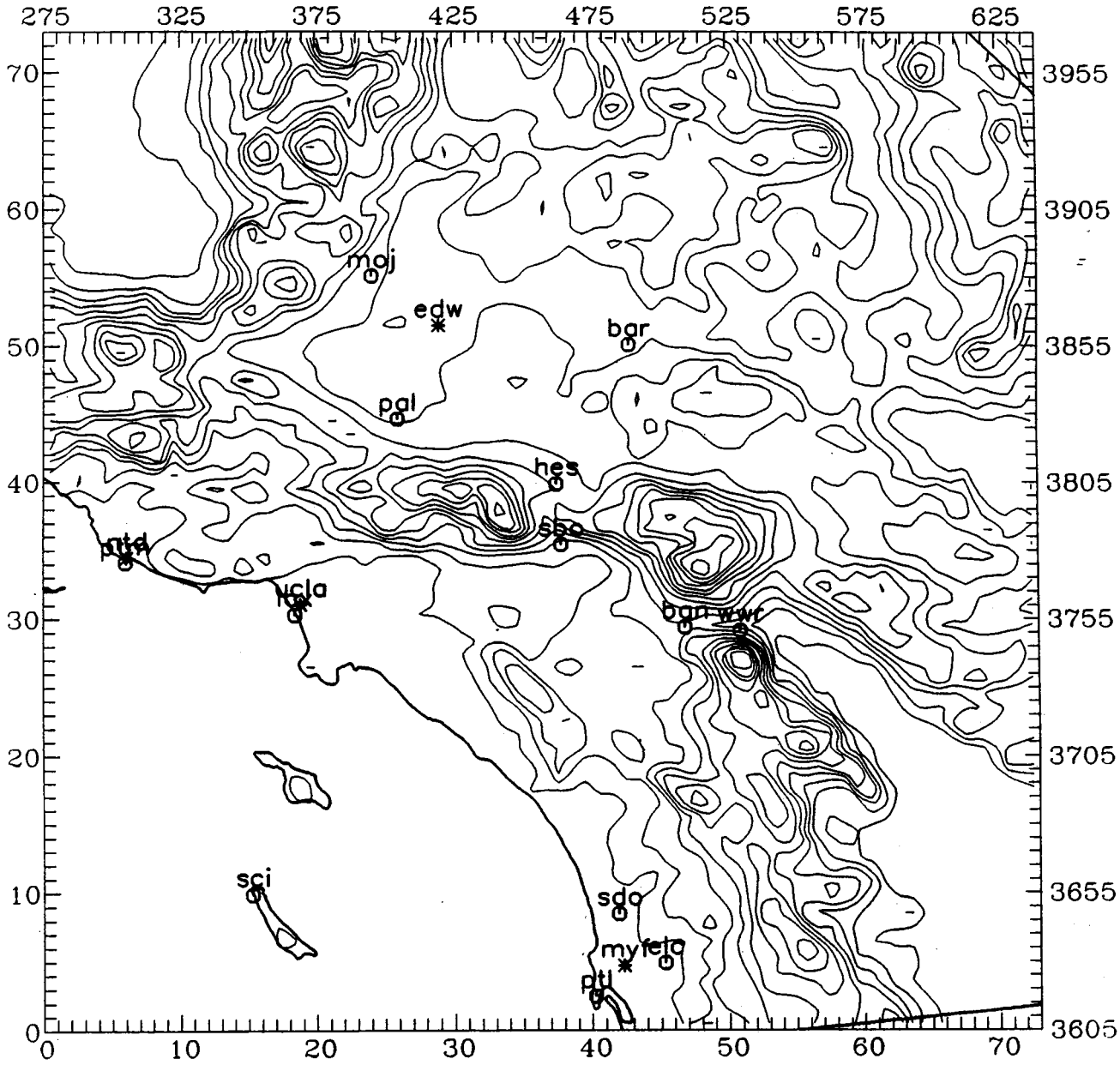

FIGURE 2-2b. Upper-air wind sites used in the data analysis.

TABLE 2-3. Meteorological monitoring sites included in the data analysis.

ID	Site Name	UTM Easting	UTM Northing
Surface Sites			
ban	Banning	509.24	3751.99
bar	Barstow	489.03	3855.11
buo	Beaumont	502.77	3754.2
bur	Burbank	375.62	3784.96
cno	Chino Airport	441.8	3758.81
crq	Carlsbad/Paloma	473.88	3665.54
czz	Campo	549.72	3609.1
dag	Daggett-Barstow	520.11	3856.23
edw	Edwards AFB	419.6	3862.11
elc	El Cajon	501.87	3630.03
emt	El Monte	404.97	3771.31
ful	Fullerton	409.4	3748.0
hes	Hesperia	462.31	3804.17
hhr	Hawthorne	377.05	3753.89
ipl	Imperial	632.91	3633.14
lax	Los Angeles Intl.	370.6	3755.08
lgb	Long Beach	393.57	3742.6
moj	Mojave	395.13	3880.1
mws	Mount Wilson	401.45	3787.98
myf	San Diego/Montgomery Field	487.83	3631.15
nfg	Camp Pendleton	467.41	3684.41
njk	El Centro	623.57	3631.91
nkx	Miramar	488.77	3634.47
nrs	Imperial Beach	488.74	3603.44
nsi	San Nicolas Island	271.69	3679.27
ntk	Tustin	423.08	3729.01
nuc	San Clemente	352.42	3654.42
nxp	Twentynine Palms	576.38	3795.54
nzj	El Toro	432.32	3725.61
nzy	North Island	479.38	3617.86
ont	Ontario Intl.	444.62	3767.67
oxr	Oxnard	315.72	3785.95
pal	Palmdale	404.62	3827.87
pmd	Palmdale Produc.	401.0	3832.35
poc	La Verne	428.05	3773.32
psp	Palm Springs	546.27	3743.23
ral	Riverside Municipal	458.42	3756.51
riv	Riverside - March Field	475.03	3748.69
san	San Diego - Lindbergh Field	484.07	3621.18
sba	Santa Barbara	239.93	3813.27
sbd	San Bernardino	478.78	3773.07
sbo	San Bernardino	464.06	3781.99
sdb	Sandberg	341.64	3846.49
sdm	San Diego - Brown	501.88	3603.43
sdo	San Diego	485.05	3647.78
see	San Diego - Gille.	502.81	3632.25
sli	Los Alamitos	402.78	3738.06
smo	Santa Monica	366.12	3765.13
sna	Santa Ana	419.35	3726.82
teh	Tehema	280.76	1106.01
toa	Torrance	376.88	3740.58

Continued

TABLE 2-3. Concluded.

ID	Site Name	UTM Easting	UTM Northing
trm	Thermal Airport	576.98	3721.25
vny	Van Nuys Airport	363.67	3787.35
wjf	Lancaster	388.3	3843.58
wwr	White Water	529.59	3750.92
Upper-Air Sites			
ban	Banning	509.24	3751.99
bar	Barstow	489.03	3855.11
edw	Edwards AFB	419.60	3862.11
elc	El Cajon	501.87	3630.03
hes	Hesperia	462.31	3804.17
lax	Los Angeles International	366.92	3756.24
moj	Mojave	395.13	3880.10
myfr	San Diego/Montgomery Field	487.83	3631.15
ntdr	Point Mugu	304.8	3776.9
pal	Palmdale	404.62	3827.87
ptl	Point Loma	476.57	3617.87
ptm	Point Mugu	304.43	3775.08
sbo	San Bernardino	464.06	3781.99
sci	San Clemente Island	351.49	3654.44
sdo	San Diego	485.05	3647.78
ucl	UCLA	369.0	3760.0
wwr	White Water	529.59	3750.92

TABLE 2-4. Vertical levels used in the preprocessing of wind data.

Level	Height (meters agl)	Level	Height (meters agl)	Level	Height (meters agl)
1	10	7	500	13	1500
2	50	8	600	14	2000
3	100	9	700	15	2600
4	200	10	800	16	3200
5	300	11	1000	17	4000
6	400	12	1200	18	5000

TABLE 2-5. Maximum mixing heights for the classification combinations.

	SoCAB	MDAB/ SSAB	SoCAB – San Bernardino	SoCAB – Banning	MDAB/ SSAB Average
1	High	High	978	1064	1295
2	High	Moderate	1130	1053	1191
3	High	Low	1508	1176	1655
4	Moderate	High	1416	1409	1430
5	Moderate	Moderate	1402	1402	1218
6	Moderate	Low	1100	1243	1403
7	Low	High	-	-	-
8	Low	Moderate	1144	1061	1273
9	Low	Low	1609	1292	1305

High-Moderate

While surface wind patterns are similar to the high-high case, flow through the Banning Pass is less persistent at the 1000 and to a lesser extent, 2000 m agl levels. Winds near Banning Pass do not become westerly at 1000 m until after 1600 PST and thus indicate a reduced mass flux from the SoCAB into the MDAB/SSAB (previously SEDAB) compared to the high-high days. Maximum mixing heights are similar for the two air basins.

High-Low

Surface winds are characterized by sea-breeze development along the coast. Despite a somewhat vigorous sea breeze at the coast and across the basin, flow through the passes is not indicated. Surface winds over the MDAB/SSAB (previously SEDAB) maintain a northerly component through 1600 PST for the high-high and high-moderate cases. For the high-low case, surface winds over the former SEDAB are southwesterly throughout the afternoon. At 1000 m agl, winds are from the north over Cajon Pass and from the east over Banning Pass for most hours of the day. At 2000 m agl, winds are variable over the passes. Thus the potential for transport from the SoCAB to the MDAB/SSAB is lower for this case compared to the high-high and high-moderate cases; but some pollutant transport from the MDAB/SSAB to the SoCAB is indicated. Compared to those for the other categories, maximum estimated mixing heights for the former SEDAB are relatively high (greater than 1600 m). Increased ventilation in the former SEDAB may have contributed to the lower observed ozone concentrations.

Moderate-High

Similar to the high-high case, surface winds for this category are characterized by sea-breeze development and inland penetration of the onshore flow. Westerly winds are evident at both Riverside and San Bernardino in the afternoon. Strong southwesterly winds (6–8 m s^{-1}) characterize the airflow in the Antelope Valley. Winds aloft are, however, somewhat different from the high-high case. Westerly flow through Banning Pass is established at 1000 m agl after 1600 PST. At 2000 m agl, winds along the coast are generally northwesterly, while winds over the MDAB/SSAB (previously SEDAB) are more variable and southerly at times.

Another difference between the high-high and the moderate-high days is the estimated maximum mixing heights for the Los Angeles Basin. As indicated in Table 2-5, maximum mixing heights for both the San Bernardino and Banning sites are 20–30 percent lower for high ozone days than for moderate ozone days in the SoCAB. The mixing heights for the moderate-high case are comparable for the SoCAB and the MDAB/SSAB (previously SEDAB).

Moderate-Moderate

Surface winds are very similar to those for the high-high and moderate-high categories. Wind speeds within the MDAB/SSAB (previously SEDAB) are generally higher, however, for the moderate-moderate case, especially during the morning hours. Wind directions within the air basin previously referred to as the SEDAB are also more uniform (generally westerly to southwesterly). The 1000 m agl winds indicate flow through both Banning and Cajon

Passes for most of the day. Flow through the passes is more pronounced and wind speeds over the former SEDAB are somewhat stronger than for the moderate-high days. At 2000 m agl, winds along the coast (e.g., at Pt. Mugu, LAX, and San Diego) are predominantly from the northwest near 2-4 ms^{-1}. Note that this is a feature that distinguishes this category from the high-high and high-moderate categories. Maximum mixing height estimates are near 1400 m for the SoCAB but lower (approximately 1200 m) for the MDAB/SSAB (previously SEDAB).

Moderate-Low

The composite wind data for this category indicate early sea-breeze development along the coastline. Winds within the interior of the SoCAB are light and variable until approximately 1600 PST, when the sea breeze penetrates into this region. Surface winds over the northern MDAB are more southerly than for the moderate-moderate case. Winds over Banning Pass are easterly to southeasterly during the first half of the day and westerly during the second half of the day for the 1000 and 2000 m agl levels. Winds near Cajon Pass are variable, although a southerly component is apparent during some morning and afternoon hours. In this regard, winds aloft most resemble those for the high-low day and do not suggest significant interbasin transport. Maximum mixing heights are relatively low in the SoCAB (1100 and 1243 m) and near average in the MDAB/SSAB (previously SEDAB) (1403 m).

Low-High

No days during the 1992 study period were characterized by low ozone concentrations in the SoCAB and high concentrations in the MDAB/SSAB (previously SEDAB).

Low-Moderate

A sea breeze develops during the mid-morning period; the onshore flow and winds across the SoCAB have a southerly component. Unlike most of the other categories, this category is characterized by persistent northwesterly winds over the Coachella Valley. The typical airflow in this area is downvalley (northwesterly) flow during the nighttime and upvalley (southeasterly) flow during the day. Flow through Banning and Cajon Passes is apparent throughout the day. Surface winds are organized and wind speeds are relatively strong. Winds at 1000 m agl are southwesterly at Banning, White Water, and San Bernardino for most of the day, except along the coast where wind directions vary throughout the day. At 2000 m agl, winds veer from southwesterly in the morning to westerly and northwesterly during the afternoon.

Low-Low

A sea breeze develops in mid-morning, but winds within the SoCAB are unorganized throughout the day. Westerly flow appears at Banning during mid to late afternoon. Southerly winds dominate at Cajon Pass and Hesperia for most of the day. Afternoon surface winds are from the southwest at speeds between 8 and 10 m s^{-1} in the Antelope Valley and from the northwest in the Coachella Valley. At 1000 and 2000 m agl, winds are from the southwest at Cajon Pass but from the east at Banning Pass during the most of the day. Maximum mixing height estimates for the SoCAB range from moderate (approximately 1300

m) for Banning to relatively high (approximately 1600 m) for San Bernardino. Estimates for the SEDAB result in an average of approximately 1305 m.

AIRCRAFT DATA

Additional meteorological and air quality data were collected during the 1992 Southern California Transport Study using an instrumented aircraft (Anderson et al., 1993). The aircraft was flown on selected days (typically twice per day) and along selected flight paths. Aircraft data are available for the SEDAB for the following days: 27 July, 30 July, 1 August, 4 August, 9 August, and 13 August 1992. An example of a typical flight path is provided in Figure 2-3; additional detail on the aircraft sampling program is provided in the referenced report. Measurements/reported parameters include: time, position, altitude, temperature, dew-point temperature, turbulence, backscatter, ultraviolet and total solar radiation, ozone, and NO-NO_x.

Four of these days for which aircraft measurements were available for the MDAB/SSAB (previously SEDAB) (27 July, 30 July, 1 August, and 9 August) were classified (as described previously) as high-high days.

- For 27 July, ozone concentrations aloft during the morning flight (0413 to 0808 PST) are low (on the order of 50 ppb) but layers of higher ozone aloft are apparent for most spiral locations (as illustrated in Figure 2-4, three layers of ozone aloft are indicated for Rialto). For Barstow (Figure 2-5), the highest ozone is within the lowest 600 m. Both of these features disappear by the time of the afternoon flight (1406 to 1747 PST). At this time ozone is relatively constant throughout the mixed layer at most sites, and the highest concentrations are found in this layer.
- For 30 July, data from the morning flight (0421 to 0744) also indicate the presence of layers of high ozone aloft. The vertical distribution patterns for ozone are generally similar to those for 27 July (Figures 2-6 and 2-7), but the concentrations are higher (in excess of 100 parts per billion by volume ppbV at some sites). There was no afternoon flight on 30 July.
- August 1 is also characterized by layers of high ozone aloft during the morning hours (0403 to 0720 PST). This is especially apparent for Rialto (Figure 2-8) where the maximum ozone concentration exceeds 15 pphmV (150 ppbV). The vertical distribution of ozone at Barstow (Figure 2-9) is different from that for 27 and 30 July (the highest ozone concentrations are not within the lowest 600 meters of the atmosphere but are found at a height of approximately 1000 m agl). During the afternoon hours (1405 to 1710 PST), the highest ozone concentrations are found in the mixed layer. A day-to-day build-up of ozone is indicated.
- For 9 August, layers of high ozone aloft characterize the morning hours (0408 to 0738 PST) for most spiral locations (Figures 2-10 and 2-11). The afternoon profiles (1420 to 1738 PST) indicate some variations in the ozone distributions aloft, especially over the Mojave, Barstow, and Banning locations.

Two of the six days were classified as high-moderate: 4 August and 13 August 1992. Note, however, that the maximum ozone concentration in the SoCAB for 4 August is just over the cut-off for this classification. The ozone concentration profiles for these days are not clearly distinguishable from those for the high-high category days.

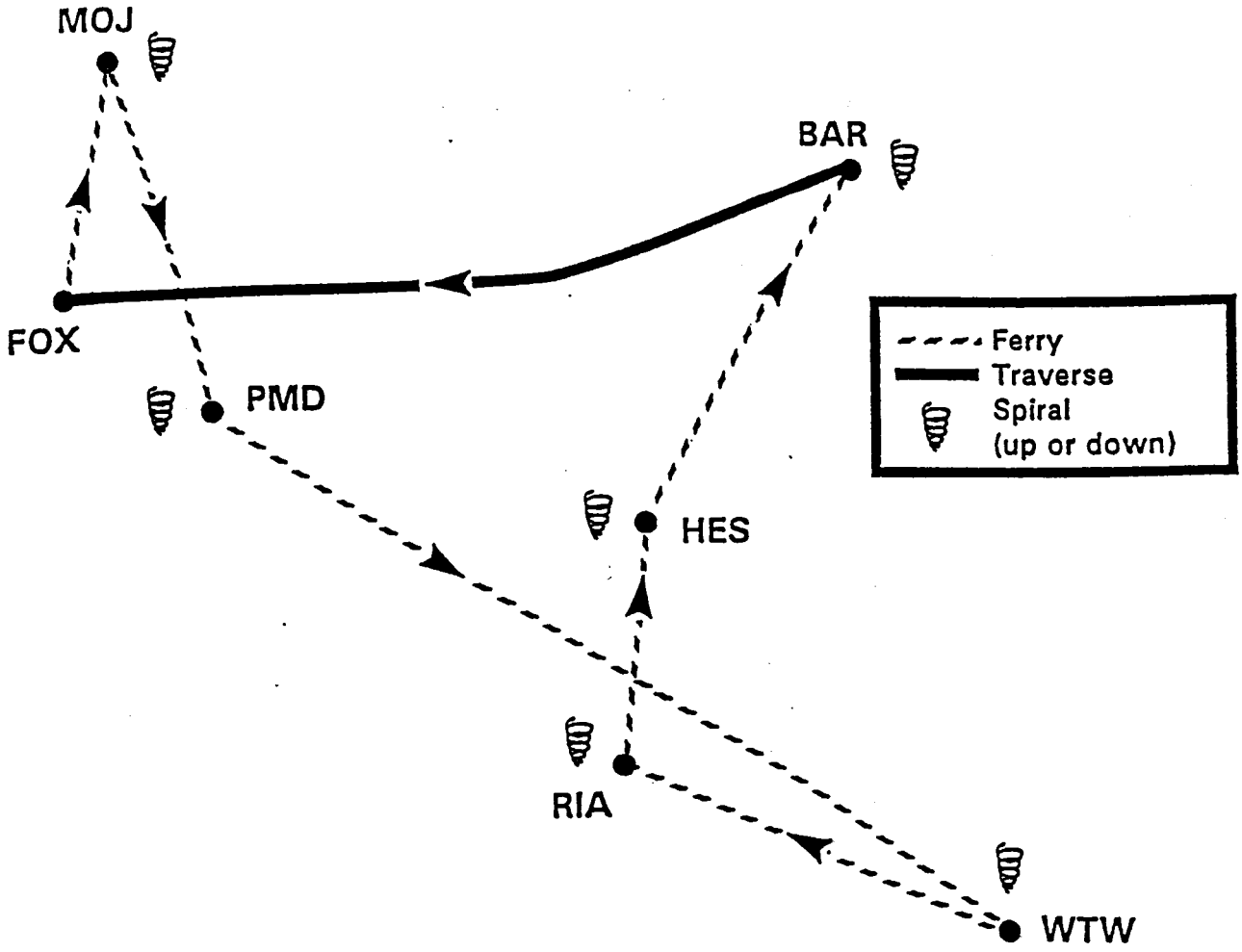

ID.	LOCATION DESCRIPTION	LATITUDE	LONGITUDE
RIA	Rialto Airport	33°07.7	117°24.2
HES	Hesperia Profiler site	34°24.0	117°24.1
BAR	Profiler site near Barstow	34°50.9	117°07.7
FOX	General Fox Airport	34°44.5	118°13.1
MOJ	Mojave Airport	35°03.5	118°09.0
PMD	Profiler site near Palmdale	34°35.6	118°02.2
WTW	Profiler site near Whitewater	33°54.5	116°45.5

FIGURE 2-3. Sample flight path for the SEDAB aircraft flights. (Source: Anderson et al., 1993).

- For 4 August, the morning profiles (0406 to 0737 PST) indicate some higher ozone aloft (compared to the surface); examples for Rialto and Barstow are provided in Figures 2-12 and 2-13. During the afternoon, the mixed layer is clearly discernible in the spirals for most locations. However, concentrations over Banning indicate higher ozone aloft, even during the afternoon hours (Figure 2-14).
- For 13 August, elevated layers of ozone are very apparent for the Rialto morning spiral (Figure 2-15) but the data for Barstow are missing. Higher ozone aloft than at the surface was also observed during the afternoon flight.

Although not the focus of this analysis, note that aircraft data are also available for the SDAB for 2 November 1992. An example flight path for the SDAB is provided in Figure 2-16. As illustrated by the spiral for Palomar Airport in Carlsbad (Figure 2-17), a layer of ozone aloft was observed during the morning flight (0659 to 10 PST). This day was not placed into one of the classification categories but moderate ozone concentrations (between 9 and 12 pphmV) were recorded. Concentrations within the SoCAB were low on both 1 and 2 November.

SUMMARY

Analysis of the composite surface and upper-level winds and maximum mixing heights for the nine different ozone classification couples for the SoCAB and MDAB/SSAB (previously SEDAB) indicates numerous similarities in the airflow patterns for all days of the 1992 study period but also some differences in both the winds and the mixing heights that enable one to distinguish among the categories. In reviewing the results of this analysis, it is important to keep in mind that the composite winds and mixing heights represent averages of the data for all days within the classification categories. As presented in Table 2-2, the total number of observations that were used in calculating the averages varied among the categories (according to the number of days within each category). The averages are therefore likely more robust for the high-high, high-moderate, and moderate-moderate categories, which contain the greatest number of days, than for the other categories. All results should be considered with this in mind.

In addition, averaging of the data for all days within each classification category only yields meaningful results if the days are similar meteorologically as well as in terms of ozone distribution. Following classification of the days into the nine categories, the Classification and Regression Tree (CART) analysis technique was applied for each category to determine whether the days within each category could be further segregated into distinct meteorological regimes. The CART results indicated that the meteorological conditions were similar among the episode days within each category. Further analysis of the airflow patterns for individual days (presented in Volume III of this report) also indicates that the day-specific airflow patterns (for the 12 days examined) generally reflect those described by the composite wind data.

The results of this analysis suggest that there is a strong correlation between high ozone concentrations in the SoCAB and high concentrations in the MDAB and SSAB. During the 1992 study period, moderate to high observed ozone concentrations in the former SEDAB were almost always associated with moderate to high ozone concentrations in the SoCAB. There were no days when high ozone was observed in the former SEDAB and concentrations within the SoCAB were low. The composite winds also indicate that transport of pollutants

from the SoCAB to the MDAB/SSAB (previously SEDAB) contributes to the high observed concentrations in the air basin formerly designated the SEDAB; the composite winds suggest the possibility of pollutant transport both near the surface and aloft.

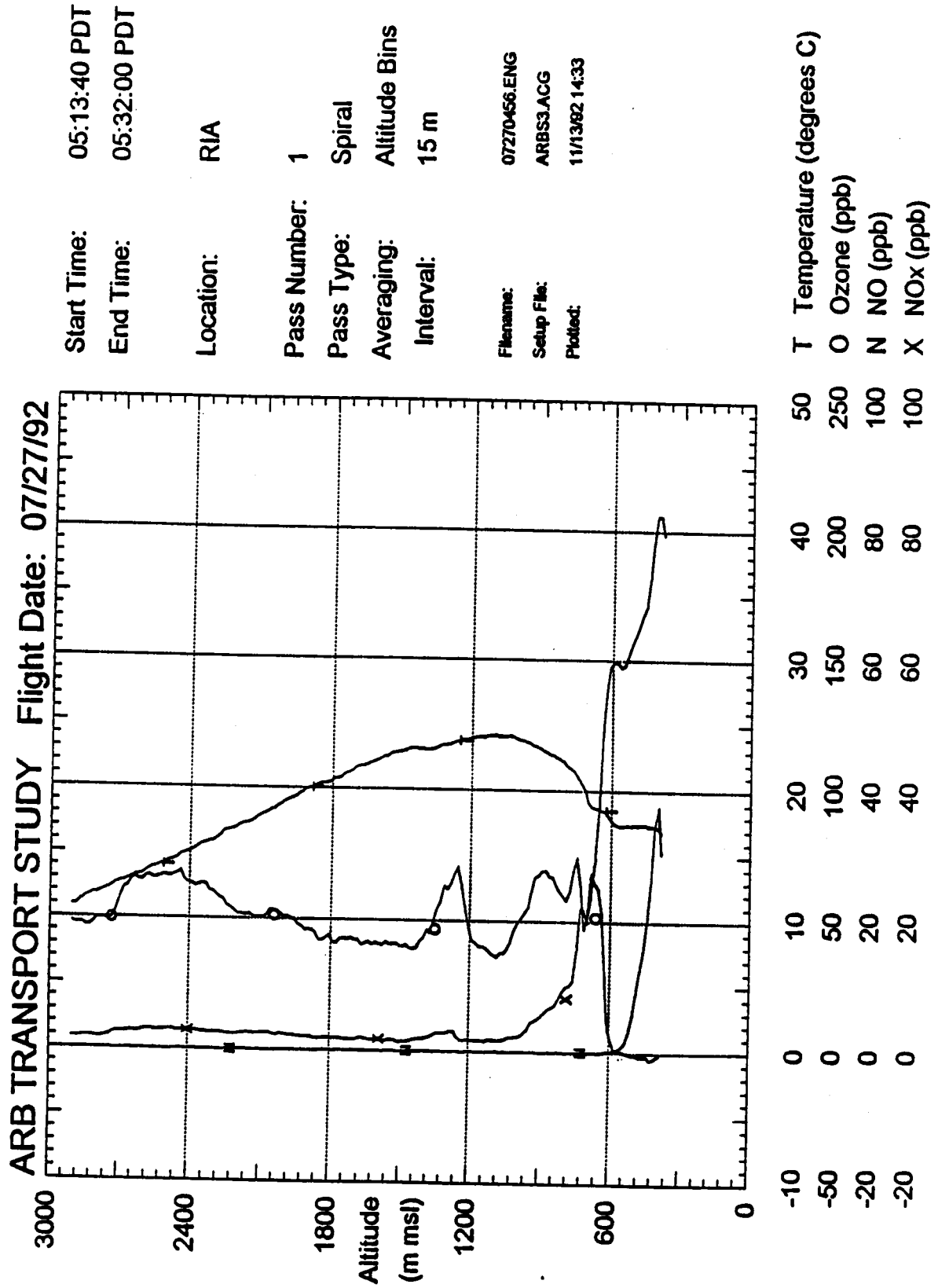

FIGURE 2-4. Vertical profiles of temperature, ozone, NO, and NO_x over the Rialto sampling location as measured by the 0413 to 0432 PST aircraft spiral for 27 July 1992. (Source: Anderson et al., 1993).

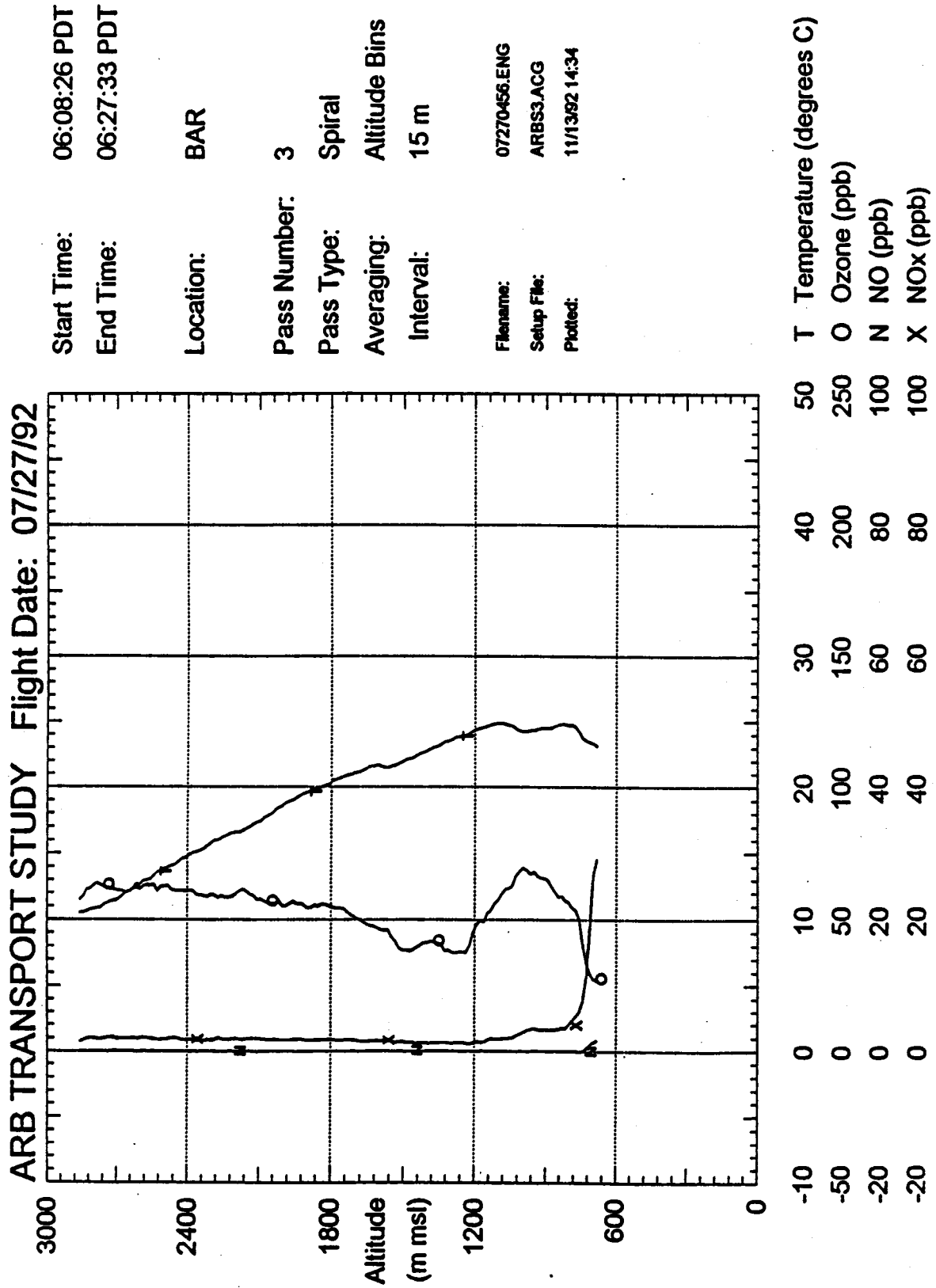

FIGURE 2-5. Vertical profiles of temperature, ozone, NO, and NO_x over the Barstow sampling location as measured by the 0422 to 0439 PST aircraft spiral for 27 July 1992. (Source: Anderson et al., 1993).

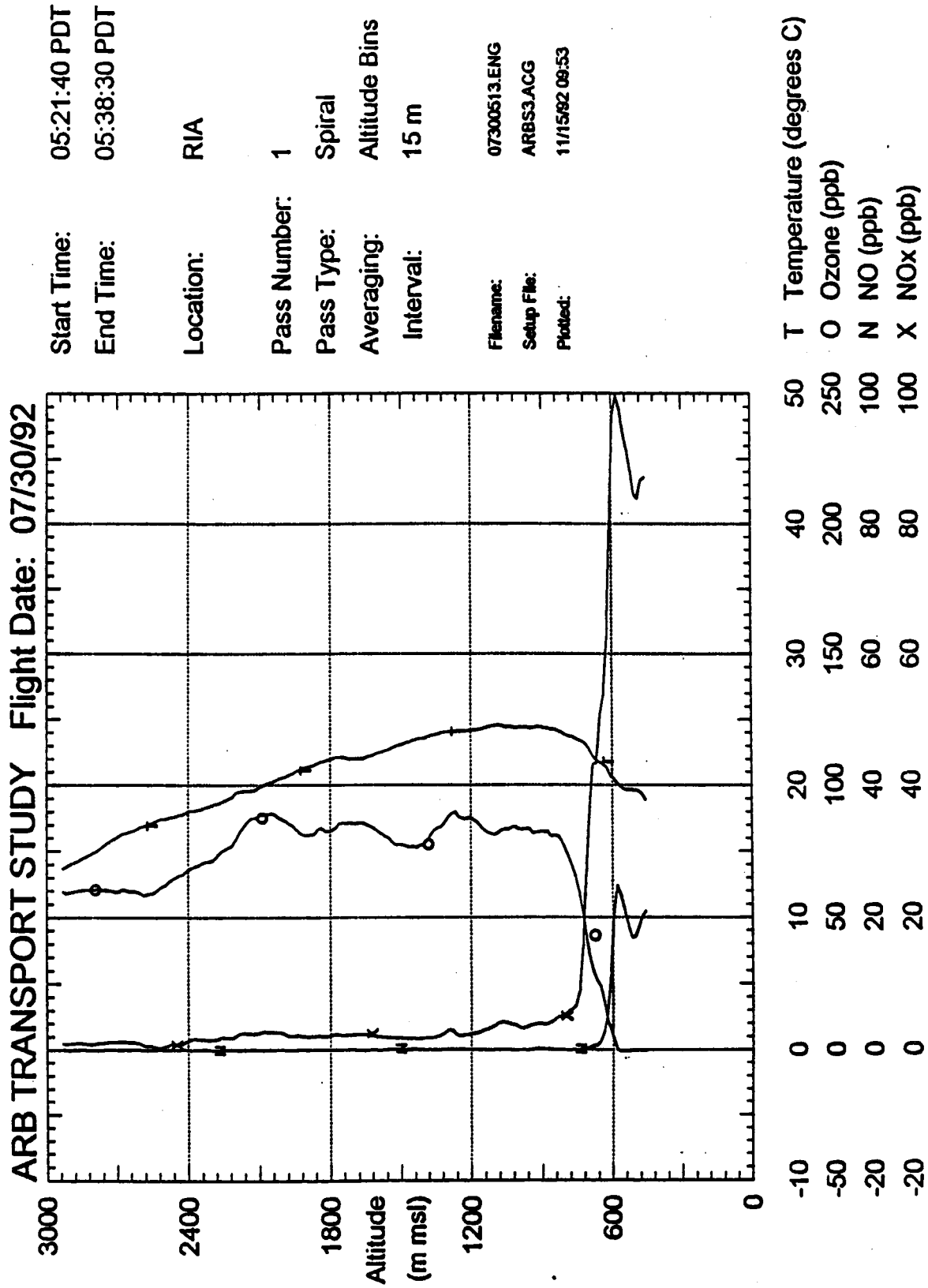

FIGURE 2-6. Vertical profiles of temperature, ozone, NO, and NO_x over the Rialto sampling location as measured by the 0422 to 0439 PST aircraft spiral for 30 July 1992. (Source: Anderson et al., 1993).

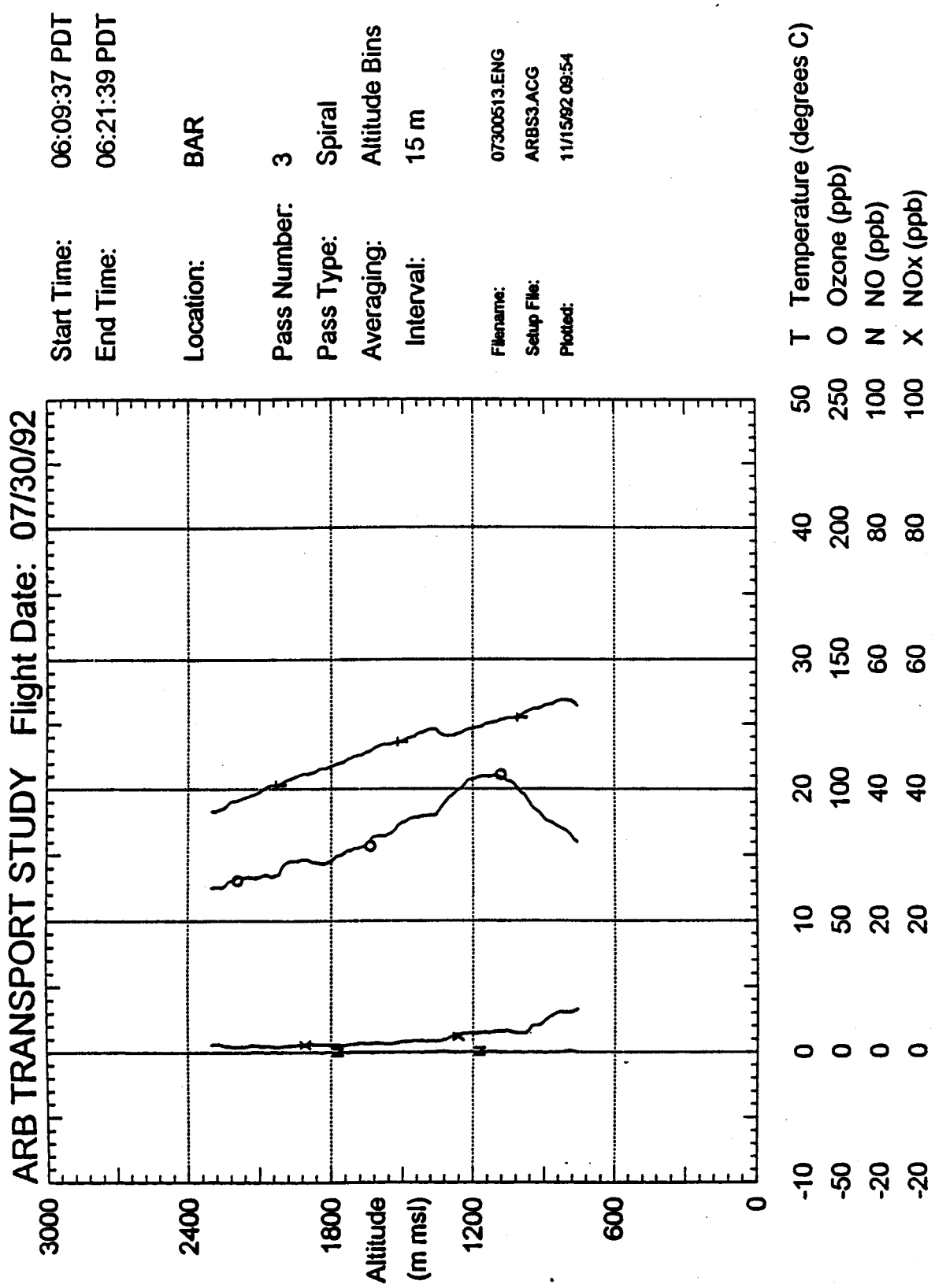

FIGURE 2-7. Vertical profiles of temperature, ozone, NO, and NO_x over the Barstow sampling location as measured by the 0510 to 0522 PST aircraft spiral for 30 July 1992. (Source: Anderson et al., 1993).

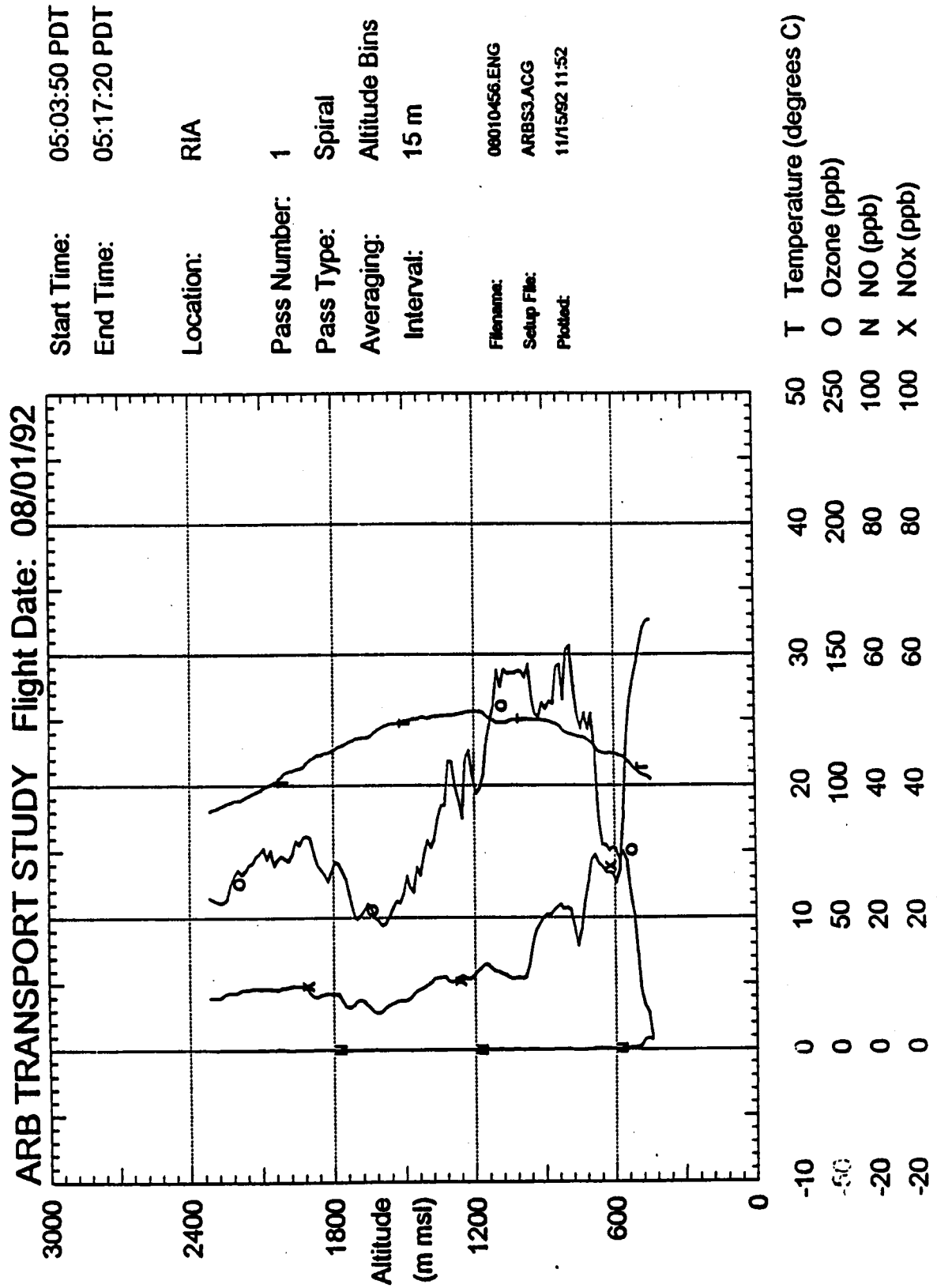

FIGURE 2-8. Vertical profiles of temperature, ozone, NO, and NO_x over the Rialto sampling location as measured by the 0404 to 0418 PST aircraft spiral for 1 August 1992. (Source: Anderson et al., 1993).

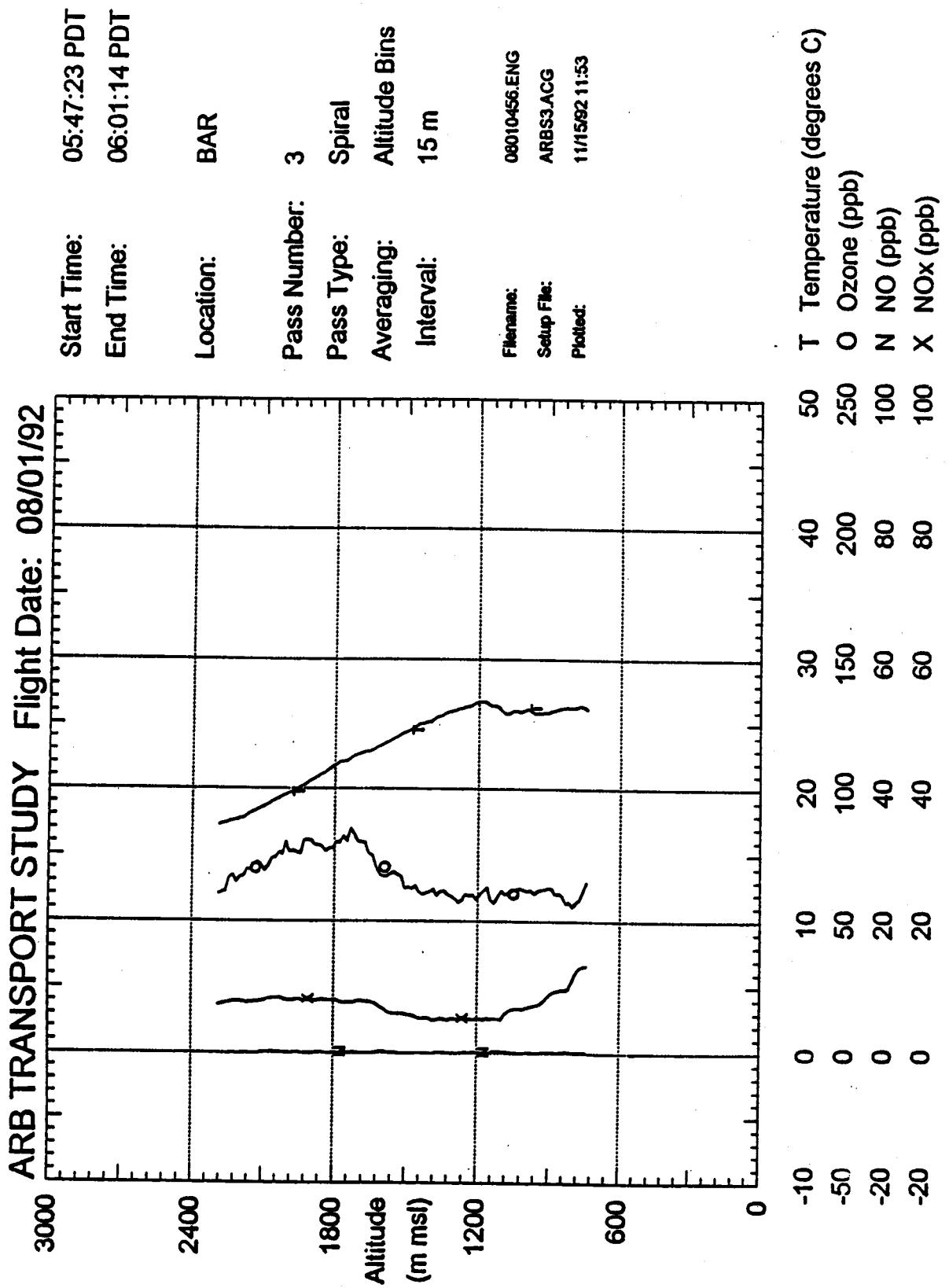

FIGURE 2-9. Vertical profiles of temperature, ozone, NO, and NO_x over the Barstow sampling location as measured by the 0447 to 0501 PST aircraft spiral for 1 August 1992. (Source: Anderson et al., 1993).

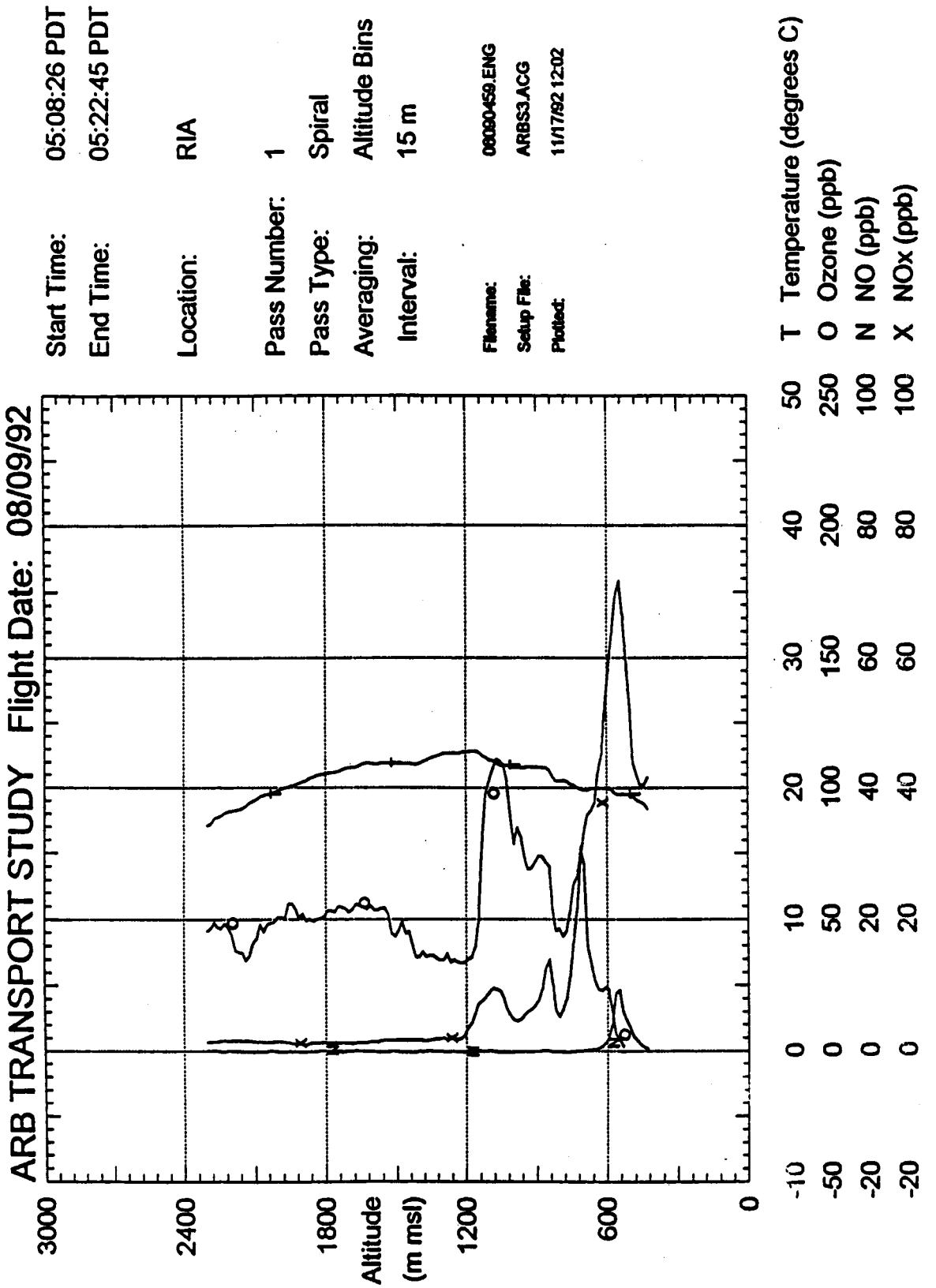

FIGURE 2-10. Vertical profiles of temperature, ozone, NO, and NO_x over the Rialto sampling location as measured by the 0408 to 0423 PST aircraft spiral for 9 August 1992. (Source: Anderson et al., 1993).

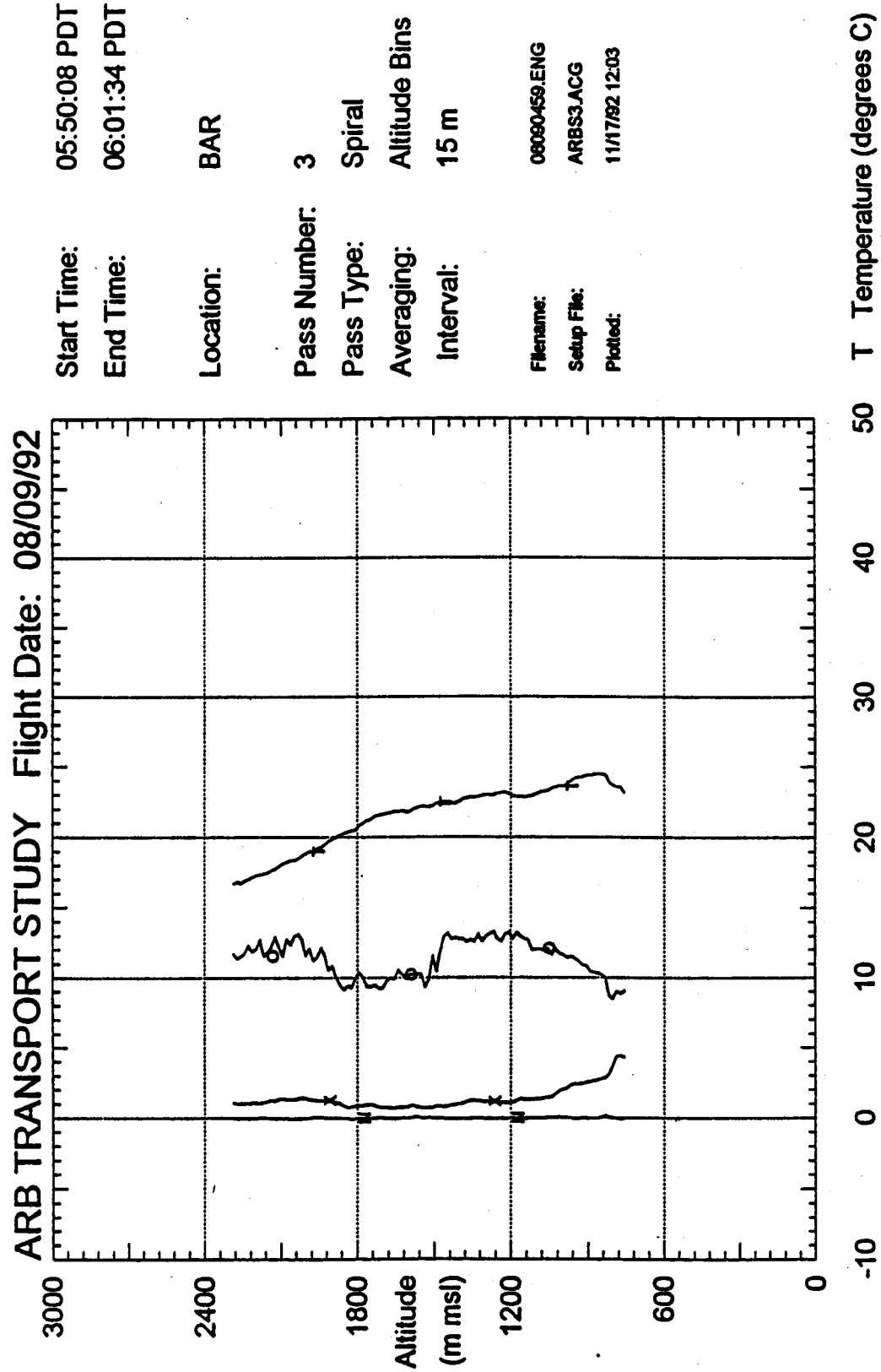

FIGURE 2-11. Vertical profiles of temperature, ozone, NO, and NO_x over the Barstow sampling location as measured by the 0450 to 0502 PST aircraft spiral for 9 August 1992. (Source: Anderson et al., 1993).

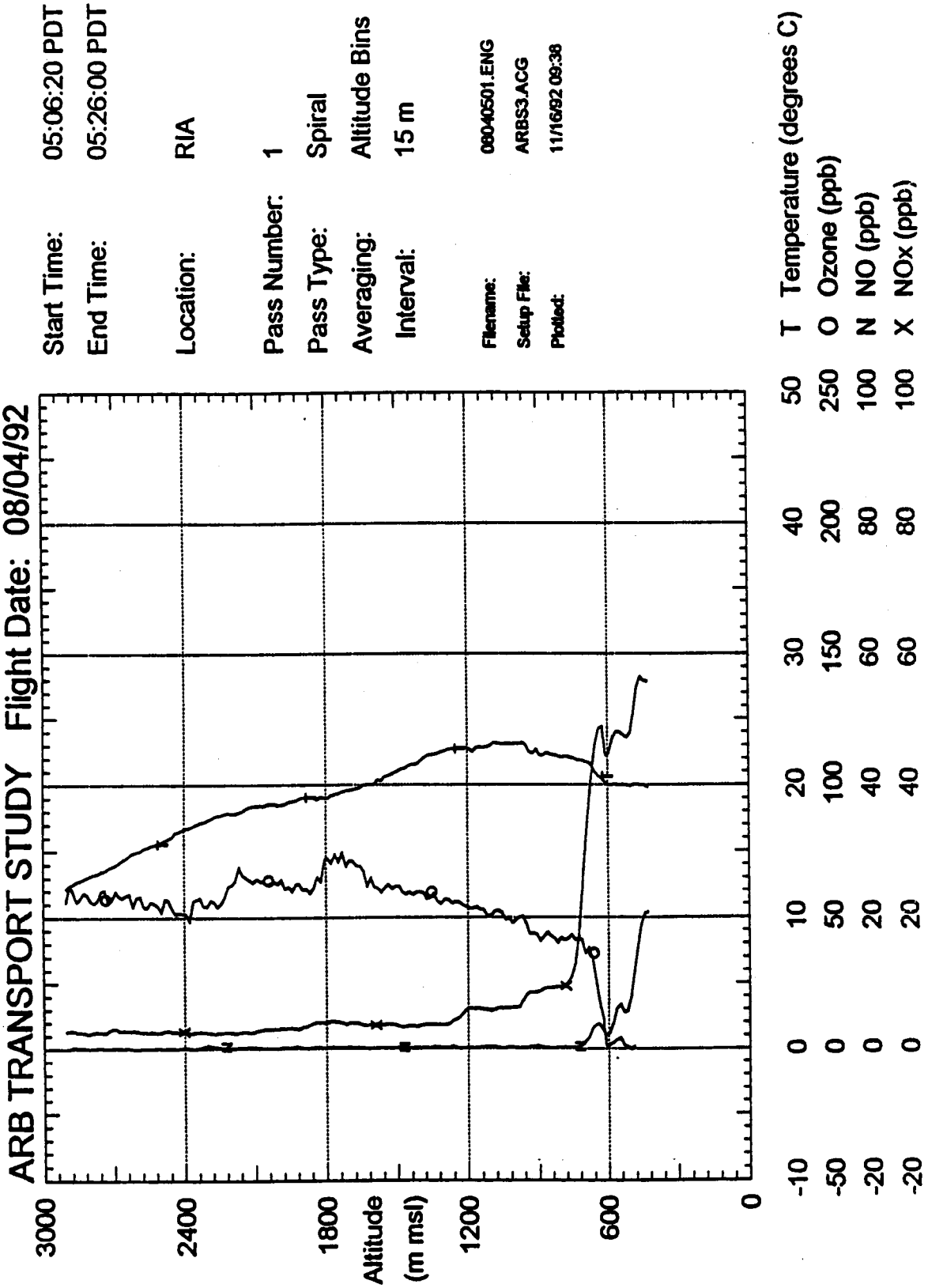

FIGURE 2-12. Vertical profiles of temperature, ozone, NO, and NO_x over the Rialto sampling location as measured by the 0406 to 0426 PST aircraft spiral for 4 August 1992. (Source: Anderson et al., 1993).

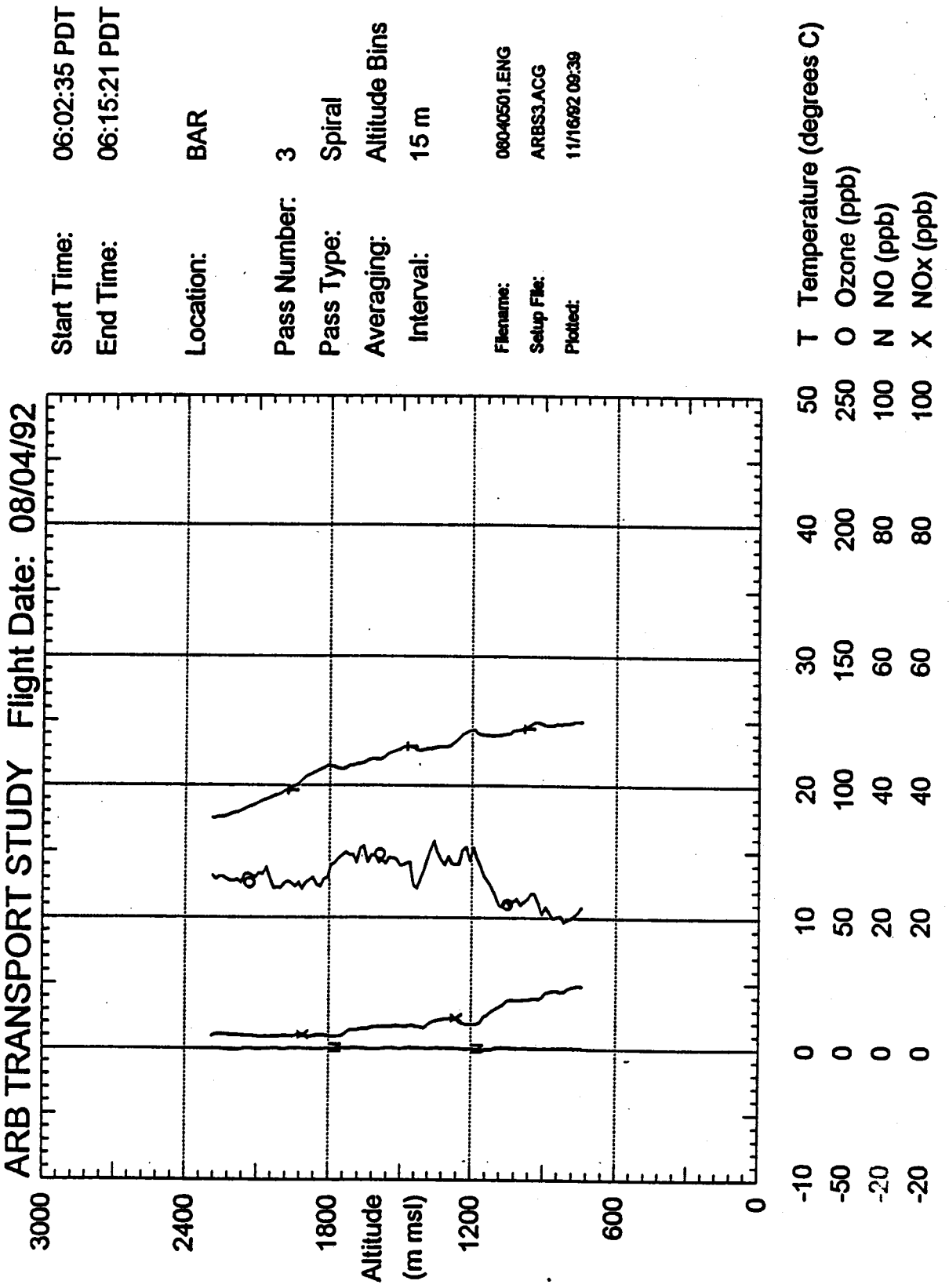

FIGURE 2-13. Vertical profiles of temperature, ozone, NO, and NO_x over the Barstow sampling location as measured by the 0502 to 0515 PST Barstow sampling location as measured by the 0502 to 0515 PST.

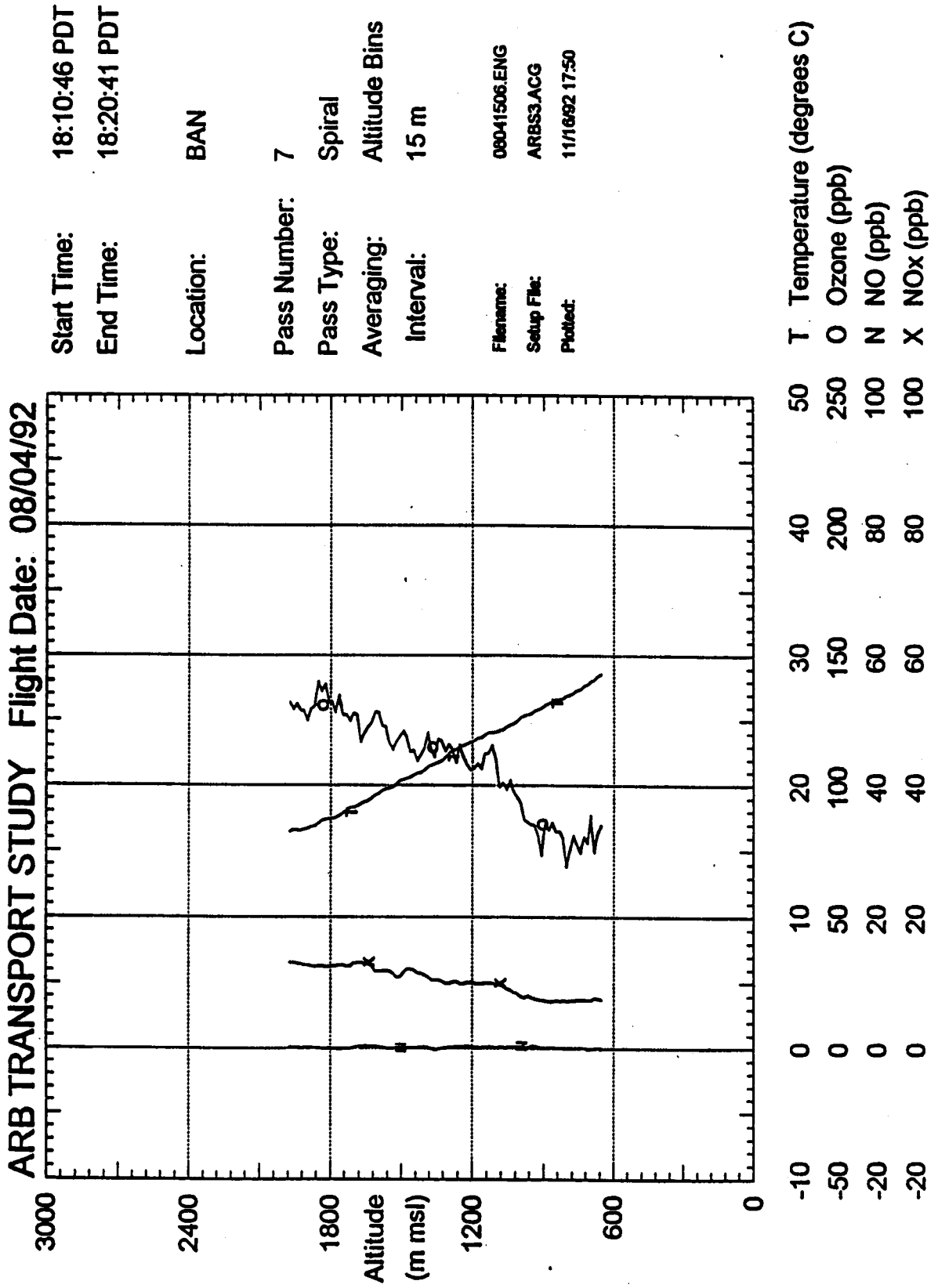

FIGURE 2-14. Vertical profiles of temperature, ozone, NO, and NO_x over the Banning Pass location as measured by the 1711 to 1721 PST aircraft spiral for 4 August 1992.

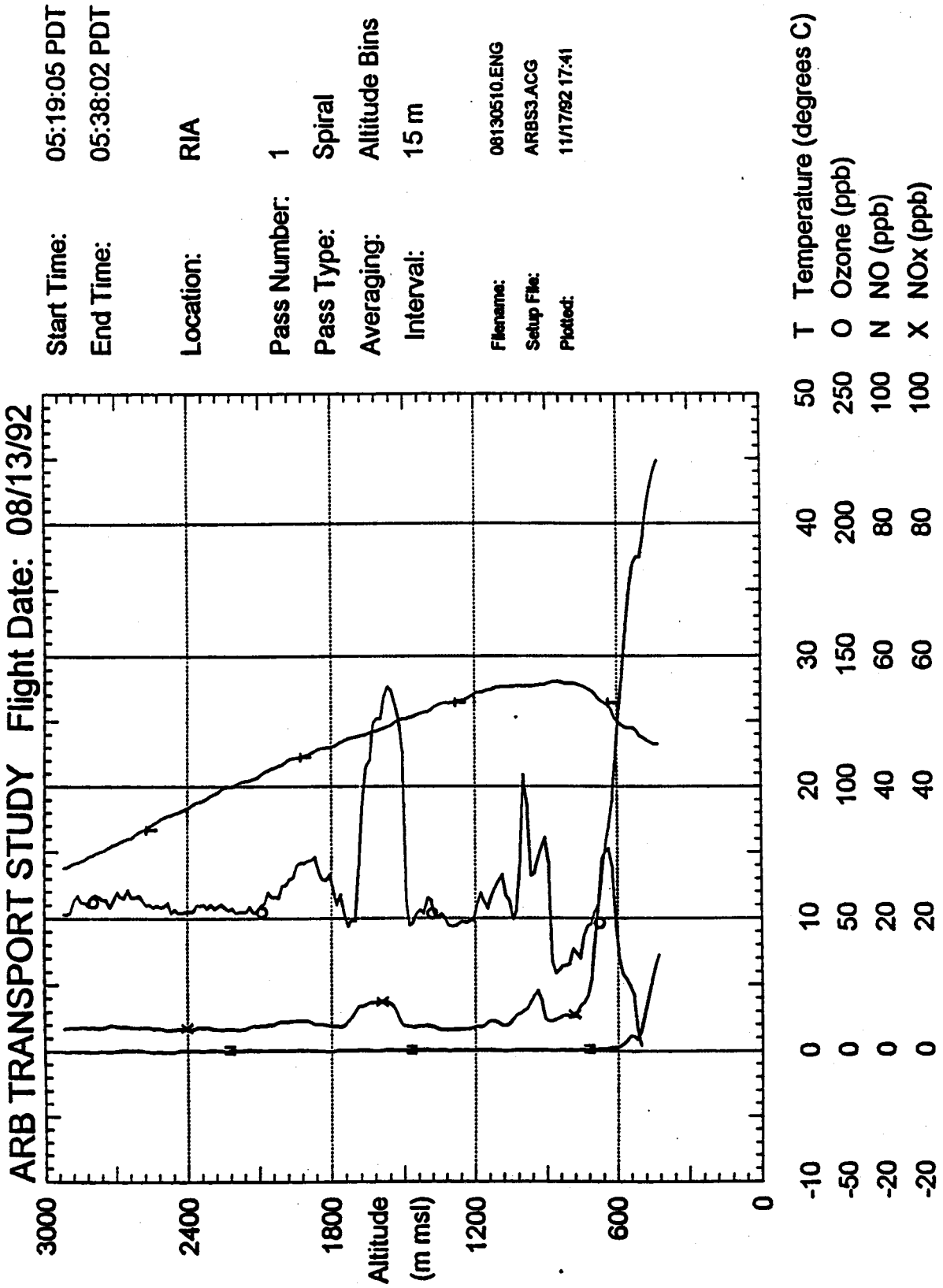

FIGURE 2-15. Vertical profiles of temperature, ozone, NO, and NO_x over the Rialto sampling location as measured by the 0419 to 0438 PST aircraft spiral for 13 August 1992.

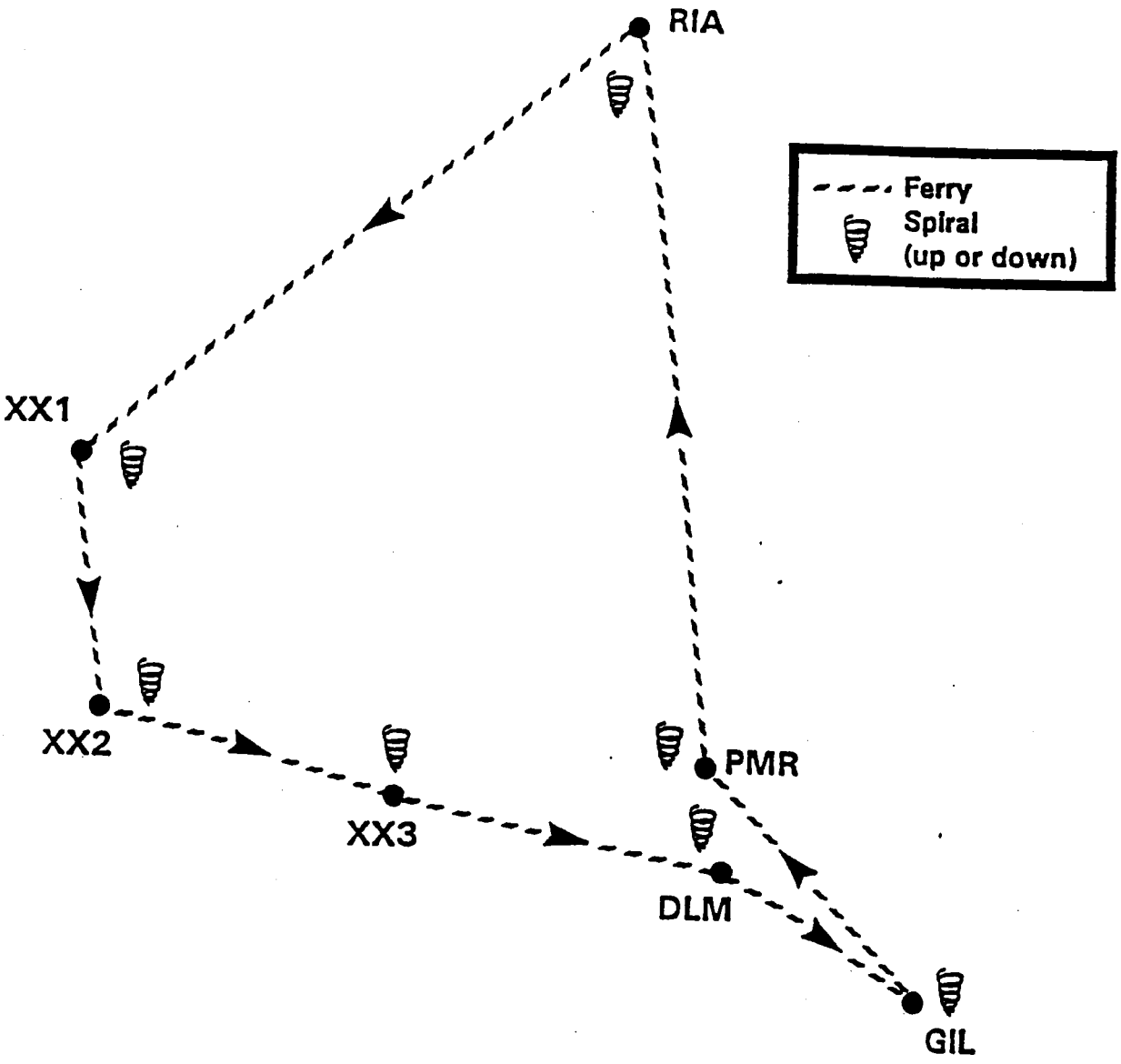

LOCATION		LATITUDE	LONGITUDE
RIA	Rialto Airport	33°07.7	117°24.2
XX1	Over-water location about halfway between Long Beach and Catalina	33°33.0	118°14.0
XX2	Over-water location about 10 miles southeast of Catalina	33°11.0	118°13.0
XX3	Over-water location about halfway between Catalina and Del Mar	33°05.0	117°45.5
DLM	Over-water location near Del Mar	32°57.5	117°17.5
GIL	Gillespie Airport	32°49.6	116°58.3
PMR	Palomar Airport	33°07.7	117°16.8

FIGURE 2-16. Sampling flight path for the SDAB aircraft flights.

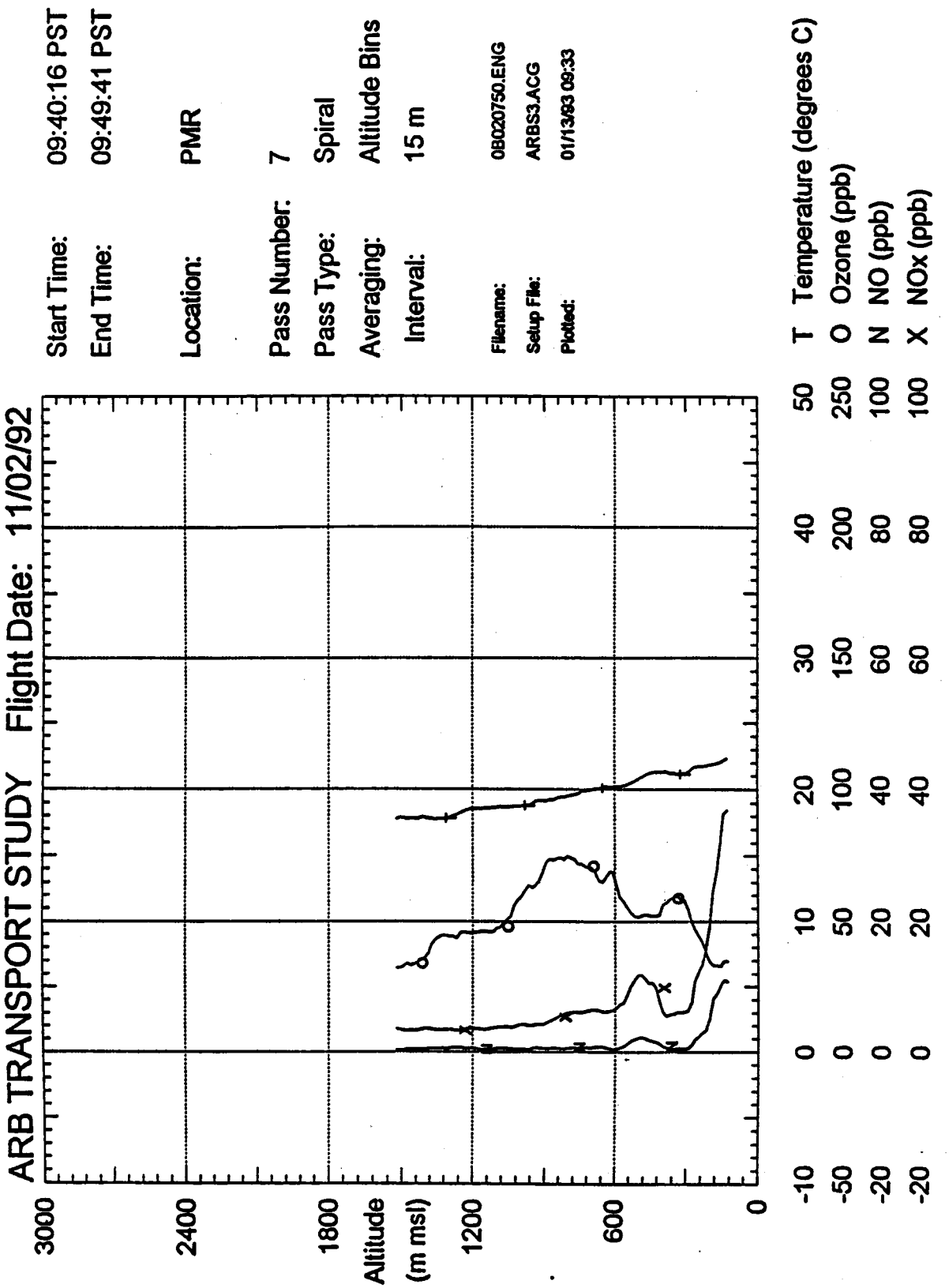

FIGURE 2-17. Vertical profiles of temperature, ozone, NO, and NO_x over the Palomar Airport sampling location as measured by the 0940 to 0950 PST aircraft spiral for 2 November 1992.

3 EVALUATION OF EPISODES IN THE MOJAVE DESERT AND SAN DIEGO AIR BASINS TO DETERMINE SHARED AND LOCAL DAYS

The objective of this phase of the study was to determine whether ozone episodes that occurred within the former SEDAB and the SDAB during the 1992 study period were the result of local emissions or the combination of local emissions and transported ozone and precursor pollutants. The Classification and Regression Tree (CART) analysis software was used to categorize the ozone episode days (with respect to meteorological and air quality conditions), and representative episodes from the major classification categories were selected for further analysis. Six episodes were selected, three distinguished by high observed ozone concentrations in the MDAB/SSAB (previously SEDAB) and three with high ozone concentrations in the SDAB. Based on this analysis, ozone episode days were classified as "local" or "shared" events; the "shared" events were further categorized as "overwhelming", "significant", or "inconsequential" transport days.

Analysis of the transport characteristics of the episodes included (1) preparation of hourly, gridded wind fields for each episode day, as well as the preceding day and (2) calculation of both two- and three-dimensional backward particle paths (trajectories). The wind fields were prepared using the Diagnostic Wind Model (DWM) (SAI, 1990). This model combines interpolation of observed wind data with the parameterization of terrain effects for those areas where data are not available. The resolution of terrain effects was important to this analysis; preliminary analysis of the radar wind profiler (RWP) data collected during the 1992 Southern California summer field study indicated that certain terrain-generated airflows, including rapidly developing downslope winds, may influence interbasin transport. Trajectories were then calculated using the gridded wind fields, and the potential for interbasin transport for the selected days, as well as meteorologically similar days (according to the results of the CART analysis), was examined.

The issue of pollutant transport between the SoCAB, MDAB, SSAB and SDAB is one that will need to be continuously examined in response to the changing emissions distributions within and among the southern California air basins. Although driven by the prevailing meteorological conditions, the extent and magnitude of pollutant transport is also influenced by the distribution of emissions sources. Consequently, changing emissions patterns (such as an expanding population to the north of the San Gabriel Mountains and an increase in commuter traffic from this area to the Los Angeles area, an increase in recreational activity in the Mojave Desert, and an increase in population in northern San Diego County) may alter the ozone and precursor transport characteristics. Thus, this type of analysis may need to be expanded and repeated for future air quality assessments.

The air quality database used for this analysis is described in Section 2 of this report. The meteorological database consists of routine and supplementary surface and upper-air wind measurements; the meteorological monitoring network is also documented in Section 2.

The CART analysis, an overview of the meteorological and air quality characteristics of the selected episode days, and methodologies and results for the wind and trajectory analyses are presented in the remainder of this section.

CART ANALYSIS

The Classification and Regression Tree (CART) analysis software is a powerful statistical analysis tool that partitions a data set into discrete subgroups based on the value of a user-defined classification variable (e.g., maximum ozone concentration). The remaining variables in the database are selected as to whether or not they provide a predictive segregation of the data between different values of the classification variable. This restriction presupposes that there is a causal relationship between the independent variables and the dependent variable. Consequently, it is necessary to construct a database of independent variables such that this relationship can be identified.

The CART technique is designed to segregate objects or, in the case of air quality analysis, days with different values of a classification variable into different terminal nodes or "bins." It accomplishes this task through the growth of a binary decision tree via a progression of binary splits of the values of the independent variables. Each split is chosen such that the segregation of different values of the dependent variable is improved. The resulting tree has multiple branches, of various complexity, each of which represents a variable path to a series of values of the dependent variable.

CART was used in this study to group or classify both episode and non-episode days according to ozone air quality and meteorological conditions. Based on this classification, six episodes, representative of certain types of episodes, were selected for further analysis including the determination of "local" versus "shared" transport characteristics and the further description of "shared" events into subcategories "overwhelming", "significant", or "inconsequential". Because it was not feasible to perform a detailed wind/trajectory analysis for each episode day that occurred during the 1992 study period, CART provided a means to group the episode days and possibly extend the findings corresponding to a detailed analysis of a subset of the days to other days with similar meteorological and air quality characteristics.

Application of CART for the Mojave Desert and Salton Sea (Previously Southeast Desert) Air Basins

The application of CART to the former SEDAB was designed to identify SEDAB ozone episodes with similar meteorological characteristics. The value of the dependent variable used for the CART application, EPSSED, signified whether the day in question was an ozone episode day or not. The value of EPSSED was initially set equal to one (episode day) if the maximum observed ozone concentration at the Lancaster monitoring site exceeded 13 pphmV or if the ozone concentration at Barstow, Twentynine Palms, or Trona exceeded 9 pphm. Otherwise, the value was set equal to zero. Use of this dependent variable resulted in a large number of misclassified days; that is, non-episode days were put into bins designated for episode days. Upon examining ozone concentrations at the various MDAB/SSAB (previously SEDAB) monitoring sites on these misclassified days, it was found that although the set of sites used in defining an episode day did not have ozone concentrations exceeding the cutoff values, nearby sites did. In effect, CART could not distinguish between these days (based on meteorology) and classified them as high ozone days (which they were). To aid in the classification process, ozone data for additional monitoring sites were used and a new

definition was given to the dependent variable. A day was classified as an ozone episode day (EPSSED=1) if the ozone concentration at Lancaster, Hesperia, Victorville, or Phelan exceeded 13 pphm or if the ozone concentration at any other site in the MDAB/SSAB (previously SEDAB) exceeded 9 parts per hundred million by volume (pphmV) on that day. Following the application of CART, the days within each bin were examined and only those meeting the original ozone-episode criteria were considered for further analysis.

The meteorological and air variables used for the CART analysis are listed and described in Table 3-1. The variables depict wind conditions and air quality in the SoCAB, former SEDAB, and SDAB. The resultant CART classification tree (optimized by CART to minimize misclassifcation of exceedance days) consisted of 26 terminal nodes. Fourteen of these were designated exceedance nodes. A review of the classification criteria for this tree, however, suggested that not all of the binary splits represented a physically meaningful segregation of the data (at least according to known characteristics of SoCAB and MDAB/SSAB ozone episodes). The complexity of the classification tree was then reduced (by invoking an optional feature of CART) and a tree with 12 nodes (and 5 exceedance nodes) was selected as the best compromise between physically meaningful splitting or classification criteria and misclassification of exceedance days. This tree is shown in Figure 3-1. This figure gives the number of episode and non-episode days that were assigned to each node. The number of episode days as defined using the original criteria (ozone concentration that exceeded 13 pphm at Lancaster or that exceeded 9 pphm at Barstow, Twentynine Palms, or Trona) is also indicated. These comprise the candidate episode days for further analysis.

The CART classification tree for the MDAB/SSAB (formerly SEDAB) provides some useful information regarding the differences in the input parameters that are important in distinguishing between the exceedance and non-exceedance days and in identifying different categories or types of exceedance days. However, an overwhelming majority of the exceedance days (85 days in all, 38 considering the original definition of an exceedance day) are classified as belonging to Node 8. Days within this node are characterized by high ozone concentrations (greater than 12.5 pphmV) in the SoCAB, predominantly west-southwesterly surface winds at Palmdale during the afternoon hours (1500-1700 PST), and moderate wind speeds near the surface and aloft (greater than 2.5 but less than 5 ms^{-1}) at most monitoring sites in the MDAB and SSAB. According to the CART analysis results, days within this node are distinguished from other days by the first two parameters given above, then by morning wind speed at the Daggett surface monitoring sites (days within this node are characterized by higher wind speeds than other days), and finally by afternoon wind direction at the Daggett site (days with east-northeasterly winds are placed in a neighboring non-exceedance node). Combined, these features suggest that transport of ozone and/or precursor pollutants is associated with the exceedance days in this node. A representative day was selected from this node for further analysis of the transport characteristics. To avoid selecting a day for which ozone concentrations in the SoCAB were unusually high, the average maximum ozone concentration for the SoCAB for all days within Node 8 was computed and the day with the maximum ozone concentration nearest the average (29 July 1992) was selected.

The next most populated exceedance node for the MDAB/SSAB CART classification tree is Node 12 (with 10 exceedance days, 5 of which meet the original exceedance criteria and are thus candidates for further analysis). Days within this node are characterized by high ozone

TABLE 3-1. Variables used in the application of CART for the MDAB/SSAB (formerly the SEDAB)..

Dependent Variable:

EPSSED - Variable = 1 if the daily maximum ozone concentration at Lancaster, Phelan, Victorville, or Hesperia exceeded 13 pphm or the daily maximum ozone concentration at remaining sites exceeded 9 pphm.

Air Quality and Miscellaneous Variables:

SCO3MX - Maximum daily ozone concentration (pphm) in the SoCAB.
SCO3MXY - Previous day's maximum daily ozone concentration (pphm) in the SoCAB.
SEDLOC - Location of maximum daily ozone concentration in the SoCAB.
= 1 for Lucerne Valley North
= 2 for Indio to Lucerne Valley
= 3 for South of Indio
= 4 if 1 and 2
= 5 if 1 and 3
= 6 if 2 and 3
= 7 if 1, 2, and 3.
SEDTIME - Timing of daily maximum ozone concentration in the former SEDAB.
= 1 if 0000 ≤ time of daily maximum ≤ 0900 PST
= 2 if 1000 ≤ time of daily maximum ≤ 1200 PST
= 3 if 1300 ≤ time of daily maximum ≤ 1500 PST
= 4 if 1600 ≤ time of daily maximum ≤ 1800 PST
= 5 if time of daily maximum ≥ 1900 PST.
EXCSD - Variable = 1 if the daily maximum ozone concentration in the SDAB exceeded 13 pphm.
SDLOC - Location of maximum daily ozone concentration in the SDAB.
= 1 for coastal (western most) sites (Oceanside, Del Mar, San Diego, Chula Vista)
= 2 for central sites (Escondido, El Cajon)
= 3 for Alpine
= 4 if 1 and 2
= 5 if 1 and 3
= 6 if 2 and 3
= 7 if 1, 2, and 3.
SDTIME - Timing of daily maximum ozone concentration in the SDAB.
= 1 if 0000 ≤ time of daily maximum ≤ 0900 PST
= 2 if 1000 ≤ time of daily maximum ≤ 1200 PST
= 3 if 1300 ≤ time of daily maximum ≤ 1500 PST
= 4 if 1600 ≤ time of daily maximum ≤ 1800 PST
= 5 if time of daily maximum ≥ 1900 PST.

Surface Wind Variables

For the wind speed variables:
1 = 3-hour average for values at hours 0600, 0700, and 0800 PST
2 = 3-hour average for values at hours 0900, 1000, and 1100 PST
3 = 3-hour average for values at hours 1200, 1300, and 1400 PST
4 = 3-hour average for values at hours 1500, 1600, and 1700 PST.
Values for the wind direction variables represent wind direction "bins" instead of actual wind directions:

1 = 345°≤ WD < 15°, calm	5 = 105°≤ WD < 135°	9 = 225°≤ WD < 255°
2 = 15°≤ WD < 45°	6 = 135°≤ WD < 165°	10 = 255°≤ WD < 285°
3 = 45°≤ WD < 70°	7 = 165°≤ WD < 195°	11 = 285°≤ WD < 315°
4 = 70°≤ WD < 105°	8 = 195°≤ WD < 225°	12 = 315°≤ WD < 345°.

Continued

TABLE 3-1. Concluded.

The following variables represent average 3-hour wind speed (m/s) and wind direction in the former SEDAB:
BAN(WS,WD)(1-4) - Banning
DAG(WS,WD)(1-4) - Daggett
HES(WS,WD)(1-4) - Hesperia
PAL(WS,WD)(1-4) - Palmdale
PSP(WS,WD)(1-4) - Palm Springs.
The following variables represent average 3-hour wind speed and direction in the SoCAB:
LAX(WS,WD)(1-4) - Los Angeles International Airport
ONT(WS,WD)(1-4) - Ontario
The following variables represent average 3-hour wind speed and direction in the SDAB:
MYF(WS,WD)(1-4) - San Diego (Montgomery Field)
NFG(WS,WD)(1-4) - Camp Pendleton

Upper-Air Wind Variables

Upper-air wind variables represent values at the 1500-m level. As only two soundings per day were available at some of the sites (0400 PST and 1600 PST), only data from these two time periods were used for each site. When a site had no data available for 0400 PST and 1600 PST, but had data for other times, the measurements taken closest in time to these two periods were used. AM corresponds to the morning sounding, PM to the afternoon sounding. "YS" was used to represent the wind speed and "YD" was used to represent the wind direction on the afternoon of the previous day. Wind direction variables took on the values of 1–12, as described in the surface wind direction section. Wind speed units are m/s. The following variables were used:
For the SoCAB:
UCLA(WS,WD)(AM,PM) - UCLA
For the Southeast Desert Basin:
BAR(WS,WD)(AM,PM) - Barstow
EDW(WS,WD)(AM,PM) - Edwards Air Force Base
HES(WS,WD)(AM,PM) - Hesperia
WWR(WS,WD)(AM,PM) - Whitewater
For the San Diego Basin:
MYF(WS, WD)(AM,PM) - San Diego (Montgomery Field)

concentrations (greater than 12.5 pphmV) in the SoCAB, predominantly westerly to west-northwesterly surface winds at Palmdale during the late morning hours (1000-1200 PST) followed by west-southwesterly surface winds at this location during the afternoon hours (1500-1700 PST), the absence of an easterly component to the morning upper-air wind directions at the Whitewater monitoring site, and moderate wind speeds aloft (greater than 2.5 but less than 5 ms^{-1}) at most monitoring sites in the MDAB and SSAB. According to the CART analysis results, days within this node are distinguished from other days by the first three parameters, some dependence on wind direction at the Palm Springs monitoring sites is also indicated but is not easily interpreted relative to transport characteristics. These characteristic features generally suggest the possibility of transport. Further analysis was conducted through examination of 20 June 1992 (selected as representative of the node based on a maximum SoCAB ozone concentration that is nearest to the average for the node, compared to the other days; it also meets the original exceedance criteria).

Together, CART Nodes 8 and 12 represent more than 80 percent of the exceedance or candidate episode days. However, one additional day was selected for further analysis and classification. One exceedance day meeting the original exceedance criteria (25 June 1992) was associated with a maximum ozone concentration in the SoCAB that was less than 12.5

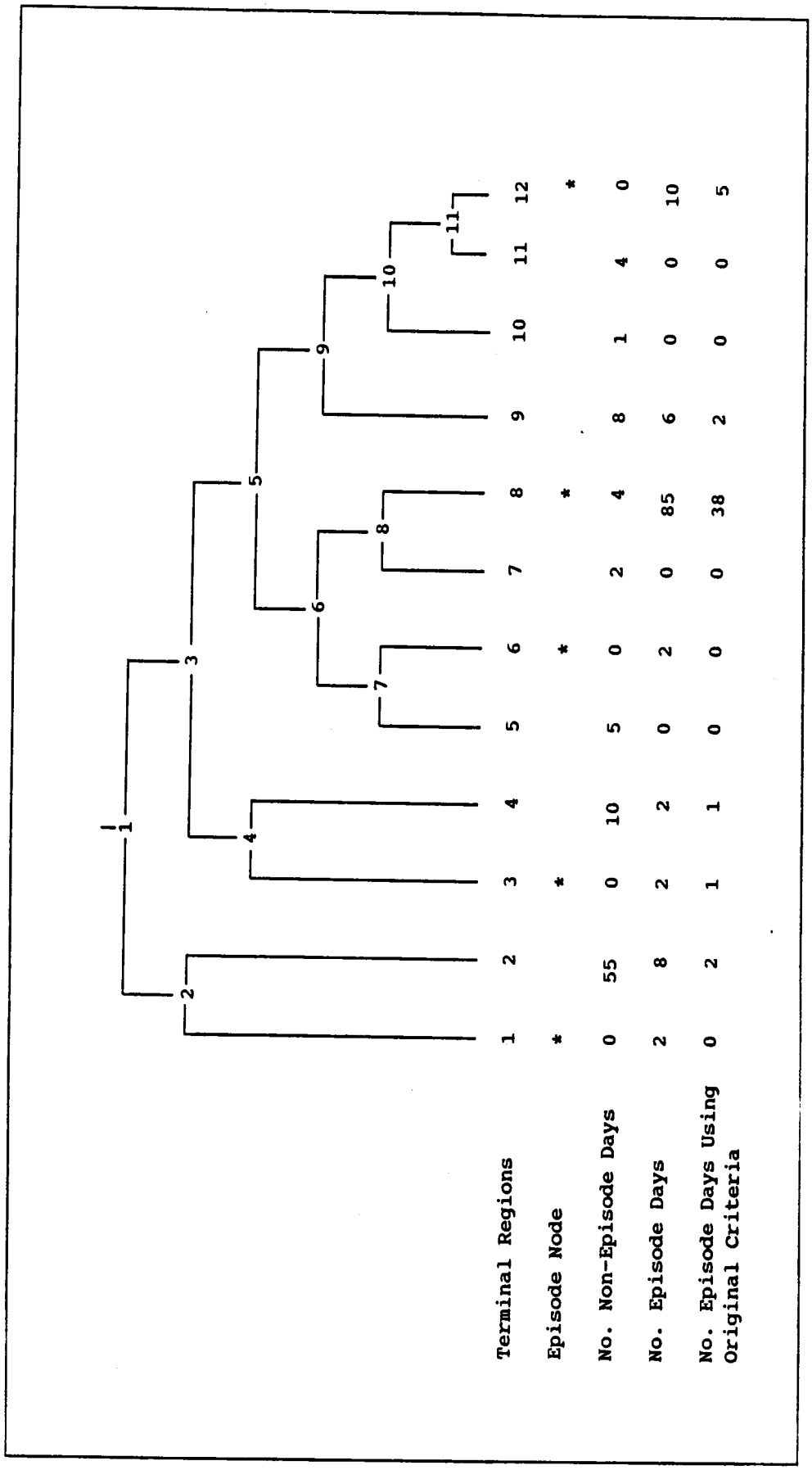

FIGURE 3-1. Southeast Desert Air Basin classification tree diagram.

pphmV. This day was placed in Node 2 (a non-exceedance node) and is thus also characterized by afternoon wind speeds at Palmdale that are greater than approximately 1.5 ms^{-1}. The maximum ozone concentration in the former SEDAB (10 pphmV) was recorded at the Twentynine Palms monitoring site at 1500, 1600, and 1700 PST. Thus the characteristics of this day are somewhat mixed with respect to transport. The relative low ozone concentrations in the SoCAB and the timing of the ozone maxima at Twentynine Palms suggest local ozone production rather than transport. However, the dependence on wind speed suggests that transport may also be important. This day was selected for further analysis as the most likely candidate for a "local" episode day for the former SEDAB.

Application of Cart for the San Diego Air Basin

Application of CART to the SDAB was designed to identify ozone episodes for this basin with similar meteorological characteristics. The dependent variable for this application was called EPSSD. The value of EPSSD was set equal to one (episode day) if the ozone concentration at any monitoring site within the San Diego Air Basin exceeded 13 pphm on that day. It was otherwise set equal to zero.

Variables used in this CART analysis are listed and described in Table 3-2. Variables represent air quality as well as wind conditions in the SoCAB and SDAB. The resultant CART tree is shown in 3-2. This figure also gives the number of episode and non-episode days that were placed in each node. All but one of the episode days were classified as belonging to a single terminal node.

Because CART was unable to identify distinct episode types for the SDAB, additional analysis of the observed meteorological and air quality data was performed. The candidate episode days, 27 September, 30 September, and 11 October, were selected as representative of a variety of upper-air wind directions, as well as representative of ozone exceedances at monitors within the SDAB. These episode days are described in more detail in the following section.

The three days selected for further analysis are generally distinguished from nonexceedance days by high ozone concentrations in the SoCAB (both for the same day and the previous day) and upper-air wind directions at San Diego that are generally southerly to west-northwesterly during the morning hours and from southerly to north-northwesterly during the afternoon hours. Several of the CART parameters pertain to surface winds at LAX and suggest typical sea breeze development; winds at Ontario are southwesterly to westerly during the morning hours and have low to moderate speeds during the afternoon hours. These parameters appear to be more related to the high concentrations in the SoCAB and thus are only indirectly related to the high concentrations in the SDAB.

OVERVIEW OF METEOROLOGY AND AIR QUALITY FOR THE SELECTED EPISODE DAYS

This section provides a brief overview of the synoptic-scale meteorological conditions and observed air quality characteristics for the selected episode days. The synoptic-scale descriptions are based on information obtained from the daily weather maps published by the National Oceanic and Atmospheric Administration. Air quality descriptions are based on analysis of hourly ozone data.

TABLE 3-2. Variables used in the application of CART for the SDAB.

Dependent Variable:

EPSSD - Variable = 1 if the daily maximum ozone concentration in the SDAB exceeded 13 pphm.

Air Quality and Miscellaneous Variables:

SCO3MX - Maximum daily ozone concentration (pphm) in the SoCAB.
SCO3MXY - Previous day's maximum daily ozone concentration (pphm) in the SoCAB.
SDLOC - Location of maximum daily ozone concentration in the SDAB.
= 1 for coastal (westernmost) sites (Oceanside, Del Mar, San Diego, Chula Vista)
= 2 for central sites (Escondido, El Cajon)
= 3 for Alpine
= 4 if 1 and 2
= 5 if 1 and 3
= 6 if 2 and 3
= 7 if 1, 2, and 3.
SDTIME - Timing of daily maximum ozone concentration in the SDAB.
= 1 if 0000 ≤ time of daily maximum ≤ 0900 PST
= 2 if 1000 ≤ time of daily maximum ≤ 1200 PST
= 3 if 1300 ≤ time of daily maximum ≤ 1500 PST
= 4 if 1600 ≤ time of daily maximum ≤ 1800 PST
= 5 if time of daily maximum ≥ 1900 PST.

Surface Wind Variables

For the following wind speed variables:
1 = 3-hour average for values at hours 0600, 0700, and 0800 PST
2 = 3-hour average for values at hours 0900, 1000, and 1100 PST
3 = 3-hour average for values at hours 1200, 1300, and 1400 PST
4 = 3-hour average for values at hours 1500, 1600, and 1700 PST.

Values for the wind direction variables represent wind direction "bins" instead of actual wind directions:

1 = 345°≤ WD < 15°, calm	5 = 105°≤ WD < 135°	9 = 225°≤ WD < 255°
2 = 15°≤ WD < 45°	6 = 135°≤ WD < 165°	10 = 255°≤ WD < 285°
3 = 45°≤ WD < 70°	7 = 165°≤ WD < 195°	11 = 285°≤ WD < 315°.
4 = 70°≤ WD < 105°	8 = 195°≤ WD < 225°	12 = 315°≤ WD < 345°.

The following variables represent average 3-hour wind speed (m/s) and wind direction in the SoCAB:
LAX(WS,WD)(1-4) - Los Angeles International Airport
ONT(WS,WD)(1-4) - Ontario
The following variables represent average 3-hour wind speed and direction in the SDAB:
MYF(WS,WD)(1-4) - San Diego (Montgomery Field)
NFG(WS,WD)(1-4) - Camp Pendleton

Upper-Air Wind Variables

Upper-air wind variables represent values at the 1500-m level. As only two soundings per day were available at some sites (0400 PST and 1600 PST), only data from these two time periods were used for each site. When a site had no data available for 0400 PST and 1600 PST but had data for other times, the measurements taken closest in time to these two periods were used. AM corresponds to the morning sounding, PM to the afternoon sounding. "YS" was used to represent the wind speed and "YD" was used to represent the wind direction on the afternoon of the previous day. Wind direction variables took on the values of 1–12, as described in the surface wind direction section. Wind speed units are m/s. The following variables were used for the South Coast Basin:
UCLA(WS,WD)(AM,PM) - UCLA
For the San Diego Basin:
MYF(WS, WD)(AM,PM) - San Diego (Montgomery Field)

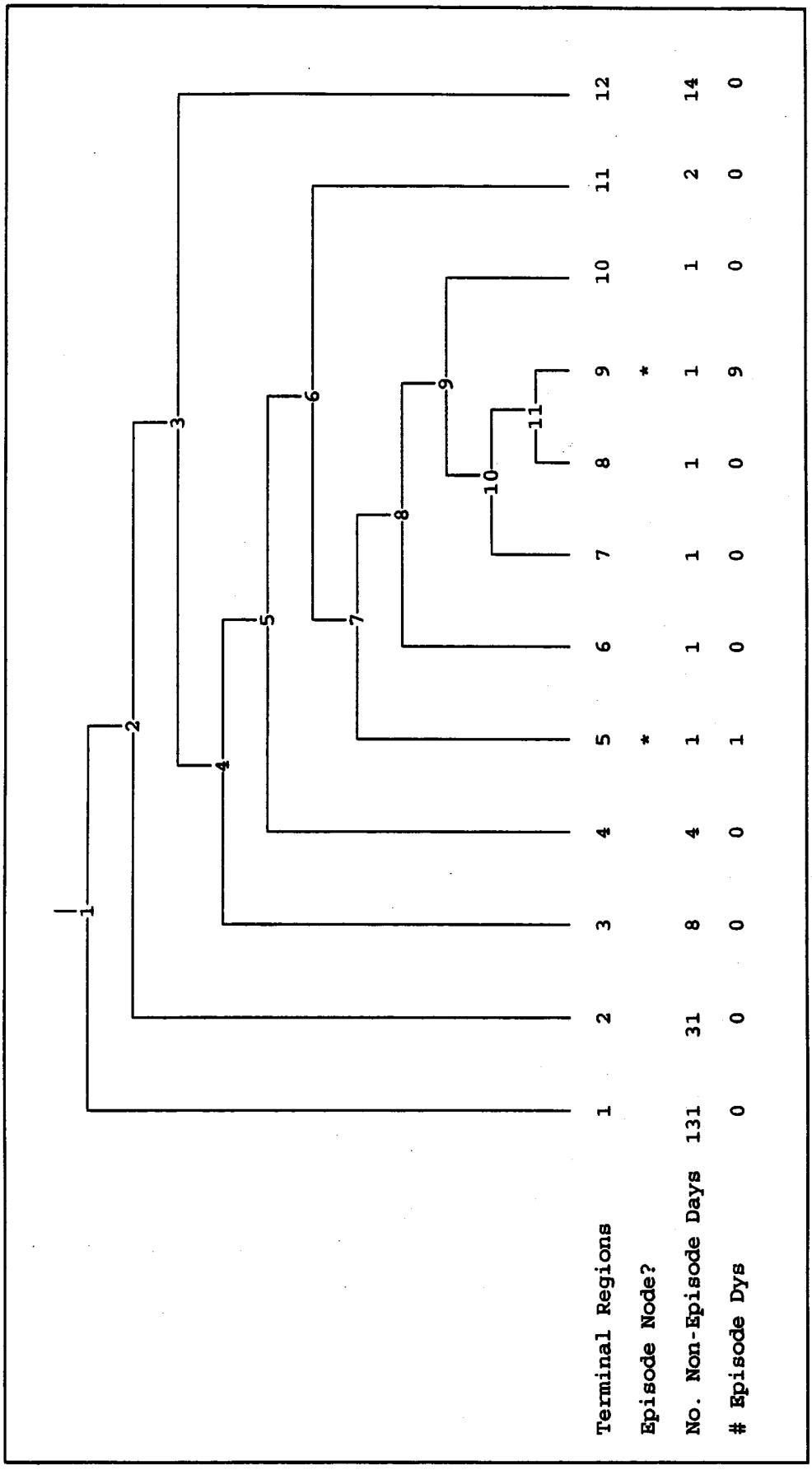

FIGURE 3-2. San Diego Air Basin classification tree diagram.

Former Southeast Desert Air Basin

For this analysis, an ozone episode for the MDAB/SSAB (previously SEDAB) is defined by an ozone concentration that exceeded 13 pphm at the Lancaster monitoring site, or a concentration greater than 9 pphm at the Barstow, Twentynine Palms, or Trona monitoring sites. The following discussions of ozone air quality focus on the measured concentrations at these sites.

20 June 1992

A thermal trough at the surface and low pressure aloft (500 mb) are indicated on the weather maps for 0400 PST for this day. Maximum temperatures reached into the 80s.

High ozone concentrations were widespread and persistent in the former SEDAB on this day. Concentrations greater than 13 pphm were recorded at 1500, 1600, and 1700 PST at Lancaster. Exceedances of the state ozone standard (concentrations greater than 9 pphm) were recorded at 1600, 1800, and 1900 PST at Barstow, at 1700 and 1800 PST at Twentynine Palms, and at 2100 PST at Trona.

25 June 1992

The surface analysis for 0400 PST indicates an area of relatively high pressure over the Pacific Ocean, northeast of the MDAB/SSAB. The 500 mb analysis for the same time indicates an area of low pressure over Central California, and moderate wind speeds aloft (approximately 15–20 m s^{-1}) over the MDAB and SSAB Maximum temperatures were in the 80s.

Ozone concentrations exceeded 9 pphm on this day at Twentynine Palms at 1500, 1600, and 1700 PST.

29 July 1992

The surface analysis for 0400 PST indicates low pressure over the central and southern portions of California. The 500 mb analysis for the same time indicates high pressure and low wind speeds (less than approximately 2.5 m s^{-1}) over the MDAB/SSAB. Maximum temperatures for the area were in the 80s.

Ozone exceedances on this day occurred during the middle of the day and two hours during the early evening. Concentrations greater than 13 pphm were recorded at Lancaster at 1700 and 1800 PST, and concentrations greater than 9 pphm were observed at Barstow at 1700 PST.

San Diego Air Basin

For this analysis, an ozone episode in the SDAB is defined as an ozone concentration greater than 13 pphm at any monitoring site within the SDAB.

27 September 1992

The surface weather analysis for this day at 0400 PST indicates an area of low pressure over the SDAB. The analysis at 500 mb, on the other hand, indicates an area of high pressure over the southern portion of California. Wind speeds aloft are light (less than approximately 2.5 m s^{-1}). Maximum temperatures for the area were in the 80s.

Ozone exceedances on this day were recorded in both the northern and the southern portions of the area and were separated by a few hours. Exceedances were recorded at Oceanside (north of San Diego) at 1400 PST and in the south at Overland two hours later (1600 PST), indicating the possibility of alongshore ozone transport from the north.

30 September 1992

The surface analysis for this day at 0400 PST indicates an area of low pressure over the SDAB. The analysis at 500 mb indicates an area of high pressure over the SDAB. Wind speeds aloft are moderate (approximately 5 m s^{-1}). Maximum temperatures for the area were in the high 80s.

Ozone exceedances on this day occurred over a three-hour period. Exceedances were recorded at Overland at 1300 and 1400 PST and further inland at Escondido at 1400 and 1500 PST.

11 October 1992

The surface analyses for this day at 0400 PST indicate low pressure over the SDAB near the surface and high pressure aloft (just north of the SDAB). Wind speeds aloft are moderate (approximately 5 m s^{-1}). Maximum temperatures for the area were in the high 70s.

Ozone exceedances on this day were recorded at Alpine at 1300, 1400, and 1500 PST.

WIND ANALYSIS

Preparation of Wind Fields for the Selected Episode Days

Hourly, gridded, horizontal wind fields were generated for each episode day and the day preceding each episode day from routine and supplementary (from the 1992 summer field study) surface and upper-air wind data using the Diagnostic Wind Model (DWM) (SAI, 1990). This model incorporates available observations and provides some information on terrain-induced airflows in regions where observations are absent.

Wind fields are generated by means of a two-step procedure. In step 1, a domain-scale mean wind is adjusted for terrain effects including the kinematic effects of terrain (lifting and acceleration of the airflow over terrain obstacles), thermodynamically generated slope flows, and blocking effects. In step 2, observational information is added to the step 1 wind field by the use of weighted interpolation.

The domain consists of 73 (5 km) cells in both the north-south and east-west directions. The domain extends from just north of Trona south to the California-Mexico border. In the east-west direction it extends from just west of Pt. Mugu eastward to approximately 50 km east of Twentynine Palms.

Surface wind data were available at 57 monitoring sites within the domain and 2 sites to the west of the domain. These sites are plotted in Figure 3-3 and listed in Table 3-3. Not all sites were operating on each of the primary episode days, as noted in Table 3-3. Upper-air wind measurements were available from radiosondes and wind profilers at 16 sites within the domain. These sites are plotted in Figure 3-4 and listed in Table 3-4. As with the surface monitoring sites, not all upper-air sites were in operation during each episode.

Generation of the wind fields involved (1) preprocessing of wind data for input into the model, (2) specification of model input parameters, and (3) exercise of the DWM. Winds were analyzed for seven levels: 10, 100, 300, 600, 1000, 1500, and 2000 meters above ground level (agl). In the preprocessing step, the data were temporally interpolated, as needed, to provide hourly inputs for the DWM as well as vertically interpolated to the model levels.

The DWM requires specification of various maximum radii of influence for the interpolation of the data. These were based on the spatial distribution of observations, and for the surface level were assigned values of 50 km over land and 250 km over water. The value was set equal to 350 km aloft. The distance from the observations at which the terrain effects begin to dominate the surface level wind field was specified to be 50 km.

The DWM also requires domain-mean wind and domain-scale stability information. For this application the domain-mean wind was set equal to the vector average of the winds at all wind sites used for the surface wind computations. Stability information, in the form of vertical temperature gradients, was estimated from typical diurnal gradient patterns for the area.

To examine the potential for pollutant transport and transport pathways, two- and three-dimensional backward particle paths were computed using the DWM wind fields as follows:

1. The times of ozone episodes (as defined earlier in this section) on each of the primary days during the episodes were determined and used as the ending times for the backward particle path calculations. The particle path ending points at these times corresponded (at a minimum) to the site or sites at which episodes occurred.

2. Using a time interval of 15 minutes, the hourly, gridded DWM wind fields were linearly interpolated in time and then interpolated in space to each particle position using an inverse-distance-squared weighting scheme.

3. The particles were then advected horizontally (and vertically for the three-dimensional cases) for the specified time interval.

4. The distance traveled by each particle during each time interval was integrated. The new position of the particle was reported at hourly intervals.

For this analysis, 24-hour two-dimensional backward particle paths were calculated for various times for the surface level, level 3 (300 m), level 5 (1000 m) and level 7 (2000 m). The three-dimensional backward particle paths ended at the surface but were advected across

the levels aloft as directed by the magnitude and direction of the vertical component of the wind. Times and ending locations varied among the episodes. Note that to compute 24-hour backward particle paths, the DWM was exercised for the day prior to each primary episode day as well.

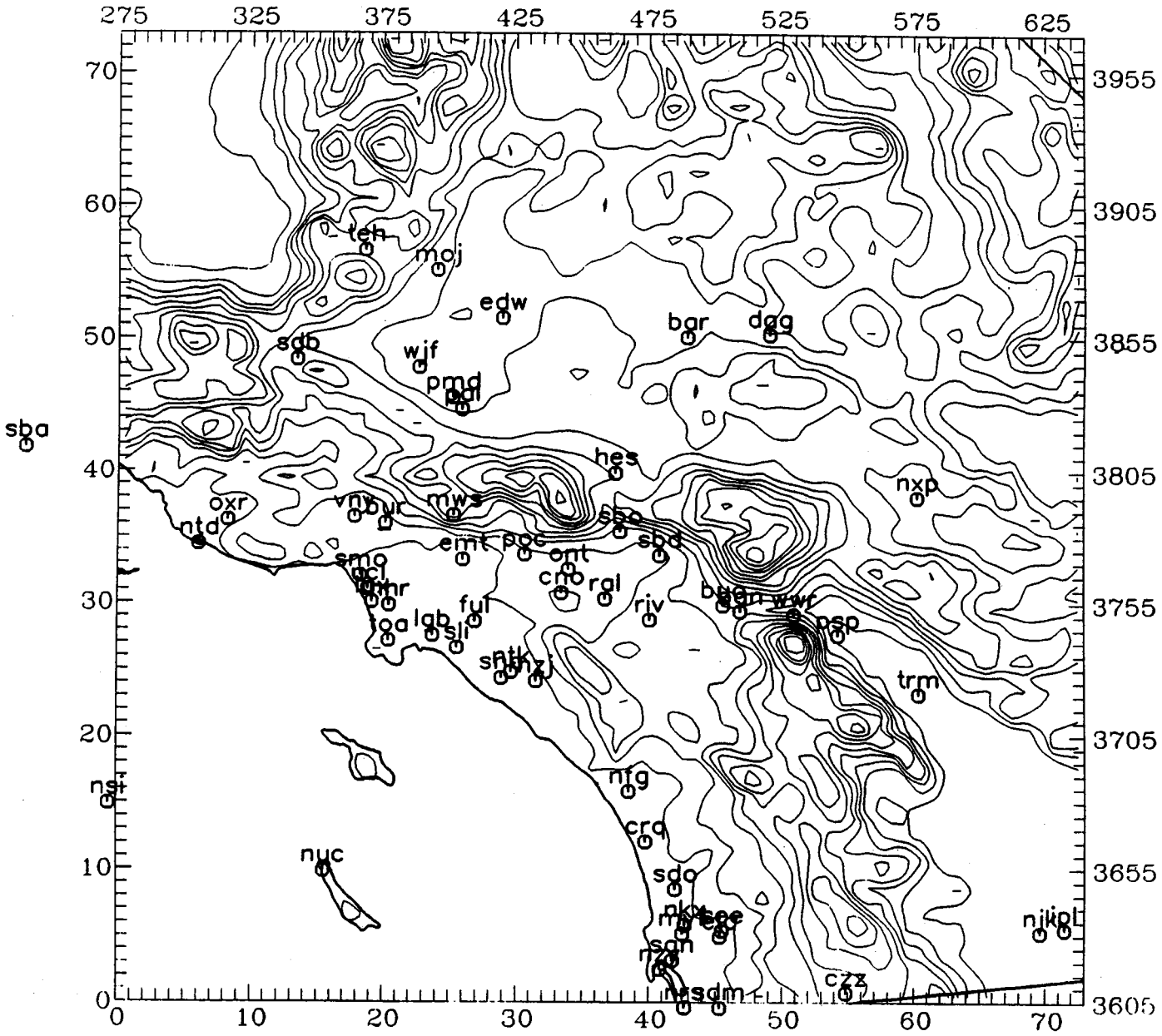

FIGURE 3-3. Surface wind sites used in the data analysis.

TABLE 3-3. Surface wind data available for episode days. Missing days denoted by "M."

ID	Site Name	UTM Easting	UTM Northing	6/20	6/25	7/29	9/27	9/30	10/11
ban	Banning	509.2	3752.0		M	M	M	M	M
bar	Barstow	489.0	3855.1					M	M
buo	Beaumont	502.8	3754.2						
bur	Burbank	375.6	3785.0						
cno	Chino Airport	441.8	3758.8						
crq	Carlsbad/Paloma	473.9	3665.5						
czz	Campo	549.7	3609.1						
dag	Daggett-Barstow	520.1	3856.2						
edw	Edwards AFB	419.6	3862.1						
elc	El Cajon	501.9	3630.0	M	M	M			
emt	El Monte	405.0	3771.3						
ful	Fullerton	409.4	3748.0						
hes	Hesperia	462.3	3804.2				M	M	M
hhr	Hawthorne	377.1	3753.9						
ipl	Imperial	632.9	3633.1						
lax	Los Angeles Intl. Airport	370.6	3755.1						
lgb	Long Beach	393.6	3742.6						
moj	Mojave	395.1	3880.1				M	M	M
mws	Mount Wilson	401.4	3788.0						
myf	San Diego/Montgomery Field	487.8	3631.1						
nfg	Camp Pendleton	467.4	3684.4						
njk	El Centro	623.6	3631.9						
nkx	Miramar	488.8	3634.5						
nrs	Imperial Beach	488.7	3603.4				M		M
nsi	San Nicolas Island	271.7	3679.3						
ntd	Pt. Mugu	304.8	3776.9	M	M	M	M		M
ntk	Tustin	423.1	3729.0						
nuc	San Clemente	352.4	3654.4	M	M		M		M
nxp	Twentynine Palms	576.4	3795.5	M		M			
nzj	El Toro	432.3	3725.6						
nzy	North Island	479.4	3617.9						
ont	Ontario Intl.	444.6	3767.7						
oxr	Oxnard	315.7	3785.9						
pal	Palmdale	404.6	3827.9				M	M	M
pmd	Palmdale Produc.	401.0	3832.3						
poc	La Verne	428.1	3773.3						
psp	Palm Springs	546.3	3743.2						
ral	Riverside Municipal	458.4	3756.5						
riv	Riverside - March Field	475.0	3748.7						
san	San Diego - Lindbergh Field	484.1	3621.2						
sba	Santa Barbara	239.9	3813.3						
sbd	San Bernardino	478.8	3773.1						
sbo	San Bernardino	464.1	3782.0					M	M
sdb	Sandberg	341.6	3846.5						
sdm	San Diego - Brown	501.9	3603.4						
sdo	San Diego	485.0	3647.8						
see	San Diego - Gille.	502.8	3632.3						
sli	Los Alamitos	402.8	3738.1						
smo	Santa Monica	366.1	3765.1						
sna	Santa Ana	419.4	3726.8						
teh	Tehema	367.6	3887.5					M	M
toa	Torrance	376.9	3740.6						
trm	Thermal Airport	577.0	3721.2						
ucl	UCLA	369.0	3760.0	M	M	M	M		M
vny	Van Nuys Airport	363.7	3787.3						
wjf	Lancaster	388.3	3843.6						
wwr	White Water	529.6	3750.9				M	M	M

Wind and Trajectory Analysis Results for the Air Basins Formerly Designated the Southeast Desert Air Basin

Wind fields and 24-hour, two- and three-dimensional particle paths for the MDAB/SSAB (formerly SEDAB) are presented in Appendices F through H. Wind fields are shown at 6-hour intervals beginning at 0400 PST, for the levels 10, 300, 1000, and 2000 m agl. Twenty-four-hour backward particle paths are shown for the hours ending 1500 PST through 2100 PST. Termination points correspond to the Trona, Lancaster, Barstow, Twentynine Palms, and Indio air quality monitoring sites. The two-dimensional particle paths are presented at levels corresponding to those for which wind fields are shown. The three-dimensional particle paths terminate at the surface level; they are, however, advected across other levels as directed by the vertical component of the wind.

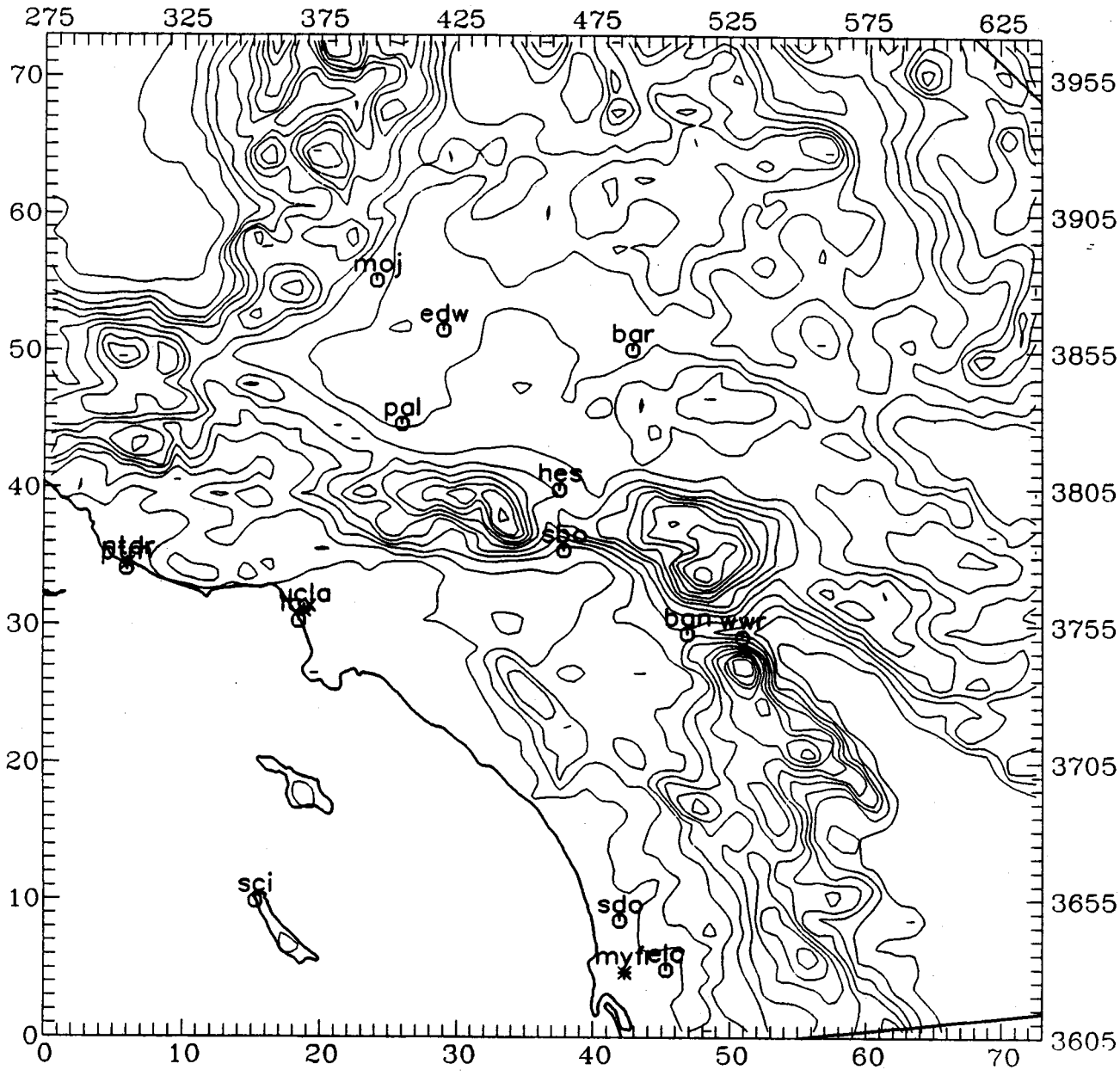

FIGURE 3-4. Upper-air wind sites used in the data analysis.

TABLE 3-4. Upper-air wind data availability for episode days. Missing days are denoted by "M."

ID	Site Name	UTM Easting	UTM Northing	6/20	6/25	7/29	9/27	9/30	10/11
ban	Banning	509.2	3752.0		M	M	M	M	M
bar	Barstow	489.0	3855.1					M	M
edwr	Edwards AFB	419.6	3862.1	M					
elc	El Cajon	501.9	3630.0	M	M	M			
hes	Hesperia	462.3	3804.2					M	M
lax	Los Angeles Intl. Airport	370.6	3755.1	M	M	M			
moj	Mojave	395.1	3880.1				M	M	M
myfr	San Diego/Montgomery Field	487.8	3631.1						
ntdr	Pt. Mugu	304.8	3776.9	M			M		
pal	Palmdale	404.6	3827.9	M	M	M			
ptm	Point Mugu	304.43	3775.08	M	M	M	M	M	
sbo	San Bernardino	464.06	3781.99					M	M
sci	San Clemente Island	351.49	3654.44	M	M	M			
sdo	San Diego	485.05	3647.78			M			
ucl	UCLA	369.0	3760.0						
wwr	White Water	529.59	3750.92				M	M	M

20 June 1992

Wind fields and 24-hour, two- and three-dimensional particle paths for the former SEDAB are presented in Appendix F.

Wind Fields

A predominance of westerly flow at all levels is evident in the wind fields for 20 June. Surface level winds at 0400 PST are very light and offshore along the coast and somewhat stronger (over 5 m s^{-1} in some locations) and from the southwest, west, and northwest over the rest of the domain. By 1000 PST winds are onshore along the coast and similar to those at 0400 PST elsewhere. By 1600 PST and continuing through 2200 PST, winds are from the southwest over most of the domain. Winds at 300 m are generally light and from the west or west-northwest for most of the day, with the homogeneity of the field being a direct result of the lack of observations for this level. (Few recordings below approximately 300 m is a limitation of the radar wind profiler. In addition, data below approximately 500 m were limited due to the removal of invalid data points during quality assurance procedures performed prior to our receipt of the data.) Winds at 1000 m vary from northwesterly and westerly at 0400 PST to westerly and southwesterly by 1000 PST (with some northeasterly flow over the Mojave area). The west/southwesterly flow continues through the remainder of the day. Winds at 2000 m are similar to those at 1000 m for most hours. A noted difference occurs at 1000 PST, during which the 2000 m winds are generally from the east.

Twenty-Four-Hour, Two-Dimensional Backward Particle Paths

Twenty-four-hour, two-dimensional backward particle paths for all levels on 20 June illustrate the predominance of flow with a westerly component. Exceedances were recorded at 1500, 1600, and 1700 PST at Lancaster, at 1600, 1700, 1800, and 1900 PST at Barstow, at 1700 and 1800 PST at Twentynine Palms, and at 2100 PST at Trona. Backward particle paths terminating at those locations in the SEDAB with episodes between 1500 and 1900

PST indicate that the particle initiation points originate over the SoCAB or over the Pacific Ocean. An exception to this is Lancaster at 1500 PST, for which the particle initiation point is in the South Central Coast Air Basin (SCCAB). The trajectory, however, does traverse the SoCAB. The particle path terminating at Trona at 2100 PST indicates an initiation point just west of the SEDAB. Particle paths at 300 m are similar for all hours and also indicate transport from the west. The particle paths for 1000 m again show transport from the west, but with a northerly component initially and a southerly component later in the day. Particle paths at 2000 m also indicate westerly flow, but with an initial southern component added. Recirculation aloft (for approximately 12 hours) over the former SEDAB is also evident. Particle paths ending at Lancaster also indicate recirculation aloft over the former SEDAB.

Twenty-Four-Hour, Three-Dimensional Backward Particle Paths

Twenty-four-hour, three-dimensional backward particle paths ending at the surface level for 20 June are similar to the two-dimensional particle paths described above. For some cases, however, the trajectories are shorter. The particle path ending at the Lancaster site at 1500 PST has an initiation point near the surface, along the border of the SoCAB and SDAB; those ending at this site at 1600 and 1700 PST indicate initiation points at an upper level over the Pacific Ocean. These latter two particle paths, do, however, traverse the SoCAB. The particle path ending at Barstow at 1600 PST remains in the surface level and indicates transport from the Burbank area. The particle paths ending at Twentynine Palms at 1700 and 1800 PST indicate near-surface transport from the Ontario area. Unlike the particle path ending at 1600 PST, which indicates transport from the Burbank area, the particle path ending at the Barstow site at 1800 PST indicates surface-level transport from Hesperia, within the SEDAB. The particle path ending at this site at 1900 PST, however, indicates near-surface level transport from the Long Beach area. The particle path ending at the Trona site at 2100 PST indicates transport from over the SCCAB.

Both the two- and three-dimensional particle paths indicate that observed ozone concentrations within the MDAB/SSAB (previously SEDAB) on 20 June were the combined result of local ozone production and ozone and precursor transport from the SoCAB and possibly the SCCAB (i.e., this episode is a "shared" ozone episode).

CART Analyses/Comparison with Results

The CART classification for this episode also indicated possible pollutant transport from the SoCAB. Classification based on morning and afternoon surface winds at Palmdale, early morning surface winds at Palm Springs, and early morning winds aloft at White Water, indicated flow from the west. A maximum ozone concentration of greater than 12.5 pphm in the SoCAB on the same day was also selected as important to the classification of this episode. The particular node selected for this classification suggested a low frequency of occurrence; 10 days out of the 206 days analyzed were placed into this bin.

Further Classification According to ARB Transport Categories

Both the particle-path and CART analysis results suggest that 20 June 1992 and other episode days within the same CART classification category as 20 June are "shared" ozone events; the potential for pollutant transport exists. Once the determination of shared was made, the relative importance of transport was estimated. This further refinement of the

classification was obtained through a comparative analysis of the upper-air wind speeds relative to all other CART nodes (for the SDAB/SSAB CART analysis) in conjunction with the maximum ozone concentrations in the SoCAB. This was done for each CART classification node. The combination of relatively low maximum ozone in the SoCAB (less than 12.5 pphmV) and low wind speeds aloft (on the average less than approximately 2.5 ms^{-1}) is designated "inconsequential", the combination of relatively high maximum ozone (greater than 12.5 pphmV) and moderate winds speeds aloft (on the average greater than approximately 2.5 ms^{-1} but greater 3.5 ms^{-1}) is designated "significant", and the combination of relatively high maximum ozone in the SoCAB (greater than 12.5 pphmV) and high wind speeds aloft (on the average greater than approximately 3.5 ms^{-1}) is designated "overwhelming". The wind speed threshold values for the various categories were determined based on the distribution of wind speeds aloft for the days within the various CART nodes.

Further classification of 20 June 1992 and other days within CART Node 12, results in a designation of "significant".

25 June 1992

Wind fields and 24-hour, two- and three-dimensional particle paths for the former SEDAB are presented in Appendix G.

Wind Fields

Westerly flow dominates the wind fields at all levels on 25 June. Surface-level winds at 0400 PST are very light and offshore along the coast. Wind speeds are slightly stronger (over 5 m s^{-1}) and winds are downslope-directed on the eastern side of the mountains near Banning. By 1000 PST winds are stronger and generally westerly over most of the domain, with onshore flow along the coast. With the exception of the return of calm conditions along the coast east of San Clemente Island at 2200 PST, the wind fields for 1600 PST and 2200 PST are very similar to those at 1000 PST. Winds at 300 m are generally dominated by a westerly component and are relatively light, increasing from approximately 1 m s^{-1} at 0400 to approximately 4 m s^{-1} by 2200 PST. Again, a lack of observations for this level (instrument limitations and erroneous data removed during quality assurance procedures) produces a relatively homogeneous field. Winds at 1000 m are generally westerly or southwesterly over most of the domain. Wind speeds at 0400 PST vary from very light along the coast to over 10 m s^{-1} through Banning Pass. Winds at 2000 m are similar to those at 1000 m for most hours.

Twenty-Four-Hour, Two-Dimensional Backward Particle Paths

As for 20 June, 24-hour, two-dimensional backward particle paths for 25 June for all levels indicate the predominance of winds with westerly components. Exceedances on this day were recorded at 1500, 1600, and 1700 PST at Twentynine Palms. Surface-level backward particle paths terminating at this site at these hours originate over the Pacific Ocean west of Los Angeles or in the Los Angeles/Long Beach areas. Residence times within the MDAB/SSAB, however, are as great as 11 hours. Particle paths at 300 m are similar for all hours; they originate over the Pacific Ocean, have relatively straight trajectories from the west, and traverse the SoCAB. The particle paths at 1000 m originate southwest of San Clemente Island and traverse the SDAB and the SoCAB prior to reaching Twentynine Palms.

Although residence times over the Pacific Ocean are longer at 2000 m than at 1000 m, the trajectories are similar.

Twenty-Four-Hour, Three-Dimensional Backward Particle Paths

Twenty-four-hour, three-dimensional backward particle paths ending at the surface level for 25 June are similar to the two-dimensional particle paths described above for this day. In some cases, however, the trajectories are shorter. The particle paths ending at Twentynine Palms at 1500, 1600, and 1700 PST have initiation points near the surface in the vicinity of Long Beach. Particle paths for all sites plotted for all times indicate transport within the lowest 100 m of the atmosphere.

Both the two- and three-dimensional particle paths indicate that observed ozone concentrations within the SEDAB on 25 June were the combined result of local ozone production and precursor transport from the SoCAB and possibly the SDAB (i.e., this episode is a "shared" ozone episode).

CART Analyses/Comparison with Results

The CART classification for this episode indicated that the maximum ozone concentrations in the SoCAB on the same day were low (≤12.5 pphm), and except for the afternoon wind direction at Ontario which was required to be from the south-southwest, surface and upper-air wind directions were varied. This episode was selected because the CART analysis did not point to strict transport conditions, and indicated the possibility of local influences. Residence times within the SEDAB of as long as 11 hours, as indicated by the two- and three-dimensional backward particle paths, suggest the possibility of local influences. The trajectories, however, do also indicate the possibility of transport. These findings indicate that this episode is possibly a "shared" ozone episode, and not a "local" episode as the CART analysis alone indicated. The particular node selected for this classification suggested a low frequency of occurrence. Only two out of the 206 days with ozone concentrations corresponding to the original exceedance criteria were placed into this bin.

Further Classification According to ARB Transport Categories

While the CART analysis results for 25 June 1992 were inconclusive relative to transport, the particle paths analysis indicates that this episode day is a "shared" ozone event. Further refinement of the classification using the approach described earlier in this section results in a designation of "significant", for 25 June and the other episode day within the CART classification category.

29 July 1992

Wind fields and 24-hour, two- and three-dimensional particle paths for the SEDAB are presented in Appendix H.

Wind Fields

As for the previous two episode days, westerly flow dominates the wind fields at all levels on 29 July. Surface-level winds at 0400 PST are very light along the coast, but in contrast to the previous two episodes, some onshore flow is present. Winds are downslope in the vicinity of Banning Pass and are moderate in speed (approximately 7 m s^{-1}). Wind speeds are generally light over the rest of the domain. By 1000 PST winds are stronger and generally from the southwest over most of the domain. Winds over the Salton Sea are southeasterly. With the exception of the return of southwesterly winds over the Salton Sea, the wind fields for 1600 PST and 2200 PST are very similar to those at 1000 PST. Winds at 300 m are generally light and from the west or west-southwest for most of the day. Winds at 1000 m are also generally westerly or southwesterly over most of the domain. Afternoon wind speeds, however, are relatively strong (approximately 10 m s^{-1}) in the northeastern portion of the domain. Winds at 2000 m are similar (but with a somewhat more southerly component in the southern portion of the domain) to those at 1000 m for most hours.

Twenty-Four-Hour, Two-Dimensional Backward Particle Paths

As for the two previously described episode days, 24-hour, two-dimensional backward particle paths for 29 July for all levels indicate predominance of winds with westerly components. Exceedances on this day occurred at 1700 and 1800 PST at Lancaster and at 1700 PST at Barstow. Surface-level backward particle paths terminating at these locations originate to the west of Los Angeles and have long residence times in the SoCAB. The particle paths at 300 m are similar for all hours and originate over the Pacific Ocean. Trajectories terminating at Barstow have relatively straight paths; those terminating at Lancaster indicate some northward directed flow. Both traverse only the northernmost portion of the SoCAB. Particle paths for 1000 m, terminating at the exceedance hours at Barstow and Lancaster, have initiation points in the SCCAB. At 2000 m, the particle paths terminating at these two sites at these times originate over the Pacific Ocean and again traverse only the northernmost part of the SoCAB.

Twenty-Four-Hour, Three-Dimensional Backward Particle Paths

The 24-hour, three-dimensional backward particle paths ending at the surface level for 29 June are similar to two-dimensional particle paths described above; however, in some cases, as with the particle paths ending at Indio at 2000 and 2100 PST, the three-dimensional paths indicate local impacts. Particle paths for all sites plotted for all times indicate transport within the lowest 200 m of the atmosphere.

Both two- and three-dimensional particle paths indicate that observed ozone concentrations within the former SEDAB on 29 June were possibly the result of transport (from the SCCAB and SoCAB) as well as due to local influences (i.e., this episode is a "shared" ozone episode).

CART Analyses/Comparison with Results

The CART classification for this episode also indicated possible pollutant transport as well as local impacts. The CART node corresponding to this episode was characterized by the following: ozone concentrations on the same day in the SoCAB were high (>12.5 pphm), afternoon surface wind directions at the Palmdale site generally had a westerly component

(transport), wind speeds aloft at Edwards Air Force Base on the previous afternoon were light (possible stagnation), early morning wind speeds at Daggett were moderate (early morning transport), varied afternoon wind directions were observed at Daggett (again, the possible indication of afternoon stagnation), and moderate, but not high wind speeds were observed during the morning hours at LAX (winds strong enough for transport, but not so strong as to blow pollutants through and out of the air basins). The particular node selected for this classification suggested a moderate frequency of occurrence; 89 days out of the 206 days analyzed were placed into this bin. Four of these days were non-episode days that were misclassified.

Further Classification According to ARB Transport Categories

Both the particle-path and CART analysis results suggest that 29 July 1992 and other episode days within the same CART classification category as 29 July are "shared" ozone events. Further classification of 29 July 1992 and other days within CART Node 8 using the procedures described earlier in this section results in a designation of "significant".

Wind Trajectory Analysis Results for the San Diego Air Basin

Wind fields and 24-hour, two- and three-dimensional particle paths for the SDAB are presented in Appendices I through K. Wind fields shown at 6-hour intervals beginning at 0400 PST for the levels 10, 300, 1000, and 2000 m agl. Twenty-four-hour backward particle paths are shown for hours ending 1500 PST through 1600 PST. Termination points correspond to the Oceanside, Del Mar, Overland, Escondido, El Cajon, and Alpine air quality monitoring sites. Two-dimensional particle paths are presented at levels corresponding to those for which wind fields are shown. Three-dimensional particle paths terminate at the surface level; they are, however, advected across other levels as directed by the vertical component of the wind.

27 September 1992

Wind fields and 24-hour, two- and three-dimensional particle paths for the SDAB are presented in Appendix I.

Wind Fields

Surface level winds at 0400 PST on 27 September are generally light and variable over most of the domain with some light offshore flow along the coast. By 1000 PST coastal winds are onshore and speeds are somewhat stronger (approximately 2 m s^{-1}). Winds elsewhere are generally light and variable. By 1600 PST, winds over most of the SoCAB are from the southwest; however, along the southern portion of the domain, winds are west-northwesterly. By 2200 PST, winds are once again mostly light and variable. Winds at 300 m are generally from the northwest over most of the domain, with some westerly flow over the San Diego/Salton Sea area at 1000 PST and over the Pacific Ocean at 1600 PST. Westerly and northwesterly winds also dominate the wind fields at 1000 m. At 2000 m, northwesterly winds prevail over land at 0400 PST, 1000 PST, and 1600 PST as well; however, some clockwise circulation is evident over the Pacific Ocean. By 2200 PST winds are very light and northeasterly over land, and somewhat stronger and southerly over water.

Twenty-Four-Hour, Two-Dimensional Backward Particle Paths

The surface-level 24-hour, two-dimensional backward particle paths for 27 September illustrate very light wind conditions prevalent on this day and the long particle residence time over the Pacific Ocean (just offshore of the SDAB). Episodes on this day occurred at 1400 and 1600 PST at Oceanside and Overland, respectively. Surface-level backward particle paths terminating at Oceanside and Overland at these times originate just west of the San Diego area. Particle paths at 300 m are similar for all hours, originate over the Pacific Ocean or near the coast of the SCCAB, and traverse the SoCAB prior to reaching the SDAB. The particle paths at 1000 m are also relatively similar for all hours. They originate northwest of the SDAB as do those at 2000 m. In general, surface-level backward particle paths indicate local or offshore influences, while those aloft indicate transport.

Twenty-Four-Hour, Three-Dimensional Backward Particle Paths

Twenty-four-hour, three-dimensional particle paths ending at the surface level for 27 September are almost identical to the surface-level two-dimensional particle paths described above; however, in some cases, as for 1600 PST, the paths originate slightly to the west of the origination locations of the two-dimensional trajectories. All trajectories meander and remain within 40 m of the surface, indicating the possibility of stagnant conditions.

The results of the two- and three-dimensional particle path analyses indicate that observed ozone concentrations within the SDAB on 27 September are the combined result of stagnant conditions near the surface and possible ozone and precursor transport from the SCCAB and SoCAB aloft (i.e., this episode is a "shared" ozone episode).

CART Analyses/Comparison with Results

All three episodes for the SDAB selected for trajectory analysis fell into the same CART node. The CART classification for this episode (and the remaining two) indicated that ozone concentrations on the same day and on the previous day in the SoCAB were high (>16 pphm and >15 pphm respectively). Classifications based on meteorological conditions were not clear-cut. Wind directions at various sites were generally westerly but included southerly and northerly flows as well. Wind speed cutoffs also varied. It appears that the high ozone concentrations in the SoCAB were the key classifiers. Although transport was not necessarily indicated, the fact that high ozone concentrations in the SoCAB were required for classification indicates that either transport of ozone or its precursors from this area, or meteorological conditions conducive to the formation of ozone over a large area (stagnation), were required. Backward particle path analyses indicated the possibility of both transport and stagnant conditions. Nine of the 10 exceedance days plus one nonexceedance day (out of the 206 days analyzed) were placed into this bin.

Further Classification According to ARB Transport Categories

The particle-path and to a lesser extent the CART analysis results suggest that 27 September 1992 and other episode days within the same CART classification category as this day are "shared" ozone events. The relative importance of transport was estimated through a comparative analysis of the upper-air wind speeds relative to all other CART nodes (for the SDAB CART analysis) in conjunction with the maximum ozone concentrations in the

SoCAB. This was done for each CART classification node. The combination of relatively low maximum ozone in the SoCAB (less than 12.5 pphmV) and low wind speeds aloft (on the average less than approximately 2.5 ms^{-1}) is designated "inconsequential", the combination of relatively high maximum ozone (greater than 12.5 pphmV) and moderate winds speeds aloft (on the average greater than approximately 2.5 ms^{-1} but less than 3.5 ms^{-1}) is designated "significant", and the combination of relatively high maximum ozone in the SoCAB (greater than 12.5 pphmV) and high wind speeds aloft (on the average greater than approximately 3.5 ms^{-1}) is designated "overwhelming". The wind speed threshold values for the various categories were determined based on the distribution of wind speeds aloft for the days within the various CART nodes.

Even further classification of 27 September 1992 and other days within CART Node 9, is not straightforward as the averaged wind speeds are close to the cut off value between "inconsequential' and "significant". However, application of the above procedures results in a designation of "significant".

30 September 1992

Wind fields and 24-hour, two- and three-dimensional particle paths for the SDAB are presented in Appendix J.

Wind Fields

With the exception of winds from the north to the east of Riverside and onshore winds near Oxnard, surface-level winds at 0400 PST on 30 September are very light and variable. By 1000 PST coastal winds are onshore, with slightly stronger speeds (approximately 2 m s^{-1}), and winds over the SDAB are northwesterly. A distinct "split" (toward the northeast and southeast) is visible in the wind field, east of San Clemente Island. By 1600 PST, winds over most of the SoCAB are westerly and southwesterly, but continue to be northwesterly over the SDAB. By 2200 PST, winds are once again mostly light and variable. Winds at 0400 PST at 300 m are light and generally westerly over the western portion of the domain, northwesterly over the northeast portion of the domain, and northerly over the southeast (San Diego) portion of the domain. By 1000 PST, winds are westerly over the SDAB and west-northwesterly elsewhere. Winds are westerly over the western portion of the domain at 1600 PST and northwesterly elsewhere. By 2200 PST, winds are homogeneous and northwesterly. Winds at 1000 m are generally westerly over the northern half of the domain and northwesterly elsewhere. Winds at 2000 m at 0400, 1000, and 1600 PST are westerly or southwesterly over the Pacific Ocean west of the Santa Catalina and San Clemente islands and northwesterly elsewhere. By 2200 PST, winds over land are light and variable, while over water the southwesterly flow continues.

Twenty-Four-Hour, Two-Dimensional Backward Particle Paths

Episodes on this day were recorded at 1300 and 1400 PST at Overland and at 1400 and 1500 PST at Escondido. Surface-level backward particle paths terminating at Overland originate near Oceanside, are blown west over the Pacific Ocean before approaching Overland from the northwest, and indicate stagnant conditions. The particle paths terminating at Escondido originate near Escondido, are also blown west, and then return from the northwest. The particle paths at 300 m are similar for all hours, originate over the Pacific Ocean or the coast of

the SCCAB, and have relatively straight paths. Most of the residence time is over water until reaching the SDAB. Except for the particle path ending at Overland (an exceedance location), which approaches from the southwest, the particle paths at 1000 m originate west of San Clemente Island, approach the coastline almost perpendicularly, and then move south through the SDAB. The particle paths at 2000 m have initiation points to the south of the SDAB. The trajectories ending at Oceanside and Escondido indicate some recirculation over the SDAB at this level.

Twenty-Four-Hour, Three-Dimensional Backward Particle Paths

As for the previous episode, the 24-hour, three-dimensional particle paths ending at the surface level for 30 September are almost identical to the two-dimensional particle paths described above. For some cases, 1600 PST for example, the origination points are slightly west of those for the two-dimensional paths. All particle paths show meandering. Unlike for the previous episode, however, particles reach 90 m. Note that the particle path reaching Escondido at 1500 PST reached approximately 90 m above the Pacific Ocean.

The two- and three-dimensional particle paths indicate that observed ozone concentrations within the SDAB are the possible result of local ozone production and ozone and precursor transport from the SCCAB as well as from points south of the SDAB (i.e., this episode is a "shared" ozone episode).

CART Analyses/Comparison with Results

As for the previous episode, the CART classification for this episode indicated that ozone concentrations on the same day and on the previous day in the SoCAB were high (>16 pphm and >15 pphm, respectively). Classifications based on meteorological conditions were not clear-cut. Again, although transport was not necessarily indicated, the fact that high levels of ozone or its precursors from this area, or meteorological conditions conducive to the formation of ozone over a large area (stagnation), were required suggests that ozone episodes witin this category are "shared" events. The backward particle path analyses indicate the possibility of some transport, mainly from areas south of the SDAB. The trajectories, however, strongly indicate stagnant conditions in the lowest layer. Nine days of the 10 episode days plus one non-episode day (out of the 206 days analyzed) were placed into this bin.

Further Classification According to ARB Transport Categories

The particle-path and to a lesser extent the CART analysis results suggest that 30 September 1992 and other episode days within the same CART classification category as this day are "shared" ozone events. Further classification of days within CART Node 9, results in a designation of "significant", with a note that with slightly different criteria a designation of "inconsequential" would have been obtained.

11 October 1992

Wind fields and 24-hour, two- and three-dimensional particle paths for the former SDAB are presented in Appendix K.

Wind Fields

Surface level winds on 11 October are almost identical to those on 27 September at all hours, remaining light throughout most of the day. Winds at 300 m are somewhat different. At 0400 PST, winds are west-northwesterly west of Santa Catalina and San Clemente islands and generally northerly or north-northeasterly elsewhere. At 1000 PST winds are westerly over most of the domain and are west-northwesterly by 1600 PST. At 2200 PST, winds are light and southerly in the eastern portion of the domain, east-southeasterly over the northwest quadrant, and form a counterclockwise eddy over the Santa Catalina/San Clemente islands area. Winds at 1000 m are generally dominated by a northern component, as are those at 2000 m. The wind fields at 2000 m, however, indicate more easterly flow, whereas those at 1000 m are more northwesterly.

Twenty-Four-Hour, Two-Dimensional Backward Particle Paths

As for the previous two episodes, the 24-hour, two-dimensional backward particle paths for 11 October indicate stagnant conditions in the SDAB. Episodes on this day occurred at 1300, 1400, and 1500 PST at the Alpine monitoring site. Surface-level backward particle paths terminating at this site originate over the Pacific Ocean and move west over the SDAB. The trajectories also indicate recirculation offshore. Particle paths at 300 m are similar for all hours. Those ending at Alpine originate southeast of Long Beach. Particle paths ending at both Escondido and Alpine at 1000 m originate in the former SEDAB, east of Mojave, and also traverse the SoCAB prior to reaching the SDAB from the northwest. Particle paths for the remaining sites originate along the coast of the SCCAB. All particle paths at 2000 m originate in the MDAB, east of Mojave, and approach the SDAB from the northwest.

Twenty-Four-Hour, Three-Dimensional Backward Particle Paths

As for the previous two episodes, the 24-hour, three-dimensional particle paths ending at the surface level for 11 October are almost identical to the two-dimensional particle paths described above. In some cases (1500 and 1600 PST), however, as for the previous episodes, the trajectories originate slightly west of those for the two-dimensional paths. Another noted difference is that the paths ending at Alpine at 1300, 1400, and 1500 PST originate within the SDAB.

Both the two- and three-dimensional particle paths indicate local ozone production as well as possible ozone and precursor transport from the SCCAB and/or MDAB/SSAB (i.e., this is a "shared" ozone episode).

CART Analyses/Comparison with Results

As for the previous two episodes, the CART classification for this episode indicated that ozone concentrations on the same day and on the previous day in the SCAB were high (>16 pphm and >15 pphm, respectively). The backward particle path analyses did indicate the possibility of some transport (especially aloft), from the Long Beach and Mojave areas. Re-circulation/stagnation within the San Diego Air Basin was also noted. Nine of the 10 episode days plus one non-episode day (out of the 206 days analyzed) were placed into this bin.

Further Classification According to ARB Transport Categories

The particle-path and to a lesser extent the CART analysis results suggest that 11 October 1992 and other episode days within the same CART classification category as this day are "shared" ozone events. Further classification of days within CART Node 9, results in a designation of "significant", with a note that with slightly different criteria a designation of "inconsequential" would have been obtained.

SUMMARY

The objective of this phase of the study was to determine whether ozone episodes that occurred within the former Southeast Desert and San Diego Air Basins during the 1992 study period were the result of local emissions or the combination of local emissions and transported ozone and precursor pollutants. The Classification and Regression Tree (CART) analysis software was used to categorize the ozone episode days (with respect to meteorological and air quality conditions) and representative episodes from major classification categories were selected for further analysis. The ozone episode days were then classified as "local" or "shared" events; the "shared" events were further categorized as "overwhelming", "significant", or "inconsequential" transport days. Based on the results of the CART analyses, six episodes were selected for further analysis. Of these, two episode days indicated the possibility of transport into the MDAB or SSAB (formerly SEDAB) from the SoCAB, one indicated the possibility of local causes within the former SEDAB and remaining three episodes indicated the possibility of transport into the SDAB from the SoCAB.

Analyses of transport characteristics of these episode days were carried out through trajectory analysis. Two- and three-dimensional particle paths were calculated using gridded wind fields, and the potential for interbasin transport for the selected days, as well as for meteorologically similar days, was examined.

The results of two- and three-dimensional particle path analyses for the MDAB/SSAB (formerly SEDAB) indicate that although local causes for one of the days was indicated by CART, all three episode days appear to be shared events. Particle paths originating in both the SoCAB and the SCCAB and ending in the former SEDAB indicate transport. Others, beginning and ending within the former SEDAB, indicate local influences. These and meteorologically similar days (according to the CART analysis) comprise more than 80 percent of the exceedance days included in this analysis. Thus most ozone episodes that occurred within the SEDAB during the summer of 1992 can be characterized as shared. The influence of transport can be further classified as "significant.

Results of two- and three-dimensional particle path analyses for the SDAB indicate that all three episode days appear to be shared events. Trajectories from both the SCCAB and SoCAB, as well as from points to the south of the SDAB, indicate the possibility of transport of ozone and precursor into the SDAB; meandering trajectories remaining over the SDAB indicate local influences. With respect to the SCCAB, note that the accuracy of the trajectories likely decreases with distance from the endpoint. These and meteorologically similar days (according to the CART analysis) comprise 90 percent of the exceedance days included in this analysis. Thus most ozone episodes that occurred within the SDAB during the summer of 1992 can be characterized as shared. The influence of transport can be further

classified as "significant with a note that with slightly different criteria a designation of "inconsequential" would have been obtained.

RECOMMENDATIONS

Use of the Classification and Regression Tree (CART) analysis technique in this study provided an insightful approach to the classification of days according to meteorological and air quality characteristics. It is interesting that most of the variables identified by CART as important to the classification were based on routine measurements. Thus, one recommendation is to expand the CART analysis to the classification of days for additional years or multi-year periods. This would provide a more extensive database for the classification of ozone events as either "local" or "shared"; and further as "overwhelming", "significant", or "inconsequential".

Improved representation of the three-dimensional airflow characteristics of the episode days selected for further analysis as part of this study, as well as other episode days that are of interest, could result from the application of a data-assimilating meteorological modeling system. This would enhance the reliability of the two- and three-dimensional trajectory calculations.

Finally, a quantitative assessment of interbasin transport (for selected days or multi-day episode periods) could be obtained through application of a photochemical grid model for the SoCAB/MDAB/SSAB/SDAB area. This would enable the calculation of pollutant flux along selected vertical planes separating the air basins. If acceptable model performance is achieved, the photochemical modeling system could also be utilized to examine the response of the simulated ozone and precursor transport to changing emissions distributions within and among the southern California air basins.

4 SUMMARY AND CONCLUSIONS

The report summarizes the methodologies and results of a data analysis study designed to examine pollutant transport within southern California, specifically between the SoCAB and the MDAB/SSAB (formerly the SEDAB) and the SDAB. Transport conditions were examined using data collected during the 1992 summer field program. These data include RWP, RASS, and aircraft data. The overall objective of the study was to provide an improved understanding of the three-dimensional meteorological and air quality characteristics of interbasin pollutant transport. The study was comprised of three major components: (1) comparison of the RWP and RASS data with routine radiosonde measurements, (2) development of a conceptual model for transport between the SoCAB and the former SEDAB, and (3) analysis of the airflow patterns and calculated trajectories for selected days representing a variety of transport conditions.

The results of the comparison of the upper-air wind and temperature data indicate that significant differences between measurements obtained using radiosondes and those obtained using RWP and RASS technologies exist. Certainly some differences are expected, given the differences in data collection methodologies and their respective error characteristics. Contamination of the RWP data by migrating birds and the subsequent application of newly developed editing routines may have contributed to the wind component differences. In addition, none of the radiosonde and RWP/RASS sites for which data were compared were collocated. The complex geography of southern California and the corresponding spatial variability in meteorological characteristics introduced by the complex terrain and the land/sea breeze circulation limited the extent to which data from non-collocated sites could be reasonably compared. A more comprehensive, site-specific examination of the agreement between RWP/RASS and radiosonde data that considers instrument calibration, siting, and the use of the moment data in addition to the hourly averages should accompany further monitoring studies of this area.

The results of the data evaluation component of this study further indicate that the use of data from relatively new types of measurement platforms, such as the RWP and RASS instruments, for analysis and modeling purposes, requires a careful review and assessment of data quality and applicability.

In the second phase of the study, each day of the 1992 analysis period was identified as belonging to one of nine categories of combinations of high, moderate, or low ozone concentrations in the SoCAB and MDAB/SSAB (formerly SEDAB) (for example, high ozone concentrations in the SoCAB and moderate ozone in the MDAB/SSAB, or high ozone in the SoCAB and high ozone in the MDAB/SSAB). Analysis of composite surface and upper-level winds and maximum mixing heights for the nine different ozone classification couples indicates numerous similarities in the airflow patterns for all days of the 1992 study period but also some differences in both the winds and the mixing heights that enable one to distinguish among the categories.

The results of this analysis suggest that there is a strong correlation between high ozone concentrations in the SoCAB and high concentrations in the MDAB and SSAB. During the 1992 study period, moderate to high observed ozone concentrations in the former SEDAB were almost always associated with moderate to high ozone concentrations in the SoCAB. There were no days when high ozone was observed in the former SEDAB and concentrations within the SoCAB were low. The composite winds also indicate that transport of pollutants from the SoCAB to the MDAB/SSAB (previously SEDAB) contributed to the high observed concentrations in the air basin formerly designated the SEDAB; the composite winds (and limited aircraft data) suggest the possibility of pollutant transport both near the surface and aloft.

In the third and final phase of the study, the CART analysis technique was used to categorize the ozone episode days (with respect to meteorological and air quality conditions) and representative episodes from the major classification categories were selected for further analysis. The ozone episode days were then classified as "local" or "shared" events; the "shared" events were further categorized as "overwhelming", "significant", or "inconsequential" transport days. Based on the results of the CART analyses, six episodes were selected for further analysis. Of these, two episode days indicated the possibility of transport into the MDAB or SSAB (formerly SEDAB) from the SoCAB, one indicated the possibility of local causes within the former SEDAB and remaining three episodes indicated the possibility of transport into the SDAB from the SoCAB.

Analyses of the transport characteristics of these episode days were carried out through trajectory analysis. Two- and three-dimensional particle paths were calculated using gridded wind fields, and the potential for interbasin transport for the selected days, as well as for meteorologically similar days, was examined.

The results of two- and three-dimensional particle path analyses for the MDAB/SSAB (formerly SEDAB) indicate that although local causes for one of the days was indicated by CART, all three episode days appear to be shared events. These and meteorologically similar days (according to the CART analysis) comprise more than 80 percent of the exceedance days included in this analysis. Thus most ozone episodes that occurred within the SEDAB during the summer of 1992 can be characterized as shared. The influence of transport was further classified as "significant.

The results of two- and three-dimensional particle path analyses for the SDAB indicate that all three episode days appear to be shared events. Trajectories from both the SCCAB and SoCAB, as well as from points to the south of the SDAB, indicate the possibility of transport of ozone and precursor into the SDAB; meandering trajectories remaining over the SDAB indicate local influences. These and meteorologically similar days (according to the CART analysis) comprise 90 percent of the exceedance days included in this analysis. Thus most ozone episodes that occurred within the SDAB during the summer of 1992 can be characterized as shared. The influence of transport was further classified as "significant" with a note that with slightly different criteria a designation of "inconsequential" would have been obtained.

References

Anderson, J. A., P. W. Hansen, J. D. Prouty, and J. M. Gardner. 1993. "Data Collected by the STI Aircraft During the 1992 ARB Southern California Transport Assessment Study. Data Volume." Sonoma Technology Incorporated, Santa Rosa, California (STI-92120-1238-DV).

ARB. 1990. "Assessment and Mitigation of the Impacts of Transported Pollutants on Ozone Concentrations within California." California Air Resources Board (Staff Report).

Cassmassi, J. C., K. R. Durkee, and K. Underwood. 1994. "Evaluation of Remote Sensing Instruments to Profile Wind and Temperature in the Boundary Layer of the South Coast Air Basin." *Regional Photochemical Measurement and Modeling Studies*, Air and Waste Management Association, San Diego, California, pp. 160-175.

Durkee, K. R., and J. C. Cassmassi. 1993. "Analysis of Wind and Temperature Profiler Data Observed in the South Coast Air Basin." *Role of Meteorology in Managing the Environment in the 90s*, Air and Waste Management Association, Pittsburgh, Pennsylvania, pp. 414-425.

Golden, J. H., R. Serafin, V. Lally, and J. Facundo. 1986. "Atmospheric Sounding Systems." *Mesoscale Meteorology and Forecasting.*, edited by P.S. Ray. American Meteorological Society, Boston, Massachusetts.

Kuo, Y.-H., and T. W. Schlatter. 1990. *Mesoscale Data Assimilation*. Advanced Study Program, National Center for Atmospheric Research, Boulder, Colorado.

NOAA. 1994. "A Multi-Year Observational Study of Atmospheric Transport Corridors and Processes in California." Prepared for California Air Resources Board by National Oceanic and Atmospheric Administration, Boulder, Colorado (Contract No. A032-145).

SAI. 1990. "User's Guide for the Urban Airshed Model, Volume III: User's Manual for the Diagnostic Wind Model (Version 1.1). Systems Applications International, Inc., San Rafael, California (SYSAPP-90/018c).

STI. 1996. "Draft Guideline for the QA and Management of PAMS Upper-Air Meteorological Data." Sonoma Technology Incorporated, Santa Rosa, California.

White, A. B. 1993. "Mixing Depth Detection Using 915-MHz Radar Reflectivity Data." Eighth Symposium on Observations and Instrumentation, American Meteorological Society, Boston, Massachusetts.